Regulation of Potassium Channels through mTOR and PDK1 in Dendritic and Mast Cells

Dissertation

der Mathematisch-Naturwissenschaftlichen Fakultät

der Eberhard Karls Universität Tübingen

zur Erlangung des Grades eines

Doktors der Naturwissenschaften

(Dr. rer. nat.)

vorgelegt von

Leonid Tyan

aus Bischkek, Kirgisische Republik

Tübingen

2012

Tag der mündlichen Qualifikation: 18.07.2012

Dekan: Prof. Dr. Wolfgang Rosenstiel

1. Berichterstatter: Prof. Dr. med. Florian Lang

2. Berichterstatter: Prof. Dr. Friedrich Götz

Acknowledgements

List of figures

List of tables

List of abbreviations

Ag	Antigen
AMPK	AMP-activated protein kinase
Anti-DNP IgE	Anti-dinitrophenyl mouse IgE
APC	Antigen-presenting cell
BMDC	Bone marrow-derived dendritic cell
BMMC	Bone marrow-derived mast cell
CCL	CC-chemokine ligand
CCR	CC-chemokine receptor
cDC	Conventional dendritic cell
CHO	Chinese hamster ovary
CTMC	Connective tissue mast cell
DC	Dendritic cell
DEPC	Diethylpyrocarbonate
ECL	Enchanced chemiluminescence
EGTA	Ethylene glycol tetraacetic acid
EIF4E	Eukaryotic translation initiation factor
EIF4EBP1	Eukaryotic translation initiation factor binding protein 1
ELISA	Enzyme-linked immunosorbent assay
ER	Endoplasmatic reticulum
F6CA	Fluorescein-6-carboxylic acid
FACS	Fluorescence activated cell sorter
FBS	Fetal bovine serum
FKBP12	FK506-binding protein 1A, 12 kDa
FLT3l	FMs-like tyrosine kinase 3 ligand
GM-CSF	Granulocyte/macrophage colony-stimulating factor
GSK	Glycogen synthase kinase
HEK	Human embryonic kidney

IFN	Interferon
IL	Interleukin
IL-1R	Interleukin-1 receptor
IP3	Inositol-(1,4,5)-trisphosphate
IRAK	Interleukin-1 receptor-associated kinase
IRF	Interferon regulatory factor
IRS	Insulin receptor substrate
K_{Ca}	Ca^{2+} activated K^+ channel
Kv	Voltage-gated K^+ channel
LC	Langerhans cell
LPS	Lipopolysaccharide
MAPK	Mitogen-activated protein kinase
MAPKAP	Mitogen-activated protein kinase-associated protein
MC	Mast cell
MHC	Major histocompatibility complex
MIIC	Major histocompatibility complex class II-rich compartments
MMC	Mucosal mast cell
MMCP	Mouse mast cell protease
mTOR	Mammalian target of rapamycine
mTORC	Mammalian target of rapamycine complex
NF-kB	Nuclear factor-kB
NK	Natural killer
PALS	Periarteriolar lymphatic sheaths
PBS	Phosphate buffered saline
PCR	Polymerase chain reaction
pDC	Plasmacytoid dendritic cell
PDK	Phosphoinositide-dependent protein kinase
PH	Pleckstrin homology
PI3	Phosphatidylinositol-3
PI3K	Phosphatidylinositol-3 kinase
PIF	Phosphoinositide-dependent protein kinase interacting fragment

PIKK	Phosphoinositide kinase-related kinase
PKB	Protein kinase B
PKC	Protein kinase C
PtdIns(3,4)P$_2$	Phosphatidylinositol (3,4) biphosphate
PtdIns(3,4,5)P$_3$	Phosphatidylinositol (3,4,5) triphosphate
PTEN	Phosphatase and tensin homologue
Rapa	Rapamycine
Raptor	Regulatory associated protein of mammalian target of rapamycine
Rheb	Ras homologue enriched in brain
Rho	Ras homologue
RICTOR	Rapamycine-insensetive major component of mammalian target of rapamycine complex 2
S6K1	S6 kinase 1
SCF	Stem cell factor
SDS	Sodium dodecyl sulfate
SEM	Standart error of the mean
SGK	Serum- and glucocorticoide-inducible kinase
STATS	Signal transducer and activator of transcription
TEVC	Two-electrode voltage clamp
T$_H$	T helper
TLR	Toll-like receptor
TNF	Tumor necrosis factor
TNF-R	Tumor necrosis factor - receptor
TSC	Tuberous sclerosis complex

1. Introduction

1.1. Role of dendritic and mast cells in immune system.

An immune system can protect the host against disease by identifying and killing pathogens and tumor cells. It detects a wide variety of agents, from viruses to parasitic worms, and needs to distinguish them from the organism's own healthy cells, tissues and harmless environmental antigens in order to function properly. Detection is complicated as pathogens can evolve rapidly, and adapt to avoid the immune system. This changes allow the pathogens to successfully infect their hosts.

Immune responses against this wide spectrum of "danger" signals are mediated by a variety of cell types and soluble factors that are generally assigned to the innate or the adaptive immune system. The innate immune system represents the first barrier against pathogens[1]. The innate immune system is evolutionary conserved and senses pathogens via pattern recognition receptors such as Nod-like receptors[2], C-type lectin receptors[3], and Toll-like receptors (TLRs)[4]. Main features of the mammalian innate immune system are the ability to rapidly recognize pathogens and/or tissue injury and the ability to signal the presence of danger to cells of the adaptive immune system. Adaptive immunity serves to detect and identify "non-self" particles via cell surface receptors such as T cell receptor on T lymphocytes and B cell receptor on B lymphocytes. Receptor engagement results in clonal lymphocyte expansion. It allows to respond to a wide range of potential antigens[1,4].

1.2. Dendritic cells.

Dendritic cells (DCs) are antigen-presenting cells, central for the development of optimal T cell immunity, that are able to initiate primary immune responses and to establish immunological memory[5,6].

Dendritic cells belong to the innate system. Cells of the innate system (DCs, natural killers, macrophages, neutrophils etc.) use a variety of pattern recognition receptors to recognize patterns shared between pathogens, for instance bacterial lipopolysaccharide (LPS),

carbohydrates, and double-stranded viral RNA[7,8]. Upon taking up an antigen (Ag), dendritic cells undergo maturation, express costimulatory molecules and MHC class II [9-11], produce certan chemokines and cytokines and migrate to the draining lymph nodes where they induce proliferation and differentiation of antigen-specific T cells[12-14].

Dendritic cells (DCs) are unique antigen-presenting cells (APCs). From the wide spectrum of immune cells only DCs are able to induce primary immune responses, thus permitting establishment of immunological memory. In the bone marrow DC progenitors give rise to circulating precursors that home to tissues, where they reside as immature cells with high phagocytic capacity (Figure 1). Following tissue damage, immature DCs capture Ag and subsequently migrate to the lymphoid organs, where they select rare Ag-specific T cells, thereby initiating immune responses. DCs present Ag to CD4$^+$ T-helper cells, which in turn regulate the immune effectors, including Ag-specific CD8$^+$ cytotoxic T cells and B cells, as well as non–Ag-specific macrophages, eosinophils, and NK cells[15]. DCs also present Ag to CD8$^+$ T cells through MHC I, which plays an important role in viral and tumor defence (Fig. 1). Moreover, DCs "educate" effector cells to home to the site of tissue injury. DCs are effective on four stages of their development: 1) bone marrow progenitors; 2) precursor DCs that are patrolling through blood and lymphatics as well as lymphoid tissues, and that, upon pathogen recognition, release large amounts of cytokines thereby limiting the spread of infection; 3) tissue-residing immature DCs, which possess high endocytic and phagocytic capacity permitting Ag capture; 4) mature DCs, present within secondary lymphoid organs, that express high levels of costimulatory molecules permitting Ag presentation[15] (Figure 1). DCs constitute a complex system of cells which, under different microenvironmental conditions, can induce such contrasting states as immunity and tolerance[15].
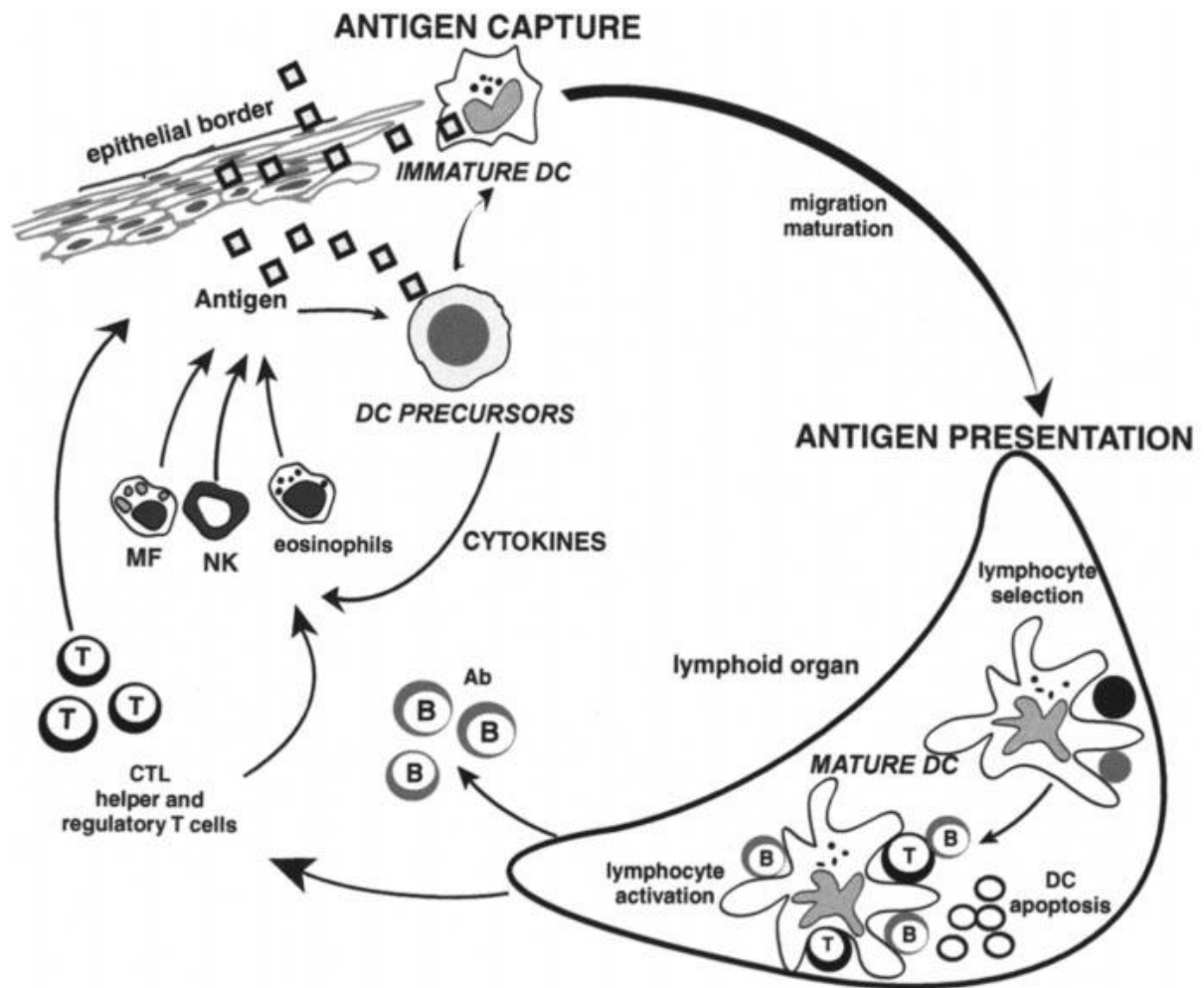
Figure 1. The life cycle of dendritic cells (DC). Circulating precursor DCs enter tissues as immature DCs. They can also directly encounter pathogens (e.g. viruses) that induce secretion of cytokines (e.g. IFNα), which in turn can activate eosinophils, macrophages (MF), and natural killer (NK) cells. After antigen capture, immature DCs migrate to lymphoid organs where, after maturation, they display peptide-major histocompatibility complexes, which allow selection of rare circulating antigen-specific lymphocytes. These activated T cells help DCs in terminal maturation, which allows lymphocyte expansion and differentiation. Activated T lymphocytes migrate and can reach the injured tissue, because they can traverse inflamed epithelia. Helper T cells secrete cytokines, which permit activation of macrophages, NK cells, and eosinophils. Cytotoxic T cells eventually lyse the infected cells. B cells become activated after contact with T cells and DCs and then migrate into various areas where they mature into plasma cells, which produce antibodies that neutralize the initial pathogen. It is believed that, after interaction with lymphocytes, DCs die by apoptosis. Taken from Banchereau et al.[15]

1.2.1. Dendritic cell classification.

There are two pathways of DC development: conventional DCs of myeloid origin and pre-DCs of lymphoid origin[15]. Evidence for the myeloid origin of DCs comes mainly from in vitro studies in which myeloid-committed precursors give rise to both granulocytes/monocytes and myeloid DCs under the influence of granulocyte/macrophage colony-stimulating factor (GM-CSF)[16]. At the steady state, conventional DCs (cDCs) display all the typical phenotypic and functional characteristics that have been originally used to describe DCs. They are veiled cells of myeloid origin capable of efficiently processing and presenting antigens and of priming naive T cells[17]. DCs can also arise from lymphoid-committed precursors[18]. By contrast with cDCs, pre-DCs must undergo an additional differentiation step, induced, in most cases, by inflammatory stimuli (microbial and endogenous stimuli that activate TLRs), to acquire the characteristics of DCs, including the efficient antigen-presenting capacity[17]. Plasmacytoid DCs (pDCs) and monocytes are classified as pre-DCs, as both can further differentiate into efficient APCs in the presence of microbial stimuli[19].

Conventional DCs are subdivided into migratory and lymphoid tissue-resident DCs. Migratory cDCs reside in nonlymphoid tissues where they continuously scan the environment to detect the presence of invading microorganisms. Upon microbial encounter tissue-resident migratory cDCs migrate to the draining lymph nodes through the afferent lymphatic vessels[17].

Lymphoid tissue-resident cDCs are not present in the afferent lymphatic system and encounter the antigen directly inside the lymphoid organs. Antigens can reach the lymphoid organs through the blood, by freely migrating through the lymphatics or associated to migratory cDCs[17]. Most thymic and splenic DCs and about half of the lymph node DCs are lymphoid tissue-resident cells[19].

cDCs are subdivided into different subtypes as well[17]. The number of subtypes is continuously growing[17]. Subset classification is based on tissue origin and the expression of particular markers for migratory cDCs, and on marker expression for lymphoid tissue-resident DCs[17,20,21].

Pathway of development determines phenotype, localization, and function of DCs[15]. Both cDC and pDC express class II major histocompatibility complex (MHC), high levels of CD11c, and the costimulatory molecules CD86 and CD40[15]. The most reliable way to distinguish this two subsets of DC is CD8α homodimer. pDCs, but not cDCs express CD8α[22].

pDCs are localized in the T cell–rich areas of the periarteriolar lymphatic sheaths (PALS) in the spleen and lymph nodes[23]. cDCs are localized in the marginal zone bridging channels of the spleen[23]. The pDCs make higher levels of IL-12 and are less phagocytic than cDCs[24]. pDCs express IFNγ under influence of IL-12 but not cDCs[25]. In vitro, the pDCs were reported to prime allogeneic CD4$^+$ and CD8$^+$ T cells less efficiently than cDCs[26]. In vivo, both pDCs and cDCs appear to prime Ag-specific CD4$^+$ T cells efficiently[27].

GM-CSF and Flt3 ligand (Flt3-L) can expand mature DC in mice[15]. Flt3-L targets primitive hematopoietic progenitors in the bone marrow, inducing their expansion and differentiation and both pDC and cDC numbers increase dramatically upon Flt3-L injection[28]. Flt3-L treatment leads to an increase in DC numbers in multiple organs in mice, including spleen, lymph nodes, blood, thymus, Peyer's patch, liver, and lungs. In contrast, GM-CSF preferentially expands the cDC subset in vivo [29].

1.2.2. Antigen capture, migration and maturation of dendritic cells.

An important attribute of DCs is their mobility. DCs migrate from the bone marrow to the peripheral tissue, then to the secondary lymphoid and nonlymphoid organs[15]. DCs accumulate rapidly (within an hour) at the sites of Ag deposition. This accumulation likely represents recruitment of circulating DC precursors, in response to the production of chemokines upon local inflammation. In vitro, immature DCs respond to a large spectrum of chemokines through specific receptors. Different DC subsets display unique sensitivity to certain chemokines. During their migration, DCs are involved in several adhesion events[15]. For instance, E-cadherin, uniquely expressed by Langerhans cells (LCs) (DCs of the epidermis), permits, through homotypic interactions, the residence of LCs in epidermis[30]. Ag encounter results in downregulation of E-cadherin that allows LC migration out of the skin[31].

Immature DCs are very efficient in Ag capture and can use several pathways, such as macropinocytosis; receptor-mediated endocytosis via C-type lectin receptors[32] or Fc$_\gamma$ receptor types I (CD64) and II (CD32) [uptake of immune complexes or opsonized particles[33]]; and phagocytosis of particles such as latex beads[34], apoptotic and necrotic cell fragments (involving CD36 and avb3 or avb5 integrins)[35], viruses, and bacteria including mycobacteria[36], as well as intracellular parasites such as *Leishmania major*[37].

Antigen uptake results in a process of maturation which includes phenotypic and functional changes and a transition from an Ag-capturing cell to an Ag-presenting cell. This transition can be also induced by activation of certain cytokine receptors (TNF-R, IL-1R) or CD40 on DCs. DC maturation starts in the periphery upon Ag encounter and/or inflammatory

cytokines, continues upon DC migration from the peripheral tissue to the draining lymphoid organs[15], is completed during the DC–T cell interaction[15].

Pathogen-related molecules such as LPS[38], bacterial DNA[39], and double-stranded RNA[40]; the balance between proinflammatory and antiinflammatory signals in the local microenvironment, including TNF, IL-1, IL-6, IL-10, TGF-b, and prostaglandins; and T cell–derived signals induce and/or regulate DC maturation. The maturation process is associated with several coordinated events such as loss of endocytic/phagocytic receptors; upregulation of costimulatory molecules CD40, CD58, CD80, and CD86; change in morphology, shift in lysosomal compartments with downregulation of CD68 and upregulation of DC–lysosome-associated membrane protein and change in class II MHC compartments[15].

Mature DCs leave the nonlymphoid organs through the afferent lymph[15].

1.2.3. Antigen processing and presentation by dendritic cells.

DCs are well equipped to capture and process antigens using MHC II and MHC I complexes.

Soluble and particulate Ags are efficiently captured by immature DCs and targeted to MHC class II compartments[41,42]. Immature DCs constantly accumulate MHC class II molecules in lysosome-related intracellular compartments identified as MHC class II–rich compartments (MIICs), with multivesicular and multilamelar structure[43]. The captured Ag is directed towards MIICs containing HLA-DM that promotes the catalytic removal of class II–associated invariant chain peptide and enhances peptide binding to MHC class II molecules[44].

To generate CD8^{+} cytotoxic killer cells, DCs present antigenic peptides on MHC class I molecules, which can be loaded through both an endogenous and an exogenous pathway[45]

The endogenous MHC class I pathway operates through the degradation of cytosolic proteins and the loading of peptides onto newly synthesized MHC class I molecules within the endoplasmic reticulum (ER). Ag processing occurs first in the cytosol through the ATP-dependent proteolytic system, which starts by ubiquitin conjugation. The ubiquitinylated proteins are directed to the proteasome, which cleaves the protein into peptides. The peptides are then translocated into the ER via ATP-dependent TAP1/2 transmembrane transporters and are trimmed into 8–10 mers, which accommodate the MHC class I-binding groove[15].

DCs have an alternative MHC class I pathway (cross-priming) that can present peptides derived from extracellular Ags[15]. There are two routes for the exogenous MHC class I pathway: 1) a TAP-independent pathway in which Ag is most likely hydrolyzed in endosomes[46] and 2) a phagosome-to-cytosol pathway that is TAP dependent[15]. This pathway

is thought to be involved in immune responses against transplantation Ags, particulate Ags, tumors[47], and viruses[48]. It is also operative in the development of tolerance[49]. The engulfment and processing of cell bodies by DCs represent a possible pathway for the loading of MHC class I [35].

1.3. Mast cells.

Mast cells are tissue-based effector cells in allergic diseases, playing a central role in the propagation of IgE-dependent allergic reactions[50], such as allergic rhinitis[51], asthma[52], anaphylaxis and delayed hypersensitivity reactions[52,53]. Upon Ag stimulation of IgE receptors (Fc$_\varepsilon$RI), mast cells release granules containing several mediators including histamine and cytokines, which participate in the regulation of other inflammatory cells [53].

Fc$_\varepsilon$RI is a tetrameric receptor that comprises an α-chain, which is responsible for binding IgE, as well as a β-chain and a disulphide-linked γ-chain homodimer, which are responsible for initiating signalling[54].

Antigen-dependent mast-cell activation is regulated by a complex series of intracellular signalling processes that is initiated following Fc$_\varepsilon$RI aggregation. Although the immediate receptor-proximal signalling events seem to be common for the release of all categories of mediators, the receptor-distal signalling events must diverge to regulate the different mechanisms by which these mediators are released[54].

The classification of rodent mast cell subtypes is based on phenotypical differences between connective tissue mast cells (CTMC), particularly of the skin and peritoneal cavity, and mucosal mast cells (MMC), particularly of the intestinal lamina propria. There are phenotypical differences between these two populations, including size and histamine content as well as proteoglycan and neutral protease composition. Furthermore, these subtypes show differences in function, including responsiveness to various secretagogues, and inhibition by drugs. The population of MMC also expands remarkably during T cell-dependent immune responses to certain intestinal parasites[55]. In contrast, CTMC exhibit little or no T-cell dependence and occur in athymic nude mice or rats in numbers similar to those present in normal animals[56]. By analogy to rodent mast cells, variations in fixation properties provided the first experimental evidence of the existence of different types of human mast cells. Accordingly, human intestinal mucosal mast cells display metachromatic staining after fixation in Carnoy's solution, but not when fixed in neutral buffered Formalin. In contrast, CTMC found in the intestinal submucosa retain metachromatic staining properties regardless of the fixative used[55]. Human mast cells also exhibit variations in morphological

characteristics such as size and cytoplasmic granule ultrastructure[57], histochemical properties, quantities of stored mediators, sensitivity to stimulation by various secretagogues, and susceptibility to various drugs[55].

1.3.1. Mast cells origin and activation.

Mast cells originate from pluripotential progenitor cells in the bone marrow. They express $Fc_\varepsilon RI$ and $Fc_\gamma RII/III$ early in development before they exhibit full granule maturation and may be recognized morphologically. Several cytokines are known to affect the growth and differentiation of mast cells, including IL-3, stem cells factor, IL-4, IL-9, IL-10, and NGF. Mast cells enter the circulation in small numbers and before they can be morphologically identified. From the circulation, mast cell precursors enter the peripheral tissues where they express their final phenotype under the influence of stem cell factor (SCF) and other locally produced cytokines[55].

IL-3 and SCF are two principal cytokines that promote mast cell proliferation and/or differentiation. IL-3 seems to be important for early mast cell proliferation. SCF is produced by stromal cells, acts to maintain mast cell viability and promotes maturation[55]. In addition, SCF promotes mast cell adhesion to fibroblasts and to extracellular matrix components[58], thus influencing mast cell migration and distribution.

Mast cell activation may be initiated upon interaction of a multivalent antigen (allergen) with its specific IgE antibody attached to the cell membrane via its high-affinity receptor, Fc_ε RI. Cross-linkage of IgE by the interaction of allergen with specific determinants on the Fab portion of the molecule brings the receptors into juxtaposition and initiates mast cell activation and mediator generation and release. Experimentally, IgE crosslinkage may be induced artificially by the use of anti-IgE antibodies or antibodies against the IgE receptor. $Fc_\varepsilon RI$ is also found on basophils, Langerhans cells, and activated monocytes. Mast cells may also be activated by nonimmunologic stimuli induced by substances such as neuropeptides, basic compounds, complement components, and certain drugs such as opiates. Morphologically, degranulation produced by immunologic and nonimmunologic stimulation appears similar. However, biochemical processes that lead to mediator release may differ[55].

IgE binds to membranes or solubilized $Fc_\varepsilon RI$ receptors with high affinity. The binding is highly specific and cannot be inhibited by an excess of any other immunoglobulins. Also, the isotype specificity is almost absolute. The binding of IgE occurs via the Fc region of the immunoglobulin in a 1:1 ratio[55].

1.3.2. Mast cells mediators.

Mast cells release and generate a heterogeneous group of mediators that differ in their potency and biological activities. Mast cell-dependent mediators may be categorized into three groups: preformed secretory granule-associated mediators, lipid-derived mediators, and cytokines[55].

Granule-associated mediators are histamine, proteoglycans, neutral proteases.

Histamine is the single amine known to be stored in human mast cells, although mast cells of other species are known to store additional amines. Decarboxylation of the amino acid histidine to form histamine takes place in the Golgi apparatus of mast cells and basophils. The histamine is then stored associated by ionic linkage with the carboxyl groups of proteins and proteoglycans of the secretory granules at acidic pH. Rat peritoneal mast cells contain 10-30 pg histamine/cell, whereas mucosal mast cells have lower amounts (1-3 pg/cell)[55]. Approximately 3-8 pg histaimine/cell is found in mast cells isolated from human lung, skin, lymphoid tissue, and small intestine [59].

Histamine dissociates from the proteoglycan-protein complex by cation exchange with extracellular sodium and at neutral pH. Specific receptors on target cell surfaces then mediate the wide-ranging biological activities of histamine. The interaction of histamine with H_1 receptors results in the contraction of airway and gastrointestinal smooth muscle and vasospasm. The distinction between H_1 and H_2 receptors is based on the inhibitory activity of certain drugs on specific pharmacological effects of histamine. Within minutes of release, histamine is metabolized into methylhistamine, methylimidazole acetic acid, or imidazole acetic acid. It is thus likely that histamine usually influences events at or near the site of release[55].

Heparine and chondroitin sulfat E are MCs proteoglycans. Both of them stabilize mast cell proteases and alter the biological activity of many enzymes. Heparin is also a potent anticoagulent[55].

Mouse MC proteases are now very well described. They include at least seven serine proteases (mouse mast cell protease (MMCP)-1 to MMCP-7). The proteases MMCP-1 to MMCP-5 are highly homologous chymases, and MMCP-6 and MMCP-7 are tryptases[60]. Mouse mast cell proteases are differentially expressed in various mast cell subsets and at specific tissue sites[55].

The activation of mast cells not only causes the release of preformed granule-associated mediators, but initiates the de novo synthesis of lipid-derived substances. Of particular

importance are the cyclooxygenase and lipoxygenase metabolites of arachidonic acid, because these products possess potent inflammatory activity[55].

1.4. Role of PI3-Kinase, mTOR and PDK1 in immune system regulation.

The phosphatidylinositol-3 kinases (PI3Ks) as well as the mammalian target of rapamycin (mTOR) pathways are two key cellular signalling pathways that affect broad aspects of cellular functions, including metabolism, growth and survival[61,62].

PI3K and mTOR signalling are connected via the serine/threonine kinase Akt.[63] Akt, also termed PKB (protein kinase B), is one of the most important survival kinases involved in regulating a similarly wide array of cellular processes as PI3K and mTOR, including metabolism, growth, proliferation and apoptosis[64]. Akt, in turn, is activated by phosphoinositide-dependent protein kinase-1 (PDK1) (Fig. 2)

1.4.1. Role of phosphatidylinositol-3-Kinase in dendritic cells.

The function of DCs is under the control of the phosphoinositide-3-kinase pathway[65]. PI3 kinase is considered to be an endogenous suppressor of IL-12 production triggered by TLR signalling and limits excessive T_H1 polarization[66]. Inhibition of PI3 kinase was also shown to enhance IFN-β synthesis downstream of TLR3 and TLR4[67]. Together with two other kinases, such as IRAK-M and SOCS-1, PI3 kinase belongs to the gate-keeping system, preventing excessive innate immune responses. PI3 kinase is stimulated by most of the activators of DCs that induce IL-12 production at an early phase and interferes at the first encounter to pathogens, providing a negative feedback regulation of IL-12 production in DCs[68].

1.4.2. Role of mTOR in immune system regulation.

Serine/threonine protein kinase mammalian target of rapamycin (mTOR) has an important role in the modulation of both innate and adaptive immune responses. mTOR plays a central role in mammalian development[69]. It is a crucial regulator of cell growth and proliferation, and of physiological events such as transcription, mRNA turnover and translation, ribosomal biogenesis, vesicular trafficking, autophagy, cytoskeletal organization and cell size[62]. mTOR regulates diverse functions of DCs and has important roles in the activation of effector T cells and the function and proliferation of regulatory T cells[70].

There are two mTOR complexes, mTOR complex 1 (mTORC1) and mTORC2. These two complexes have different sensitive to rapamycin, which inhibits mTORC1, but not mTORC2.

mTOR kinase, functioning in mTORC1 and mTORC2, acts as a coordinator of signalling pathways that shape the response of cells to various stimuli. Immune cells, using receptors that signal through mTOR directly or indirectly, modulate host responses based on their 'perception' of environmental danger[70].

mTORC1 is a regulator of cell growth and other processes downstream of phosphatidylinositol-3-Kinase (PI3K)–AKT (also known as PKB, protein kinase B), WNT–GSK3 (glycogen synthase kinase 3) and AMP-activated protein kinase (AMPK) signalling[70] (Fig. 2)

Tuberous sclerosis complex 1 (TSC1) and TSC2 together form a functional complex that acts as the upstream inhibitor of mTORC1. Growth factors, cytokines, costimulatory molecules and antigen receptors activate PI3K, which subsequently activates AKT[70]. Fully activated AKT inhibits TSC2 by phosphorylating it[71], thereby negating the inhibitory effect of TSC2 on mTORC1. Activation of the Ras–MAPK (mitogenactivated protein kinase) pathway also leads to the inhibition of the TSC1–TSC2 complex. Alternatively, cellular stress and DNA damage can inhibit mTORC1 by promoting the regulatory capacity of TSC1–TSC2[62]. The inhibitory activity of the TSC1–TSC2 complex is mediated by inhibiting Rheb (Ras homologue enriched in brain), a Ras-like GTPase and a positive regulator of mTORC1[72]. Removal of TSC1–TSC2-dependent inhibition allows mTORC1 to phosporylate S6 kinase 1 (S6K1; also known as RPS6KB1) and the eukaryotic initiation factor EIF4EBP1 (eukaryotic translation initiation factor (EIF4E) binding protein 1). Phosphorylated S6K1 promotes mRNA translation and cell growth by enhancing the biosynthesis of the translational apparatus in the cell[70]. The phosphorylation of EIF4EBP1 prevents it from inhibiting EIF4E, which also stimulates translation[62]. WNT proteins bind to the Frizzled family of receptors, which are involved in the regulation of effector T cell development, Treg cell activation and DC maturation[73]. The WNT pathway influences the mTORC1 pathway by inhibiting GSK3, which in the absence of WNT signalling is an additional negative regulator of mTORC1[74].

mTORC2-dependent signalling is not so well explored like signalling through mTORC1 due to the lack of mTORC2-specific inhibitors. Studies targeting Rictor (rapamycin-insensitive major component of mTORC2)[70] (Fig.3) through small interfering RNA[75] and studies of *Rictor*-knockout mice[76] have shown the importance of mTORC2 in mammalian development and several cellular processes. mTORC2-mediated phosphorylation of Akt is stimulated by insulin and can be blocked by PI3K inhibitors[77]. However, knockdown of

Rictor does not decrease S6K1 activation, indicating that mTORC2 does not activate mTORC1[78]. Targeting *Rictor* has also demonstrated that mTORC2 regulates actin cytoskeleton through the small GTPase Ras homologue (Rho) and protein kinase C14[70]. The TSC1–TSC2 complex has been shown to regulate cell adhesion and migration[79], but it is not clear whether it signals to and regulates mTORC2. Regulation of cell movement and adhesion is an important feature of effective immune responses, so it is possible that mTORC2 might also modulate immune reactivity [70].

1.4.3. S6K1-mediated regulation of mTOR signalling.

mTOR is a crucial coordinator of signalling pathways, so it is not surprising that feedback inhibition through S6K1 is an important component of the pathway. Activated S6K1, the main effector of uninhibited mTORC1, negatively regulates input from the PI3K–AKT signalling pathway to mTORC1 by phosphorylating and initiating degradation of insulin receptor substrate 1 (IRS1), which is the molecular intermediate between insulin receptor and PI3K[80]. It has not yet been determined whether S6K1 can also negatively regulate input from other receptor systems that activate mTOR through PI3K. On the other hand, activated S6K1 can also positively regulate mTOR activation. GSK3, which is constitutively activated in the absence of growth factors, negatively regulates mTOR pathway by stimulating the TSC1–TSC2 complex[70]. Under certain conditions, activation of S6K1 can negatively regulate GSK3[81], thus leading to mTOR deinhibition.
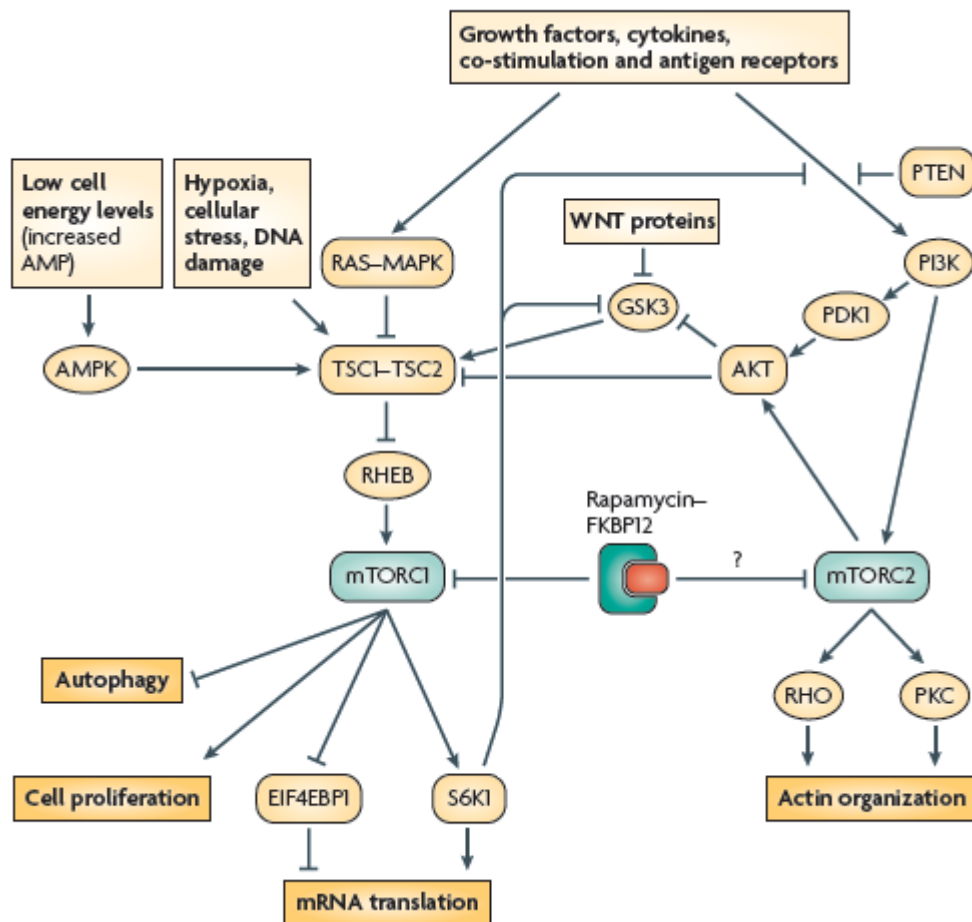
Figure 2 mTORC1 and mTORC2 signalling pathways. Mammalian target of rapamycin complex 1 (mTORC1) is the direct target of the rapamycin–FK506-binding protein 1A, 12 kDa (FKBP12) complex and regulates cell growth and size by controlling mRNA translation, ribosome biogenesis and autophagy. Diverse signals, arising from growth factors (such as insulin and FMs-like tyrosine kinase 3 ligand (FLT3L)), various cytokines, ligated co-stimulatory molecules and antigen receptors, WNT proteins, cellular energy levels, as well as hypoxia, cellular stress and DNA damage determine mTORC1 activity. These signals all mediate their effects through the tuberous sclerosis complex 1 (TSC1)–TSC2 complex, which is the main negative regulator of mTORC1. Activation of Ras–MAPK (mitogen-activated protein kinase) and phosphoinositide 3-kinase (PI3K)–Akt signalling results in inhibitory phosphorylation of TSC2 and removes repression of Rheb (Ras homologue enriched in brain), which is the mTORC1 stimulator. Activation of PI3K–Akt signalling is negatively regulated by phosphatase and tensin homologue (PTEN). Activated mTORC1 promotes mRNA translation by stimulating s6 kinase 1 (S6K1; also known as RPs6KB1) and inhibiting EIF4EBP1 (eukaryotic translation initiation factor-binding protein 1). Activated S6K1 can also feed back to negatively regulate input from PI3K–Akt by facilitating the degradation of

24

signalling intermediates between surface receptors (such as the insulin receptor) and PI3K. Low energy and nutrient levels (signalling through AMP-activated protein kinase; AMPK), as well as hypoxic conditions, increase the TSC1–TSC2-mediated inhibition of mTORC1 that is downstream of input from glycogen synthase kinase 3 (GSK3). mTORC2 is not inhibited directly by rapamycin, but long-term rapamycin administration disrupts its assembly in some cells. mTORC2, activated by PI3K, directly phosphorylates Akt. mTORC2 also regulates actin cytoskeletal dynamics through the small GTPase Ras homologue (Rho) and protein kinase C (PKC). PDK1, phosphoinositide-dependent kinase 1. Taken from Thomson et al[70].
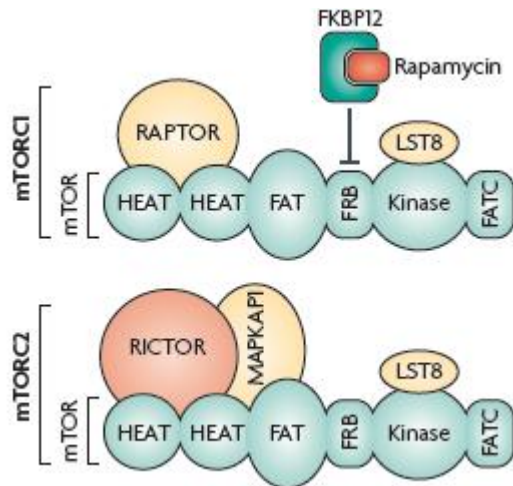
Figure 3. **Mammalian target of rapamycine.** Mammalian target of rapamycin (mTOR) is a large (~289 kDa) atypical kinase, which, like other members of the phosphoinositide kinase-related kinase (PIKK) family, contains a carboxy-terminal serine/threonine protein kinase domain[62]. Also consistent with other PIKKs, mTOR contains a FRAP–ATM–TTRAP (FAT) domain and a C-terminal FAT (FATC) domain that might have a role in its structure and stability[82]. Mammalian LST8 (also known as GβL) associates with the kinase domain of mTOR and is thought to facilitate mTOR signalling, but its precise role has yet to be defined[83]. In addition, mTOR seems to be involved in various protein–protein interactions that determine its physiological role. It has been established that mTOR exists in at least two distinct complexes, mTOR complex 1 (mTORC1) and mTORC2. mTOR and LST8, together with the regulatory associated protein of mTOR (Raptor) form mTORC1. Raptor is essential for mTORC1 activity and is proposed to interact with mTOR through shared HEAT domains[72]. Rapamycin binds to the immunophilin FK506-binding protein 1A, 12 kDA (FKBP12) to form a drug–receptor complex that specifically and effectively blocks the activity of mTORC1. The rapamycin–FKBP12 complex binds next to the kinase region of mTOR in the FKBP12–rapamycin-binding (FRB) domain[84] and disrupts the *in vitro* and *in vivo* activity of the complex, potentially by disrupting the interaction between Raptor and mTOR14. mTORC2 also contains LST8, but instead of Raptor, it associates with rapamycin-insensitive companion of mTOR (Rictor) and possibly MAPKAP1 (mitogen-activated protein kinase-associated protein 1; also known as SIN1)[72]. Unlike mTORC1, mTORC2 is resistant to direct inhibition by rapamycin. It is unknown what prevents the interaction between the rapamycin–FKBP12 complex and the FRB domain on mTORC2[62] Taken from Thomson et al.[70]

1.4.4. mTOR in dendritic cell differentiation, maturation and function.

Rapamycin exerts numerous effects on DC differentiation, maturation and function.

It was showed that mTOR inhibition suppressed interleukin-4 (IL-4) dependent maturation through the posttranscriptional downregulation of the IL-4 receptor (IL-4R) complex in mouse bone marrow-derived DCs. Rapamycin inhibited the expression of costimulatory molecules by DCs both *in vitro* and *in vivo* and suppressed their IL4-induced production of IL-12 and tumour necrosis factor (TNF) as well as their T cell stimulatory function[85]. mTOR inhibition during DC differentiation inhibits the upregulation of CD86 expression that is induced by Toll-like receptor ligands (such as LPS or CpG DNA) or by a CD40-specific monoclonal antibody[86]. mTOR inhibition also decreases the production of nitric oxide by LPS-stimulated macrophages, an effect that is due in part to impaired secretion of interferonβ (IFNβ), which is an autocrine cofactor for nitric oxide production. Furthermore, the inactivation of mTOR decreases the secretion of IL-2 by DCs following their stimulation through the C-type lectin receptor dectin-1[87]. Therefore cytokine production through the activation of C-type lectin receptors involves mTOR.

Rapamycin impairs macropinocytosis and endocytosis of antigens by cultured mouse immature bone marrow-derived DCs[88]. Rapamycin also inhibits endocytosis *in vivo* in mouse splenic DCs[85]. Human monocyte-derived DCs that have differentiated in the presence of rapamycin have decreased expression of antigen uptake receptors (such as CD32, CD46, CD91 and CD205) and decreased receptor-mediated and fluid phase endocytosis and phagocytosis of bacteria and apoptotic cells[89].

DC survival is important for the induction of immune responses. Blocking of GM-CSF signalling by rapamycin induced the apoptosis of both human monocyte-derived DCs and DCs derived from CD34$^+$ precursor cells, but not of monocytes or macrophages[70]. By contrast, the frequency of apoptotic or dead cells was consistently lower than 10% in rapamycin-conditioned, bone marrow-derived mouse DC cultures and *in vivo* generated DCs from rapamycin-treated mice[85].

mTOR plays a role in DC migration. By increasing the expression of CC-chemokine receptor 7 (CCR7), rapamycin increases the migration of human DCs in response to CC-chemokine ligand 19 (CCL19) *in vitro* and mouse DC migration to lymph nodes *in vivo*[90]. Similarly, functional expression of CCR7 is retained on rapamycin-conditioned mouse DCs[86], which promotes their homing to secondary lymphoid tissue during inflammatory responses following allogeneic haematopoietic cell transplantation[91]. Intact *in vivo* migration of rapamycin-conditioned DCs to secondary lymphoid tissue has also been reported in a heart

allograft model[92]. Retention of this *in vivo* migratory ability is probably crucial for the immunoregulatory properties that have been ascribed to rapamycin-conditioned DCs, as it allows these cells to reach appropriate T cell areas in the lymphoid tissue[70].

The coordinated secretion of pro- and anti-inflammatory cytokines is essential for effective immune responses. mTOR suppresses the activation of caspase 1 and therefore the production of bioactive IL-1β[87]. mTOR inhibition elicits *de novo* production of IL-1-β by otherwise phenotypically immature, mouse bone marrow-derived DCs both *in vitro* and *in vivo*[93]. Moreover, IL-1β production by rapamycin-conditioned DCs promotes overexpression of the transmembrane form of the IL-1R family member, IL-1R-like 1, which is the recently identified receptor for IL-33 and promotes T helper 2 (T$_H$2) cell responses[94]. In keeping with this function, IL-1β-induced IL-1R-L1 expression suppresses the responses of rapamycin-conditioned mouse DCs to CD40 ligation, an effect that is absent in *Il1rl1*$^{-/-}$ DCs[93]. So, IL-1ß production upregulates IL-1R-L1 expression and mTOR inhibition impedes the maturation of DCs and their ability to stimulate effector T cell responses.

PI3K negatively regulates TLR-mediated IL-12 production by mouse DCs[66], a feedback mechanism that might prevent excessive T$_H$1 cell polarization. One of the kinases downsream from PI3K is mTOR. Blocking mTOR increases IL-12 production by LPS-stimulated DCs, an effect that is mediated by inhibiting the autocrine secretion of IL-10 (which normally inhibits IL-12 production in a negative feedback mechanism). Consistent with this observation, the activation of mTOR by the transduction of a constitutively active form of Rheb inhibits IL-12 production. In related study, the activation of mTOR in mononuclear phagocytes increased the activity of signal transducer and activator of transcription 3 (STAT3) and the production of IL-10, but decreased the production of proinflammatory molecules (such as IL-12) and the activation of nuclear factor-κB (NF-κB); mTOR inhibition had reciprocal effects[95]. Similarly, rapamycin increased IL-12 production and decreased IL-10 production by human DCs stimulated with LPS or *Staphylococcus aureus*[96]. Such findings imply that mTOR pathways might regulate the T$_H$1–T$_H$2 cell balance by modulating the production of IL-10 and IL-12 by DCs. Rapamycin-treated monocytes induce the polarization of T$_H$1 cells and T$_H$17 cells[96], and rapamycin greatly increases the expression of IL-12p40 and the levels of *IL-23p19* mRNA and IL-23 protein in human macrophages infected with *Mycobacterium tuberculosis*[97]. Therefore these data identify the mTOR pathway as a key regulator of immune homeostasis.

The mTOR pathway has recently been implicated in the regulation of production of type 1 IFNs (IFNα and IFNβ), which are crucial for antiviral immunity, by plasmacytoid DCs[98]. mTOR associates with myeloid differentiation primary-response gene 88 (MyD88), an

adaptor protein that is used by many TLRs, to allow the activation of IFN regulatory factor 5 (IRF5) and IRF7, which are transcription factors for type 1 IFN genes3[99]. Thus, inhibition of mTOR signalling during pDC activation through TLR9 blocks the interaction between TLR9 and MyD88 and the subsequent phosphorylation and nuclear translocation of IRF7, resulting in impaired IFNα and IFNβ production[100]. Decreased IFNα levels in the serum and decreased production of IFNα by pDCs in response to stimulation with CpG DNA or a viral vaccine lead to impaired adaptive CD8$^+$ T cell-mediated immune responses[101].

Taken together, these data suggest that mTOR exerts numerous effects on DC differentiation, maturation and function. It interferes with antigen uptake and might modulate antigen presentation. Its differential effects on cytokine production and chemokine receptor expression regulate interactions between innate and adaptive immune responses[70].

1.4.5. Role of mTOR for mast cells.

Key components of the mTORC1 pathway are phosphorylated following FcεRI aggregation and Kit ligation in mast cells[102]. The mTORC1 pathway appears to contribute to the overall signaling cascade required for Ag- or SCF-induced cytokine production and SCF-mediated chemotaxis and cell survival in mast cells[102]. Kim M.S. et al. show that the mTORC1 complex is a point of divergency for the PI3K-regulated signaling downstream of Fc$_ε$RI and Kit for the selective regulation of specific mast cell functions. The ability of rapamycin to significantly inhibit cytokine production, chemotaxis, and mast cell survival supports a role for mTORC1 pathway in these responses[102].

1.4.6. Role of phosphatidylinositol-3-kinase in mast cells.

Mast cell function critically depends on phosphatidylinositol-3-kinase[103-105]. PI3-kinase is activated following FcεRI stimulation[106]. Mast cell adhesion[107], mast cell degranulation, and the expression and release of certain cytokines[108] are reduced upon PI3-kinase inhibition. Mast cells derived from mice lacking the PI3-kinase p110δ catalytic subunit showed decreased degranulation and cytokine release responses to antigen-IgE stimulation[109]. In addition, mast cell adhesion, mast cell migration and anaphylactic response is impaired in mice lacking PI3-kinase p110δ[110]. Thus, PI3-kinase p110δ plays a critical role in mast cell function.

1.4.7. PDK1 in immune system.

PI3K induces the synthesis of membrane- associated PtdIns (3,4,5)-triphosphate (PIP3), which provides membrane docking sites for pleckstrin homology (PH) domain-containing signaling molecules such as PDK1[102].

Phosphoinositide-dependent protein kinase-1 (PDK1) is a member of the AC kinase family and consists of a kinase domain, a hydrophobic pocket (known as the PDK1-interacting fragment (PIF) pocket) involved in substrate recognition, and a PH domain specific for phosphatidylinositol (3,4,5) triphosphate (PtdIns(3,4,5)P$_3$) and phosphatidylinositol (3,4) biphosphate (PtdIns(3,4)P$_2$)[111]. PDK1 activates its target kinases through the phosphorylation of their T loop. Under basal conditions, PDK1 exists in an active, phosphorylated form. Because this characteristic could result in a noncontrolled activation of the substrates, PDK1 recognizes its targets only when they are phosphorylated at a Ser/Thr residue in a hydrophobic motif. This preactivation step is achieved by stimulation with extracellular agonists[112]. For example, PKB requires, prior to phosphorylation by PDK1, another phosphorylation event by mTOR/rictor together with its binding to PtdIns(3,4,5)P3[113], whereas RSK isoforms need first the phosphorylation by Erk1/2 in order to become then activated by PDK1. In contrast with RSK and PKB, PKC isoforms are constitutive targets of PDK1[112]. Indeed, phosphorylation by PDK1 stabilizes their conformation after synthesis[114]. In the past few years, the crucial role of PDK1 in embryo development[115] as well as in the normal functions of the liver[116] and the heart[117] has been well studied using specific tissue deletion in mice. Recently, several studies have addressed the role of PDK1 in T lymphocytes. Using *in vitro* models, Nirula *et al.[118]* showed that PDK1 was involved in the production of IL-4 by T$_H$2 cells[112].

1.5. Mast and dendritic cells ion channels.

Molecular biology and patch-clamp analyses in recent years have shown that non-excitable cells such as mast and dendritic cells express a variety of ion channels permeable for K$^+$, Cl$^-$, Ca^{2+} or non-selective for cations[119-121].

In dendritic cells downstream targets of the PI3K pathway include ion channels[122].

DCs express voltge-gated outwardly rectifying K$^+$ channels[119]. It was shown that DCs express voltage-gated K$^+$ channels Kv1.3 and Kv1.5[120,122]. Kv channels are upregulated upon

DC maturation as induced by LPS[120,122]. Moreover, Kv channels sustain Ca^{2+} influx through Ca^{2+} release-activated channels (CRAC), which are also expressed in DCs[123], by maintaining the negative membrane potential and providing the necessary electrical driving force in DCs. Accordingly, Kv channel inhibitors impair Ca^{2+}- dependent cytokine production, maturation, and migration of murine DCs[124]. Kv channels in DCs are under tonic inhibition by phosphoinositide-3-kinase[122]. PI3K negatively regulates TLR-mediated proinflammatory cytokine production in DCs and belongs to the gate-keeping system, preventing excessive proinflammatory immune responses[68]. PI3K-dependent inhibition of Kv channels may contribute to the PI3K-mediated DC suppression. That's why it was interesting to check whether kinases downstream from PI3K, such as mTOR, regulate Kv channel activity in DCs.

Mast cell stimulation involves activation of ion channels, such as Ca^{2+}[125], K^{+}[126] and Cl^{-}[127,128] channels. Upon mast cell activation, store-operated and receptor-mediated Ca^{2+} channels allow the entry of Ca^{2+} into the cell, which triggers exocytosis and degranulation[129,130]. The electrical driving force for Ca^{2+} entry is provided by cell membrane potential, which is maintained by the activity of K^{+} channels[131]. Accordingly, cell membrane depolarization decreases Ca^{2+} influx and subsequent degranulation[132]. Ca^{2+}-activated K^{+} channels are critical in this scenario, as pharmacological inhibition of these channels disrupts mast cell degranulation[133]. Most recently it was shown that the Ca^{2+}-activated K^{+} channel in mouse BMMCs is absent in gene targeted mice lacking $K_{Ca}3.1$ channels and that $K_{Ca}3.1$ is a critical regulator of mast cell degranulation[121].

1.5.1. Voltage-gated K^{+} channels Kv1.3 and Kv1.5.

Voltage-gated K^{+} channels consist of two types of protein subunits: α subunits, which contain the ion conducting pore[134], and accessory subunits, which modify the intrinsic properties of the α subunits[135,136]. The α subunits have six full membrane spanning domains (S1–S6) and one loop domain (P) that contributes to the channel pore along with the S5 and S6 domains[137] (Fig. 4). Both the amino and carboxy termini of the α subunits are intracellular. Functional Kv channels consist minimally of four identical (homotetrameric) or closely related (heterotetrameric) α subunits[137]. In addition to the pore-forming domain, other distinct functional domains of the α subunits have been mapped, including a voltage sensor (S4) and a domain involved in tetramerization between α subunits and required for α subunit interaction with accessory Kv β subunits (N-terminus)[138].
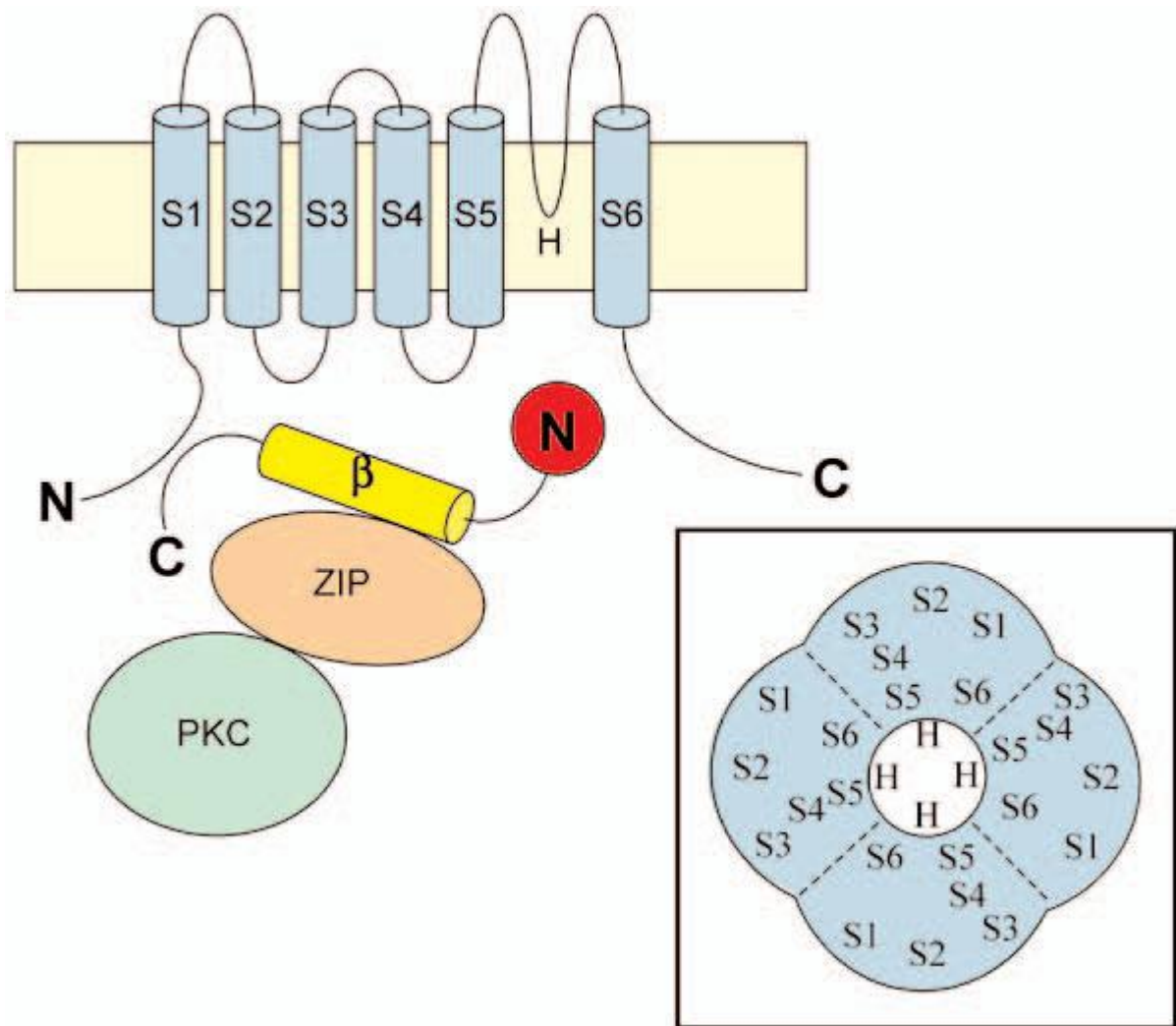
Figure 4. Schematic representation of voltage-gated K+ channel (Kv) structure and some interacting proteins. Kv subunits consist of six transmembrane segments (S1–S6) and a P loop. Both N- and C-terminal regions are intracellular. S5, S6, and P contribute to the pore region, whereas S4 is the voltage-sensing domain. The C-terminal region of Kv β subunits interact with the N-terminal domain of Kv α subunits in a region that governs α-subunit tetramerization. The β subunits can bind to adaptor proteins ZIP1 and ZIP2 that couple Kv channel complexes to protein kinase C (PKC). This complex mediates the effects of PKC activation on some Kv channel complexes. The insert shows schematic the localization of domains in the four subunits that compose the Kv channel complex viewing from outside the channel pore. Taken from Cox R.[137]

Functional Kv1.3 and Kv 1.5 channels are opened by membrane depolarization, with half maximal opening occurring at -40 mV to -35 mV[139]. With cell depolarization, a conformational change moves the voltage sensor in the S4 transmembrane domain and opens the channel pore[140]. There are several potent and relatively selective inhibitors of Kv1.3. These include ShK (K_d 11 pM), a 35-amino acid polypeptide derived from the Caribbean Sea anemone *Stichodactyla helianthus*, and margatoxin (K_d 110 pM), which is derived from the

scorpion *Centruroides margaritatus*[141]. Both bind to the outer mouth of the channel and physically obstruct ion conduction. Once bound, their dissociation is very slow so that their effects may persist for several hours[137]. The specificity of ShK for Kv1.3 is greatly enhanced by the substitution of the critical Lys22 in ShK with diaminopropionic acid (ShK-Dap22)[142] or by attachment of L-phosphotyrosine to the N-terminus (ShK(L5))[143]. These analogues are remarkably stable in cell culture systems and *in vivo*. PAP-1 [5-(4-phenoxybutoxy)psoralen] is the first relatively specific small molecule blocker of Kv1.3 (Kd 2 nM)[144]. A further useful tool for the study of Kv1.3 is a fluorescein-6-carboxylic acid (F6CA)-labelled analogue of ShK[137].

1.5.2. Ca^{2+}-activated K^+ channel $K_{Ca}3.1$.

Ca^{2+}-activated K^+ channels $K_{Ca}3.1$ (also known as $IK_{Ca}1$ or SK4) have a similar topological structure to Kv1.3, but rather than containing a voltage sensor in the S4 domain, they bind calmodulin tightly near the C-terminus, which serves as the Ca^{2+} sensor[145]. $K_{Ca}3.1$ channels are thus opened by a rise in cytosolic free Ca^{2+} $[Ca^{2+}]_i$ due to the Ca^{2+}-calmodulin-mediated cross-linkage of subunits in the channel tetramer[146]. Channel function is reported to be increased by the membrane-associated protein kinase A through phosphorylation of either the channel protein itself or a closely associated accessory protein in oocytes and T84 cells[147]. In $CD4^+$ T cells, $K_{Ca}3.1$ activity is increased by the nucleoside diphosphate kinase B, which phosphorylates $K_{Ca}3.1$ on histidine 358[148]. In contrast, histidine 358 is dephosphorylated by the mammalian protein histidine phosphatase, which directly binds to the $K_{Ca}3.1$ protein and negatively regulates T cell Ca^{2+} flux by decreasing $K_{Ca}3.1$ activity[149]. $K_{Ca}3.1$ modulation in T cells is thus one of the rare examples of histidine phosphorylation/dephosphorylation influencing a biological process in mammals[145].

Some inhibitors of $K_{Ca}3.1$ were used for study functions of this channel. Charybdotoxin is a 37-amino acid peptide isolated from the venom of the scorpion *Leiurus quinquestriatus* and blocks $K_{Ca}3.1$ with a K_d of 5 nM but also blocks the large conductance K^+ channel $K_{Ca}1.1$ (BK_{Ca}) and Kv1.3 with similar potency[141]. Another more potent but less commonly used peptidic $K_{Ca}3.1$ blocker is maurotoxin (K_d 1 nM) from the venom of the Tunisian scorpion *Scorpio maurus* [125]). In contrast to charybdotoxin, maurotoxin does not affect $K_{Ca}1.1$ but instead potently inhibits the voltage-gated Kv1.2 channel (K_d 100 pM). Structural modification of the azole antimycotic clotrimazole (K_d 70–250 nM) has resulted in the generation of the small molecule TRAM-34, which specifically blocks $K_{Ca}3.1$ with a K_d of 20 nM. TRAM-34 blocks $K_{Ca}3.1$ by binding to internal residues below the selectivity filter, in

contrast to charybdotoxin, which binds to the external pore[145,150]. ICA-17043 (K_d 11 nM) is another small molecule blocker with high specificity for $K_{Ca}3.1$[151]. Interestingly, $K_{Ca}3.1$ channels can be activated by a number of benzimidazolones and benzothiazoles, which increase the Ca^{2+} sensitivity of these Ca^{2+}/calmodulin-gated channels[145]. The 'classic' activator 1-ethyl-2-benzimidazolinone activates heterologously expressed $K_{Ca}3.1$ with an EC50 of 30 mM and achieves maximal K^+ currents at 100 mM in the presence of 100 nM free Ca^{2+}, which is below the resting Ca^{2+} of most cell types[152]. A more potent $K_{Ca}3.1$ activator is the recently described benzothiazole SKA-31 [naphtho(1,2-*d*)thiazol-2-ylamine], which activates $K_{Ca}3.1$ with an EC50 of 250 nM[145,153].

1.6. Aim of study.

Dendritic and mast cells functions are regulated by signalling pathways including the phosphatidylinositol-3-kinase - pathway[54,122,154,155]. The PI3 kinase pathway is partially effective in dendritic and mast cells through alteration of their ion channel activity [122,156].

PI3 kinase-dependent signalling includes activation of the phosphoinositide-dependent kinase PDK1[157], which phosphorylates and thus activates the protein kinase B/Akt isoforms [158], the serum- and glucocorticoid-inducible kinase (SGK) isoforms[159], and the protein kinase PKCδ[160,161].

In dendritic cells Kv channels are under tonic inhibition by PI3K[122]. Moreover, PI3K negatively regulates TLR-mediated proinflammatory cytokine production in DCs and belongs to the gate-keeping system, preventing excessive proinflammatory immune responses[66,68]. PI3K-dependent inhibition of Kv channels may contribute to the PI3K-mediated DC suppression.

In mast cells Ca^{2+}-activated K^+ channels are critical to counteract cell membrane depolarization upon Ca^{2+} influx, and thus help to maintain Ca^{2+} influx and subsequent degranulation[132].

Both PI3K on the one hand and ion channels on the other hand are important for the regulation of MC and DC functions. Therefore a question, whether and how PI3K-downstream kinases PDK1 and mTOR regulate ion channels in DCs and MCs, is of huge interest.

The present study has three aims: 1) to elucidate whether Kv channels in dendritic cells are influenced by mTOR and to confirm the findings in the *Xenopus* oocyte expression system; 2) to study whether $K_{Ca}3.1$ channels in mast cells are influenced by mTOR; 3) to define the role of PDK1 in the regulation of mast cell functions and to explore the possible role of PDK1 in the regulation of $K_{Ca}3.1$ channel activity in mast cells.

2. Materials and Methods

2.1 Materials

2.1.1. Tissue culture

2.1.1.1. Equipment

Centrifuge RotiFix 32	Hettich Zentrifugen, Tuttlingen, Germany
Eppendorf pipettes 1000 µl, 100 µl, 10 µl	Eppendorf AG, Hamburg, Germany
Heraeus Incubator	Thermo Electron Corporation, Dreieich, Germany
Neubauer counting chamber	Brand, Wertheim, Germany
Pipetus® pipetting aid	Hirschmann Laborgeräte, Eberstadt, Germany
Syringe BD 10 ml, Luer-Lok™ Tip	Becton Dickinson Labware, Franklin Lakes, USA
Tissue Culture Dishes 60x15 mm	Becton Dickinson Labware, Franklin Lakes, USA
Vortex Genie	Scientific Industries, Bohemia NY, USA
Eppendorf cups 1.5 ml	Eppendorf AG, Hamburg, Germany
Needles BD Microlance™ 3, 0.55x25 mm	Becton Dickinson Labware, Franklin Lakes, USA
PP-Test tubes 15, 50 ml	Greiner bio-one, Frickenhausen, Germany
Stripette® 5, 10, 25 ml	Corning Incorporated, Corning NY, USA

2.1.1.2. Chemicals

Fetal Bovine Serum (FBS)	GIBCO, Carlsbad, Germany
Gentamycin	Sigma-Aldrich, Steinheim, Germany
GMCSF mouse recombinant	Peprotech/Tebu, Cölbe, Germany
L-Glutamine	Invitrogen, Karlsruhe, Germany
MEM Non-Essential Amino Acids	Sigma-Aldrich, Steinheim, Germany
N-Acetyl-D-sphingosine (C2-ceramide)	Invitrogen, Karlsruhe, Germany
Penicillin-Streptomycin	GIBCO, Carlsbad, Germany
Phosphate buffered saline (PBS)	Sigma-Aldrich, Steinheim, Germany
Rapamycin from *Streptomyces tygroscopicus*	GIBCO, Carlsbad, Germany
RPMI 1640	Sigma-Aldrich, Steinheim, Germany

Trypan blue solution 0,4%	Invitrogen, Karlsruhe, Germany
ß-Amyloid	Sigma-Aldrich, Steinheim, Germany
β-mercaptoethanol	Invitrogen, Karlsruhe, Germany

2.1.1.3. Culture medium composition
Complete medium

RPMI-1640

Fetal bovine serum (FBS)	10 %
L-Glutamine	1 %
Non-essential amino acids (NEAA)	1 %
Penicillin/streptomycin (P/S)	1 %
ß-mercaptoethanol	0.05 %

2.1.2. Patch Clamp

2.1.2.1. Technical Equipment

Borosilicate glass filaments	Harvard Apparatus, March-Hugstetten, Germany
DMZ puller	Zeitz, Augsburg, Germany
EPC-9 amplifier	Heka, Lambrecht, Germany
ITC-16 Interface	Instrutech, Port Washington, N.Y., USA
Microscope Axiovert 100	Zeiss, Oberkochen, Germany
MS314 electrical micromanipulator	MW, Märzhäuser, Wetzlar, Germany
pH Meter 646	Carl Zeiss , Oberkochen, Germany
Pulse software	Heka, Lambrecht, Germany

2.1.2.2. Chemicals

Ampuwa	Fresenius KABI, Bad Homburg, Germany
$CaCl_2$ x 2 H_2O	Carl Roth, Karlsruhe, Germany
D-(+)-Glucose	Sigma-Aldrich, Steinheim, Germany
Ethylene glycol tetraacetic acid (EGTA)	Sigma-Aldrich, Steinheim, Germany
HEPES	Sigma-Aldrich, Steinheim, Germany
KCl	Sigma-Aldrich, Steinheim, Germany
KGluconate	Sigma-Aldrich, Steinheim, Germany
KOH	Sigma-Aldrich, Steinheim, Germany
MgATP	Sigma-Aldrich, Steinheim, Germany
$MgCl_2$ x 6 H_2O	Sigma-Aldrich, Steinheim, Germany
NaCl	Sigma-Aldrich, Steinheim, Germany
EGTA	Sigma-Aldrich, Steinheim, Germany
Na_2ATP	Sigma-Aldrich, Steinheim, Germany
NaOH	Sigma-Aldrich, Steinheim, Germany
Antigen DNP-HSA (50ng/ml)	Sigma-Aldrich, Steinheim, Germany
Ca^{2+} ionophore ionomycin	Sigma-Aldrich, Steinheim, Germany

2.1.2.3. Buffer composition
Standard Ringer – bath solution

NaCl	145 mM/l
KCl	5 mM/l
$MgCl_2$ x 6 H_2O	2 mM/l
HEPES	10 mM/l
$CaCl_2$ x 2 H_2O	1 mM/l
Glucose	20 mM/l pH 7.4

2.1.2.4. Pipette solution
K pipette solution for dendritic cells

KCl	80 mM/l
KGluconate	60 mM/l
$MgCl_2$ x 6 H_2O	1 mM/l

MgATP	1 mM/l
EGTA	1 mM/l
HEPES/KOH	10 mM/l

pH = 7.2

Pipete solution for mast cells

KGluconate	120 mM/l
KCl	5 mM/l
$MgCl_2$	1,2 mM/l
EGTA	2 mM/l
HEPES	10 mM/l
$CaCl_2$	1,26 mM/l
MgATP	2 mM/l

pH = 7.2

2.1.3. Immunostaining

2.1.3.1. Technical equipment

FACS Calibur	Becton Dickinson, Heidelberg, Germany
FACS tubes, 1.3 ml, PP, round bottom	Greiner bio-one, Frickenhausen, Germany

2.1.3.2. Antibodies and chemicals

Annexin-V-Fluos	Roche Diagnostics, Penzberg, Germany
FITC-conjugated anti-mouse CD11c, clone HL3 (Armenian Hamster IgG_1, λ2)	BD Pharmingen, Heidelberg, Germany
FITC-conjugated dextran	Sigma-Aldrich, Steinheim, Germany
PE- conjugated anti mouse ICAM-1 (CD-54), clone 3E2 (Armenian Hamster IgG1, κ)	BD Pharmingen, Heidelberg, Germany
PE-conjugated anti-mouse CD86, clone GL1 (Rat IgG_{2a}, κ)	BD Pharmingen, Heidelberg, Germany

PE-conjugated rat anti-mouse I-A/I-E, clone M5/114.15.2 (IgG2b, κ)	BD Pharmingen, Heidelberg, Germany
Sodium azide	Sigma-Aldrich, Steinheim, Germany

2.1.3.3. Buffers
FACS buffer

PBS

0.1 % heat-inactivated FBS

2.1.4. Voltage Clamp

2.1.4.1. Technical Equipment
8-channel-multi-pipette Research pro	Eppendorf, Hamburg, Germany
Borosilicate glass filaments	Harvard Apparatus, March-Hugstetten, Germany
DMZ puller	Zeitz, Augsburg, Germany
Gene clamp 500 amplifier	Axon Instruments, Foster City, CA, USA
KL1500 LCD	Carl Zeiss MicroImaging, Oberkochen, Germany
Microscope Stemi 200	Carl Zeiss MicroImaging, Oberkochen, Germany
pH Meter 646	Carl Zeiss , Oberkochen, Germany

2.1.4.2. Chemicals
$CaCl_2$ x 2 H_2O	Carl Roth, Karlsruhe, Germany
HEPES	Sigma-Aldrich, Steinheim, Germany
KCl	Sigma-Aldrich, Steinheim, Germany
$MgCl_2$ x 6 H_2O	Sigma-Aldrich, Steinheim, Germany
NaCl	Sigma-Aldrich, Steinheim, Germany
Sodium pyruvate	Sigma-Aldrich, Steinheim, Germany
Tetracycline	Sigma-Aldrich, Steinheim, Germany
Theophylline	Sigma-Aldrich, Steinheim, Germany
Gentamycin	Sigma-Aldrich, Steinheim, Germany

2.1.4.3. Buffers composition

ND-96 – bath solution

NaCl	96 mM/l
KCl	2 mM/l
$MgCl_2$ x 6 H_2O	1 mM/l
HEPES	5 mM/l
$CaCl_2$ x 2 H_2O	1,8 mM/l
NaOH pH 7.4	

ND-96 – storage solution

NaCl	96 mM/l
KCl	2 mM/l
$MgCl_2$ x 6 H_2O	1 mM/l
HEPES	5 mM/l
$CaCl2$ x 2 H2O	1,8 mM/l
C3H3NaO3	5mM/l
Theophylline	5 mM/l
Gentamycin	50 μg/ml
Staurosporine	50 μg/ml
pH 7.4	

OR-2

NaCl	82,5 mM/l
KCl	2 mM/l
$MgCl_2$ x 6 H_2O	1 mM/l
HEPES	5 mM/l
pH 7.4	

OR-2 with collagenase

NaCl	82,5 mM/l

KCl	2 mM/l
$MgCl_2$ x 6 H_2O	1 mM/l
HEPES	5 mM/l
Collagenase	2mg/ml
pH 7.4	

2.1.4.4. Pipette solution

KCl	3M/l

2.1.5. Preparation of cRNA

2.1.5.1 Technical equipment

Eppindorf Biophotometer	Eppendorf, Hamburg, Germany
Eppindorf Concentrator	Eppendorf, Hamburg, Germany

2.1.5.2 Chemicals

Sodium acetate	Sigma-Aldrich, Steinheim, Germany

2.1.6. Intracellular Calcium Imaging

2.1.6.1. Technical equipment

Camera Proxitronic	Proxitronic, Bensheim, Germany
Centrifuge RotiFix 32	Hettich Zentrifugen, Tuttlingen, Germany
Discofix® Stopcock for Infusion Therapy	B. Braun, Melsungen, Germany
Filter Set for Fura-2	AHF Analysentechnik AG, Tübingen, Germany
Filter tips 10, 100, 1000µl	Biozym Scientific, Hess. Oldendorf, Germany
Filter wheel	Sutter Instrument Company, Novato, USA

Infusion Regulator Dosi-Flow 10	Dahlhausen, Köln/Sürth, Germany
Lambda 10-2	Sutter Instrument Company, Novato, USA
Lamp XBO 75	Leistungselektronik Jena GmbH, Jena, Germany
Metafluor software	Universal Imaging, Downingtown, USA
Microscope Axiovert 100	Zeiss, Oberkochen, Germany
Microscope cover glasses round, 30mm diameter, 0.13-0.16 mm	Karl Hecht KG, Sondheim, Germany
Neutral densitiy filters 10, 20, 40, 60%	AHF Analysentechnik AG, Tübingen, Germany
Objective fluar 40x/1.3 oil	Carl Zeiss, Oberkochen, Germany
Syringe BD 10 ml, Luer-Lok™ Tip	Becton Dickinson Labware, Franklin Lakes, USA
Syringe BD Perfusion™ 50 ml	Becton Dickinson Labware, Franklin Lakes, USA
Tissue Culture Dishes 35x10 mm	Becton Dickinson Labware, Franklin Lakes, USA
Winged Needle Infusion Set Butterfly®-21	Hospira Venisystems, Donegal Town, Ireland

2.1.6.2. Chemicals

Ampuwa	Fresenius KABI, Bad Homburg, Germany
$CaCl_2$ x 2 H_2O	Carl Roth, Karlsruhe, Germany
Ethylene glycol tetraacetic acid (EGTA)	Sigma, Taufkirchen, Germany
Fura-2 AM	Molecular probes, Goettingen, Germany
Glucose	Carl Roth, Karlsruhe, Germany
HEPES	Sigma, Taufkirchen, Germany
Immersol 518F	Carl Zeiss, Göttingen, Germany
Ionomycin	Sigma, Taufkirchen, Germany
KCl	Carl Roth, Karlsruhe, Germany
$MgCl_2$ x 6 H_2O	Sigma, Taufkirchen, Germany
$MgSO_4$ x 7 H_2O	Sigma, Taufkirchen, Germany
Na_2HPO_4 x 2 H_2O	Sigma, Taufkirchen, Germany
NaCl	Sigma, Taufkirchen, Germany
N-methyl-D-glucamine (NMDG)	Sigma, Steinheim, Germany
Poly-L-Lysine	Sigma, Taufkirchen, Germany
Silicone grease	Carl Roth, Karlsruhe, Germany
Thapsigargin	Molecular Probes, Leiden, The Netherlands

2.1.6.3. Buffer composition
Standard Ringer

NaCl	125 mM/l
KCl	5 mM/l
$MgSO_4$ x 7 H_2O	1.2 mM/l
HEPES	32.2 mM/l
Na_2HPO_4 x 2 H_2O	2 mM/l
Glucose	5 mM/l
$CaCl_2$ x 2 H_2O	2 mM/l
pH 7.4	

Ca^{2+}-free Ringer

NaCl	125 mM/l
KCl	5 mM/l
$MgSO_4$ x 7 H_2O	1.2 mM/l
HEPES	32.2 mM/l
Na_2HPO_4 x 2 H_2O	2 mM/l
Glucose	5 mM/l
EGTA	0.5 mM/l
pH 7.4	

2.1.7. Degranulation assay (ß-hexosaminidase release) and histamine release.

2.1.7.1. Technical equipment

Magellan™ software	Tecan Group Ltd., Männedorf, Switzerland
multi well plates; 24, 96 well	Corning Inc., Corning NY, USA
Sunrise™ Microplate Reader	Tecan Trading AG, Switzerland

2.1.7.2. Chemicals and Kits

Anti-DNP IgE antibody	Sigma-Aldrich, Steinheim, Germany
Tyroide's salt	Sigma-Aldrich, Steinheim, Germany
DNP-HSA	Sigma-Aldrich, Steinheim, Germany
p-nitrophenyl N-acetyl-ß-D-glucosaminide	Sigma-Aldrich, Munich, Germany
Triton X-100	Sigma-Aldrich, Steinheim, Germany
Ampuwa	Fresenius KABI, Bad Homburg, Germany
Histamine ELISA kit	IBL Int, GmbH, Hamburg, Germany

2.1.7.3. Buffers.

Citrate buffer   0,2 M pH = 4,5
TRIS buffer   1M   pH = 9,0

2.1.8. Immunoblotting

2.1.8.1. Technical equipment

Agarose gel electrophoresis chamber	BioRad, München, Germany
Centrifuge 5415R	Eppendorf, Hamburg, Germany
Densitometer Quantity One	BioRad, München, Germany
Gel tips	Alpha Laboratories, Hampshire, UK
Kodak film	Sigma, Hannover, Germany

2.1.8.2. Chemicals

ß-mercaptoethanol	Sigma, Taufkirchen, Germany
Acrylamide/bisacrylamide	Carl Roth, Karlsruhe, Germany
BenchMark prestained protein ladder	Invitrogen, California, USA
Detection reagent	GE Healthcare, München, Germany
Glycine	Sigma, Taufkirchen, Germany
Loading buffer (4x)	Carl Roth, Karlsruhe, Germany
Milk powder	Carl Roth, Karlsruhe, Germany
Nitrocellulose membrane	VWR, Darmstadt, Germany

Phenyl-methanesulfonyl fluoride solution	Sigma, Taufkirchen, Germany
Ponceau S	Sigma, Taufkirchen, Germany
Protease inhibitor	Sigma, Taufkirchen, Germany
Sodium dodecyl sulfate (SDS)	Sigma, Hannover, Germany
TEMED	Carl Roth, Karlsruhe, Germany
Triethanolamine-buffered saline (TBS)	Sigma, Taufkirchen, Germany
Tween-20	Böhringer Ingelheim, Mannheim, Germany

2.1.8.3. Antibodies and Kits

Enhanced chemiluminescence (ECL) Kit	Amersham, Freiburg, Germany
Rabbit polyclonal phospho (p) NDRG1 (Thr^{346})	Cell Signaling, Germany
Rabbit polyclonal p-PKCδ (Thr^{505})	Cell Signaling, Germany
Rabbit polyclonal PKCδ	Cell Signaling, Germany
Rabbit monoclonal GAPDH	Cell Signaling, Germany

2.1.8.4. Buffers

Lysis buffer

Tris	50mM
NaCl	150mM
Triton-X	1%
Nadeoxycholat	0,5%

Running buffer

Tris	25 mM/l
Glycine	250 mM/l
SDS	0,1 %

Transfer buffer

Tris	25 mM/l
Glycine	192 mM/l

Methanol   20 %   pH 8.3

Wash buffer (PBS-T)
1x PBS
Tween-20   0.05 %

2.1.9 Animals.

2.1.9.1 Mice.

Generation and basic properties of PDK1 hypomorphic mice were described previously[115]. Genotyping was made by PCR on tail DNA using PDK1 and neo-R-specific primers as described[115]. Mice had free access to standard mouse diet (Altromin, Lage, Germany) and tap water. For the the part of mTOR study were used wild type mice with background C57/BL6

2.1.9.2 Xenopus laevis.

Female Xenopus laevis frogs were maintained at the animal facility of the Physiological Institute, University of Tübingen. Frogs were kept humanely in accordance with the German law for the welfare of animals and were approved by local authorities.

All animal experiments were conducted according to the guidelines of the American Physiological Society as well as the German law for the welfare of animals and were approved by local authorities

2.2. Methods

2.2.1. Cell culture

Dendritic cells were cultured from mouse bone marrow following an established protocol[16] with slight modifications. The cells were isolated from femur and tibias of 7-11 weeks old wild type mice. After removing skin and muscle mass from the bone, the bone marrow-derived cells were flushed out off the bone marrow cavity from the femur and tibia with sterile, icecold PBS using a small needle fixed on a syringe. The extracted cells were centrifuged at 1500 rpm for 5 min at 4°C. The supernatant was discharged and the cells were resuspended in complete cell culture medium and centrifuged. Subsequently, the DCs were resuspended again and counted using a Neubauer counting chamber. Cells were seeded out into 60x15 mm petri dishes at a density of 2×10^6 cells per dish. Finally, GM-CSF (35 ng/mL) was added to the culture media.

The cells were cultured for 1 week with changes of the medium on days 3 and 6. For the first medium change, fresh medium as well as GM-CSF was added to the culture. On day 6, nonadherent and loosely attached cells were harvested and the removed volume of the culture medium was replaced by fresh medium and GM-CSF. At day 7, the cells were seeded out into several petri dishes in an amount of 5×10^5 cells per dish. For cell treatment, the substances of interest were added to the respective dishes for a certain time period indicated in the respective experiments. Experiments were performed on mature DCs and carried out on days 7-9. The expression of CD11c and maturation markers was monitored by FACS analysis.

Femoral bone marrow derived mast cells (BMMC) from 6-8 week-old $pdk1^{+/+}$ and $pdk1^{hm}$ naive mice were cultured for 4 weeks in RPMI 1640 (GIBCO, Carlsbad) containing 10% fetal calf serum, 1% penicillin/streptomycin, 20 ng/ml interleukin-3 (RD systems, Wiesbaden-Nordenstadt, Germany), and 100 ng/ml of the c-kit ligand stem cell factor (SCF, Peprotech, Tebu-bio, Rocky Hill, NJ, USA). BMMC maturation was confirmed by flow cytometry (FACS Calibur, Becton Dickinson) using the following specific fluorescent-labelled antibodies: Phycoerythrin-labelled anti-FcεRI (eBioscience GmbH, Frankfurt, Germany), allophycocyanin-labelled anti-CD117 (BD Pharmingen, Heidelberg, Germany) and fluorescein-isothiocyanate-labelled anti-CD34 (BD Pharmingen). For experiments BMMCs were sensitized for 1 h with monoclonal mouse anti-dinitrophenyl mouse IgE (anti-DNP IgE, 10 μg/ml per 1 x 106 cells, clone SPE-7, Sigma-Aldrich, Munich, Germany) in culture

medium and then challenged acutely with dinitrophenyl-human serum albumin (DNP-HSA, 50 ng/ml, Sigma-Aldrich).

2.2.2. Immunostaining and flow cytometry

Maturation of the DCs was confirmed by flow cytometry using a FACS Calibur. Measurements were carried out on day 7 of DC culture as well as after time periods the indicated in the particular experiments. Cells (4×10^5) were incubated in 100 µl FACS buffer containing fluorochrome-conjugated antibodies at a concentration of 10 µg/ml. DCs were stained for their surface markers CD11c, CD86, CD54 (ICAM-1), and MHCII (I-A/I-E). The amount of apoptotic cells was verified by estimating the amount of Annexin-V binding. After incubating with the respective antibodies for 60 minutes at 4^0C, the cells were washed twice and resuspended in FACS buffer for flow cytometry analysis. A total of 2×10^4 cells were analyzed for each experiment.

2.2.3. Intracellular Calcium Imaging

The measurements of intracellular calcium concentration $[Ca^{2+}]_i$ were performed using an inverted phase-contrast microscope connected to the following accessories: a camera, a light source, a filter wheel with different excitation filters, a shutter element, a perfusion system inserted into a measuring chamber, a water bath, and a pump to allow a continous exchange and removal of the added bath solutions.The cells were continously superfused during each experiment. Experiments were performed at 37°C in Ringer solution.

Cells were incubated with 2 µM Fura-2/AM for 30 minutes at 37°C. The chamber was then mounted onto the microscope and both inlet and outlet equipment for exchanging the bath solution were fixed to the chamber cavity. To generate a Fura-2 fluorescence ratio, cells were excited alternatively at 340 and 380 nm and the light was deflected by a dichroic mirror into either the camera or the objective. For the latter, an oil-immersion objective suitable for fluorescence microscopy was used. When the light was deflected into the camera, the emitted fluorescence intensity was recorded at 505 nm and data acquisition was performed every 6-10 seconds by using Metafluor computer software. For data analysis, the obtained data were converted to Excel for further evaluation. As a measure for the increase of cytosolic Ca^{2+} activity, the slope and peak of the changes in the 340/380 nm ratio in response to changing the

measurement conditions were calculated for each cell and experiment. Though, the deviation between the lowest and the highest point of the increase in $[Ca^{2+}]_i$ reflected the peak, whereas the ratio change per time represented the slope of the reaction. For intracellular calibration purposes, 10 μM ionomycin was applied at the end of each experiment. Adding of ionomycin to the Ca^{2+}-containing Ringer solution yielded a maximum value Rmax at saturating free Ca^{2+} levels. Administration of ionomycin in Ca^{2+}-free Ringer solution yielded a minimum value Rmin at zero free Ca^{2+} levels.

2.2.4. Patch clamp

Patch clamp experiments were performed at room temperature in voltage-clamp, fast-whole-cell mode according to Hamill et al[162]. The cells were continuously superfused through a flow system inserted into the dish. The bath was grounded via a bridge filled with NaCl Ringer solution. Borosilicate glass pipettes, manufactured by a microprocessor-driven DMZ puller, were used in combination with a MS314 electrical micromanipulator. The currents were recorded by an EPC-9 amplifier using Pulse software and an ITC-16 Interface.

For voltage-gated potassium channels (Kv channels) whole-cell currents were elicited by 200 msec square wave voltage pulses from -90 to +90 mV in 20 mV steps delivered at 20 ms intervals from a holding potential of -70 mV. The currents were recorded with an acquisition frequency of 10 kHz and 3 kHz low-pass filtered.

The composition of the bath solution differed depending on Kv currents were measured. The patch clamp pipettes were filled with an internal solution, which composition differed between K_v current (KCl/K^+-gluconate pipette solution).

For Ca^{2+}-activated K^+ channel ($K_{Ca}3.1$) Whole-cell currents were determined as 10 successive 400-ms square pulses from the -35 mV holding potential to potentials between -115 mV and +65 mV. The currents were recorded with an acquisition frequency of 10 kHz and 3 kHz low-pass filtered.

The patch clamp pipettes were filled with a correspondent internal solution (see 2.1.2.4. Pipette solution). Where indicated the antigen DNP-HSA (50 ng/ml, Sigma-Aldrich) or the Ca^{2+} ionophore ionomycin (1 μM, Sigma-Aldrich) were added to the bath solution.

The offset potentials between both electrodes were zeroed before sealing, and the potentials were corrected for liquid junction potentials as estimated according to Barry &

Lynch[163]. The original whole-cell current traces are depicted without further filtering and currents of the individual voltage square pulses are superimposed. The applied voltages refer to the cytoplasmic face of the membrane with respect to the extracellular space. The inward currents, defined as flow of positive charge from the extracellular to the cytoplasmic membrane face, are negative currents and depicted as downward deflections of the original current traces.

2.2.5. Degranulation assay (ß-hexosaminidase release) and histamine release

Mature bone marrow-derived mast cells (0.3 x 106 per well) were seeded in a 96-well plate in fresh medium with 10 µg/ml anti-DNP IgE antibody for 1 h. Afterwards cells were washed in Tyrode's salts and challenged with DNP-HSA (50 ng/ml) for 15 min at 37°C. 20 µl supernatant and 20 µl of 2 mM p-nitrophenyl Nacetyl-β-D-glucosaminide diluted in 0.2 M citrate buffer, pH 4.5, were mixed and incubated for 2 hours at 37°C. The reaction was terminated by the addition of 60 µl 1M TRIS buffer, pH 9.0, and the absorbance was measured at 405 nm in an ELISA microplate reader.

The data are evaluated as the percent of the total release (0.1 % Triton X-100) corrected for spontaneous release.

Histamine release from mast cells was measured by ELISA according to the instructions of the manufacturer (IBLHamburg GmbH, Hamburg, Germany).

2.2.6. Immunoblotting

Mast cells were seeded in a 6-well plate in fresh medium with 10 µg/ml anti-DNP IgE antibody for 1 h. Afterwards cells were washed in PBS and challenged with DNP-HSA (50 ng/ml) for 5 min at 37°C. Then the cells were washed twice in PBS, then solubilized in lysis buffer containing protease inhibitor cocktail, 0.4% β-mercaptoethanol and phenylmethanesulfonyl fluoride solution. Samples were stored at -80°C until use for western blotting. Cell lysates were separated by 10% SDS-PAGE and blotted on nitrocellulose membranes. The blots were blocked with 5% nonfat-milk in triethanolamine-buffered saline (TBS) and 0.1% Tween-20. Then the blots were probed overnight with one of the following rabbit polyclonal antibodies: phospho (p) NDRG1 (Thr346), p-PKCδ (Thr505), PKCδ or rabbit monoclonal GAPDH (Cell Signaling, Germany). p-PKCδ was diluted 1:500, all other antibodies were diluted 1:1000 in TBS with 5% BSA 0.1% Tween-20, washed 3 times for 15 min/wash, probed with secondary antibodies (anti-rabbit, Cell Signaling) diluted 1:5000 for 1

h at room temperature, and washed 3 times for 15 min/wash. Antibody binding was detected with the Western blotting detection reagents (Amersham ECL Western Blotting Detection Reagents, GE Healthcare, UK). Densitometer scans of the blots were performed using Quantity One.

2.2.7. Preparation of cRNA

Mutant DNAs including Kv1.3, Kv1.5, mTOR were used as a template to synthesize cRNA. Also, using the same method, cRNAs of Kv1.3, Kv1.5, mTOR were synthesized. The RNA synthesis protocol possesses two steps:

1. Linearization of the plasmid DNA containing the sequence of interest;
2. Generation of cRNA itself.

2.2.7.1 Plasmid DNA linearization

Endonucleases were used to obtain a cut at 3' end of the insert. Specific restriction enzymes as shown in table 1 were used to linearize specific plasmids.

Table 1. Plasmids containing the desired genes encoding for specific proteins and restriction endonuclease enzymes used to linearize each plasmid.

Protein	Plasmid	Restriction Endonuclease
Kv1.3	pSpG4T	EcoRI
Kv1.5	pbluescript	BamHI
mTOR	pGHγ	NotI

The reaction mixture as presented in the table below (table 2) was prepared and incubated for 2 hours at 37ºC. Afterwards DNA was precipitated with 1 volume of isopropanol (50 μl) and 1/10 volume (5 μl) of 3 M sodium acetate, at a pH of 5.2, and incubated for 10 minutes at room temperature. The reaction mixture was centrifuged at 17,000 rpm for 15 minutes at 4ºC. After removal of the supernatant, the pellet was washed twice with 70 % ethanol (100 μl) at 17,000 rpm for 10 minutes. Ethanol was removed from the last wash and the pellet was dried using the Eppendorf Concentrator (Eppendorf, Hamburg, Germany) at 35-45º C for 5 minutes.

Table 2. Reaction mixture used to linearize DNA plasmid.

Reaction mixture	Quantity
10X Buffer	5 µl
Plasmid DNA (10 µg)	20 µl
Restriction enzymed (20U)	2 µl
Water	23 µl

2.2.7.2. cRNA synthesis

The linearized DNA produced by the method mentioned above was used as a template to generate cRNA. The reaction mixture listed below (table 3) was put in a sterile eppendorf tube.

Table 3. Reaction mixture used to synthesise RNA from the linearized DNA.

Reaction mixture	Quantity
Linearized DNA (1 µg)	10 µl
10 X Buffer	2.5 µl
rNTPs	1 µl
Cap analogue	2.5 µl
RNase inhibitor	1 µl
Water	8 µl

The reaction mixture was gently spanned and the appropriate RNA polymerase (Table 4) was added and pulse spanned again. RNA polymerase T7 were used, and the mixture was then incubated at 37ºC for 1 hour. 1 µl of DNAse was added in the reaction mixture afterwards to remove the possible DNA contamination. Finally the reaction mixture was incubated at 37ºC for 15 min by shaking.

Table 4. RNA polymerases used to prepare cRNA and amount of cRNA injected into oocytes.

Protein	RNA Polymerase	cRNA (ng/oocyte)	Exp. time (days)
Kv1.3	T7	1	4
Kv1.5	T7	1	4
mTOR	T7	15	5

To purify the generated RNA, 125 μl of phenolchloroform mixture was mixed with 100 μl DEPC water and centrifuged at a maximum speed for 2 minutes. After that the upper inorganic phase was carefully taken into a new eppendorf tube, 12.5 μl of 3 M sodium acetate (pH 5.2) was added, as well as, 375 μl of ethanol (100% concentration) then mixed by pulse vortex and further incubated at -70 ºC overnight.

After incubation, the mixture was centrifuged at 17000 rpm for 15 minutes at 4º C. The supernatant was removed and the pellet was washed twice with 200 μl of 70% ethanol. Finally the pellet was left to dry at room temperature and reconstituted in 25 μl of DEPC water and vortexed. Then cRNA concentration was measured by taking 1 μl of cRNA in 69 μl water using an Eppendorf Biophotometer (Hamburg, Germany). Finally, to confirm quality of generated cRNA its quality was checked by gel electrophoresis.

2.2.8. Xenopus laevis oocyte preparation and maintenance

To study function and plasma membrane abundance of transporters Xenopus laevis oocytes were used. Prior to operation the frogs were anaesthetized by submersion in a 0.1% 3-aminobenzoic acid ethyl ester solution (Sigma, St. Louis, Mo, USA) and placed on ice for surgery. Through a small abdominal incision (1-2 cm in length) small pieces of ovary were removed carefully and the wound was subsequently closed with a reabsorbable suture. To prevent drowning, frogs were kept wet but not under water until reflexes were fully recovered. The ovarian sacs were manually separated and oocytes enzymatically defolliculated and thus singularized by treatment of ovarian lobes with a Ca^{2+}-free OR2-collagenase solution (OR2 supplemented with 1-2mg/ml collagenase (Worthington Biochemical Corp., NJ, USA)) for about 2 h at room temperature (at app. 22°C), then slightly shaken in the flask to ensure even digestion. To remove all degraded elements obtained at this point, the oocytes were washed in a Ca^{2+}-free OR2- solution. To stop defolliculation, oocytes were repeatedly washed with ND96 solution (96 mM NaCl, 2 mM KCl, 1.8 mM $CaCl_2$, 1 mM $MgCl_2$, and 5 mM HEPES, pH 7.4) and singularized oocytes were stored in a ND-96 storage

solution (complemented after sterilization with 5 mM Sodium pyruvate, 50 μg/ml gentamycin and staurosporine (to prevent infections) and 0.5 mM theophylline (inhibits the further maturation)). Large oocytes (stage V-VI) showing evenly colored poles and a sharp border between both poles were selected and microinjected with an appropriate amount of cRNA using a nanoliterinjector 2000 (World Precision Instruments, Berlin, Germany) with glass capillaries (WPI, Sarasota, FL, USA) mounted in a micromanipulator controlled by nanoliterinjector 2000. During injection permanent care was taken to avoid contamination of cRNA with RNases (by cleaning the space around, as well as, by using sterile pipettes, gloves, and DEPC water for dilution of cRNA) or small particles which could clog the injection capillaries. A glass capillary tip was manually broken under the microscope to provide an orifice with a diameter of about 10-20 μm and in order to seal the pipette from air it was backfilled with paraffin oil. Then cRNA was loaded into the capillary (usually ~ 2 μl) by suction and oocytes were placed into a 35 mm petri dish with a polypropylene mesh glued to the bottom to fix the oocytes. A certain amount of cRNA was injected in each oocyte (see Table 4). After injection, oocytes were kept in petri dishes containing app. 3 ml ND 96 storage solution in an incubator at about 15° C. Oocytes were also separated to each others. Daily, dead and damaged oocytes were removed and the sterile ND-96 storage solution which had been exchanged using a sterile pipette. Under these conditions oocytes were kept stored as long as 3-5 days after injection until the cRNA was expressed.

2.2.9. Protein expression in Xenopus laevis oocyte

Oocytes were injected with cRNA of mTOR, Kv 1.3, Kv1.5.

After expression time as detailed in Table 4, studies on the activity of the transporters, tracer uptake measurements were carried out.

2.2.10. Two-electrode-voltage clamp

Two-electrode voltage clamp (TEVC) technique is the most widely used electrophysiological technique for the measurement of whole cell currents through ion channels or electrogenic transporters expressed in Xenopus oocytes by allowing the scientists to control the membrane potential (clamping) and thus measuring currents flowing through

ion channels, electrogenic transporters or pumps. Two glass microelectrodes are impaled into the oocyte (just under the cell membrane), a membrane potential recording electrode and a current-delivering electrode. The membrane voltage electrode connects to a feedback amplifier where the signal is compared to the voltage clamp command given by a generator. The highly amplified difference of these signals is applied as a current through the current-delivering electrode, across the membrane, and to the bath-grounding electrode. All electrogenic fluxes across the membrane are now measured as a deflection from the baseline current. The ground electrodes were made of 3 % Agar and 3 M KCl, whereas the microelectrodes were backfilled with 3 M KCl. With a Faraday cage the whole setup was carefully grounded and shielded against external currents. To reduce vibrations, which may otherwise damage the membrane around the site of electrode impalement, the whole setup is mounted on a pneumatic anti-vibration table[164-166].

For the experiments glass capillaries were used with a thin filament (silver chloride coating on the Ag/AgCl2 electrode) inserted into that glass capillary. Electrodes were backfilled with 3 M KCl and connected to the feedback amplifier. The electrode resistance varies between 0.3 MΩ (Mohms) and 3 MΩ. The flow rate of the superfusion was 20 ml/min and, in theory, a complete exchange of the bath solution was reached within about 10 s. However, due to unstirred layers the full exchange of fluid around the oocyte may be slower. [167-169].

The electrode offset, in the bath solution just before impaling the oocyte, was set to 0 mV. Using micromanipulators (Leitz, Wetzlar, Germany), under a low magnification stereomicroscope (5-20X), in the presence of light within the oocyte was impaled with the microelectrodes at opposite poles. After impalement of both electrodes the amplifier was turned to the voltage clamping mode at the voltage-clamp feedback gain 1. Currents were filtered at 10 Hz. Currents were measured with a Geneclamp 500 amplifier (Axon Instruments, Foster City, CA, USA) and recorded with a MacLab D/A converter (AD Instruments, Castle Hill, Australia) on a computer for data storage and subsequent analysis using chart or scope software. Electrogenic transporters were measured at a fixed holding potential and varying application of different concentrations of substrate[164,165,170,170].

2.2.11. Statistics

Data are provided as means ± SEM, n represents the number of independent experiments. All data were tested for significance using Student's unpaired two-tailed t-test or ANOVA. $P<0.05$ was considered to indicate statistical significance.

3. Results

3.1. Dendritic cells.

3.1.1. Effect of rapamycine on voltage-gated K+ channel activity in cultured dendritic cells.

Ion channel activity in mouse bone marrow-derived dendritic cells (DCs) was analyzed utilizing whole cell patch-clamp experiments. As shown in Fig. 5, DCs express Kv channels. They presumably belong to Kv1.3 and Kv1.5 families[122,124]. As illustrated in Fig. 5, the Kv currents in wild type DCs (background C57/BL6) were down-regulated by 12 hours preatreament of the cells with 100nM rapamycine (Rapa). The mean peak density was decreased from 64,455 ± 13,13, pA/pF (+100 mV; n= 9) in untreated cells to 10,664 ± 1,323, pA/pF (+100 mV; n= 8) following a 12 hours pretreatment with Rapa.
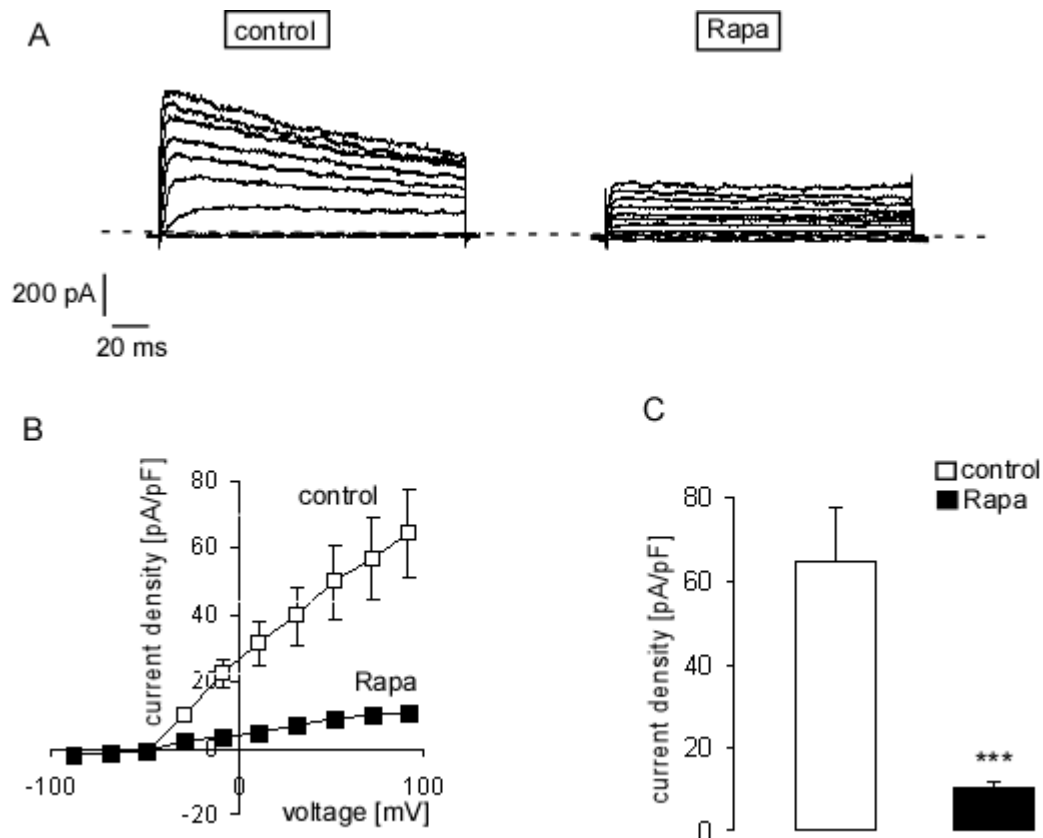
Figure 5. Effect of rapamycin (Rapa) on voltage-gated K$^+$ (Kv) channel currents in cultured bone marrow-derived mouse dendritic cells (DCs). *A*: representative tracings illustrating whole cell Kv currents in bone marrow-derived DCs cultured under control conditions (control) and following overnight treatment of the cells with 100 nM rapamycin. The currents were recorded from the cells with similar capacitance elicited by 200-ms depolarizing pulses ranging from -90 to +90 mV in 20-mV and 20-s increments from a holding potential of -80 mV. *B*: mean current-voltage (*I-V*) relationships (SE, *n* =8–9) of peak Kv current density in DCs without (□) and with (■) prior overnight treatment with 100 nM rapamycin. *C*: Kv current density (current amplitude normalized to cell capacitance) at +90 mV in control and Rapa-treated (100 nM, 12 h) cells. *** (P<0.001) two-tailed unpaired Student's *t*-test.

Pretreatment of the cells with rapamycin was followed by a gradual decline of Kv channel currents: the mean peak current density at +90 mV after 1 hour, 3 hours, 6 hours and 12 hours incubation with Rapa was (in pA/pF): 29,505 ± 4,026 (n= 9), 29,565 ± 11,6 (n= 6), 19,336 ± 5,796 (n=6) and 10,664 ± 1,323 (n= 8), respectively. The dose-response dependence revealed

that 50 nM and 100 nM Rapa led to statistically significant decline of Kv current density (mean peak density at +90 mV in DCs after 12 hours incubation with 10 nM, 50 nM and 100 nM Rapa was (in pA/pF): 45,21 ± 7,03 (n= 14), 18,202 ± 3,295, (n= 9) and 10,664 ± 1,323 (n= 8), respectively (Fig. 6).
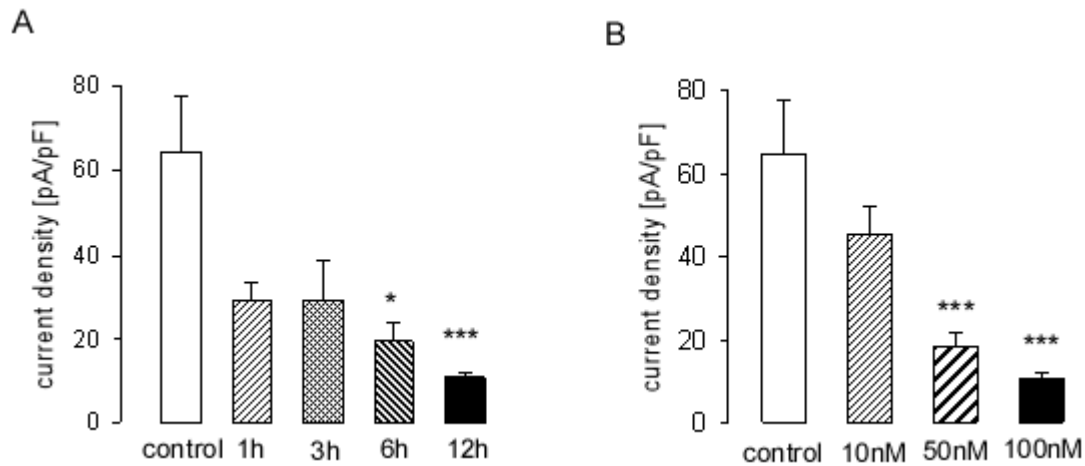
Figure 6. Time and concentration dependence of rapamycine effect on Kv channels. *A*: time dependence of rapamycin effect on Kv current density at +90 mV (means ±SE, *n* =6–9) in DCs without (open bar, control) and with (closed bars) pretreatment with 100 nM rapamycin for the indicated time points (in hours). *P < 0.05, ***P < 0.001, significant difference from control (ANOVA). *B*: dose dependence of rapamycin effect on Kv current density at +90 mV (means ±SE, *n* =8–14) in DCs without (open bar, control) and with 12-h pretreatment (closed bars) with rapamycin at indicated concentration (in nM). ***P < 0.001, significant difference from control (ANOVA).

The rising phase of activating channel currents was analyzed by single exponential fitting. Activation time constants were not different between control and rapamycin-treated DCs (Fig. 7*A*). Fitting the current decay after activation at depolarizing potentials to a single exponential function demonstrated a significant difference at + 70 mV (Fig. 7*B*). Pretreatment with rapamycin resulted in a smaller inactivation time constant, suggesting that rapamycin causes faster Kv channel inactivation.
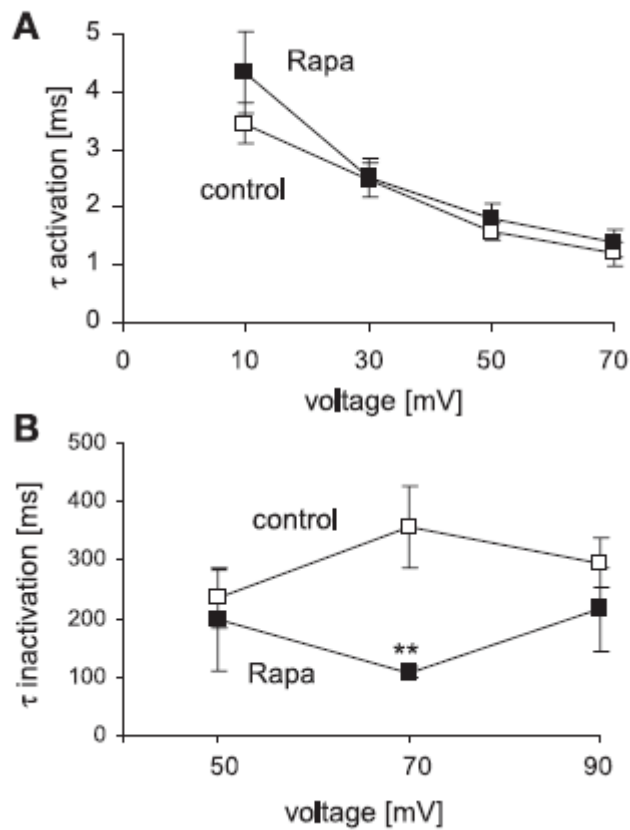
Figure 7. Rapamycin affects onset of inactivation, but not activation, of Kv currents in DCs. *A*: activation time constants (activation) was determined by fitting single exponential functions to the rising phase of currents at voltages from +10 to +70 mV of control cells (*n* =8) and cells pretreated with rapamycin (100 nM, overnight, *n*=9). *B*: inactivation time constants (inactivation) were determined by fitting single exponential functions to the decaying phase of currents at voltages from +50 to +90 mV of control cells (*n* = 8) and cells pretreated with rapamycin (100 nM, overnight, *n* = 9). **P* <0.01, statistical significance according to two-tailed unpaired Student's *t*-test analysis.

3.1.2. Stimulation of Kv 1.3 and Kv 1.5 by mammalian target of rapamycin (mTOR) .

The inhibitory effect of rapamycin on Kv channel activity suggests that Kv1.3 and/or Kv1.5 channels could be regulated by mTOR. To test this hypothesis directly, cRNA encoding Kv1.3 or Kv1.5 was injected into *Xenopus* oocytes without or with additional injection of cRNA encoding mTOR.

In *Xenopus* oocytes expressing Kv1.3, but not in waterinjected oocytes, Kv currents were observed with typical properties of Kv1.3 (Fig. 8). The Kv current was significantly increased by additional coexpression of mTOR (Fig. 8). The activation of Kv1.3 by mTOR was abolished by the mTOR inhibitor rapamycin (75 nM). Preincubation of rapamycin for 12 h did not significantly modify the Kv1.3 current in the absence of mTOR. The current amplitude at +50 mV in Kv1.3-expressing oocytes was 908 ± 56 pA ($n = 4$) in the absence and 940 ± 101 pA ($n = 4$) in the presence of rapamycin. However, rapamycin virtually abrogated the stimulating effect of mTOR coexpression on Kv1.3 (Fig. 8, *B* and *C*).
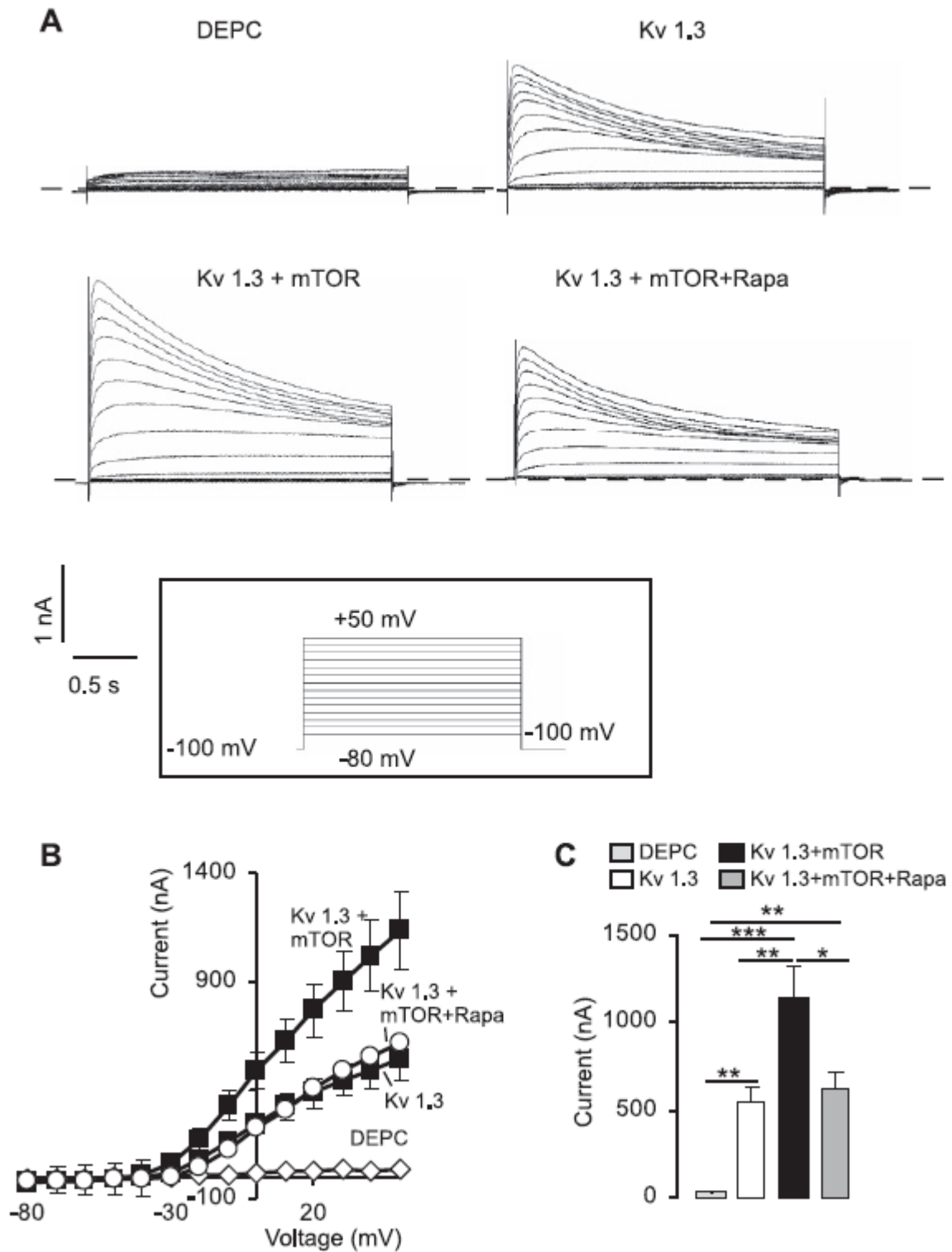
Figure 8. Stimulation of Kv1.3 by mammalian target of rapamycin (mTOR). *A*: representative currents recorded from the oocyte injected with diethylpyrocarbonate (DEPC)-H_2O (*top left*) or expressing human Kv1.3 (*top right*) or Kv1.3 + mTOR (*bottom left*) or Kv1.3 + mTOR incubated with rapamycin (75 nM, overnight, *bottom right*). The voltage protocol is shown (not to scale), whereby cells were held at -100 mV and voltage steps were

applied in +10-mV increments for 2,000 ms from -80 mV to +50 mV. *B*: mean *I-V* relationships (±SE, *n* = 9–13) of peak Kv1.3 currents in *Xenopus* oocytes injected with water (◊), expressing Kv1.3 alone (■), expressing Kv1.3 + mTOR (■), and expressing Kv1.3 + mTOR, incubated with rapamycin (75 nM, overnight, ○). *C*: mean peak amplitude (±SE, *n* = 9–13) of Kv1.3 currents at +50 mV in *Xenopus* oocytes injected with water (DEPC, light gray bar), expressing Kv1.3 (open bar), expressing Kv1.3 + mTOR (closed bar), and expressing Kv1.3 + mTOR, incubated with rapamycin (75 nM, overnight, dark gray bar). *$P < 0.05$, **$P < 0.01$, ***$P < 0.001$, significant difference between indicated groups (ANOVA).

In *Xenopus* oocytes expressing Kv1.5, the effect of mTOR on the voltage-gated current was similar as in Kv1.3-expressing oocytes (Fig. 9). The Kv1.5 currents were again significantly increased by additional coexpression of mTOR (Fig. 9), an effect abolished by rapamycin (Fig. 9, *B* and *C*). In the absence of mTOR, preincubation with rapamycin (75 nM, 12 h) did not significantly modify the Kv1.5 current. The current at +50 mV in Kv1.5-expressing oocytes was 901 ± 81 pA (*n* = 9) in the absence and 876 ± 66 pA (*n* = 8) in the presence of rapamycin.
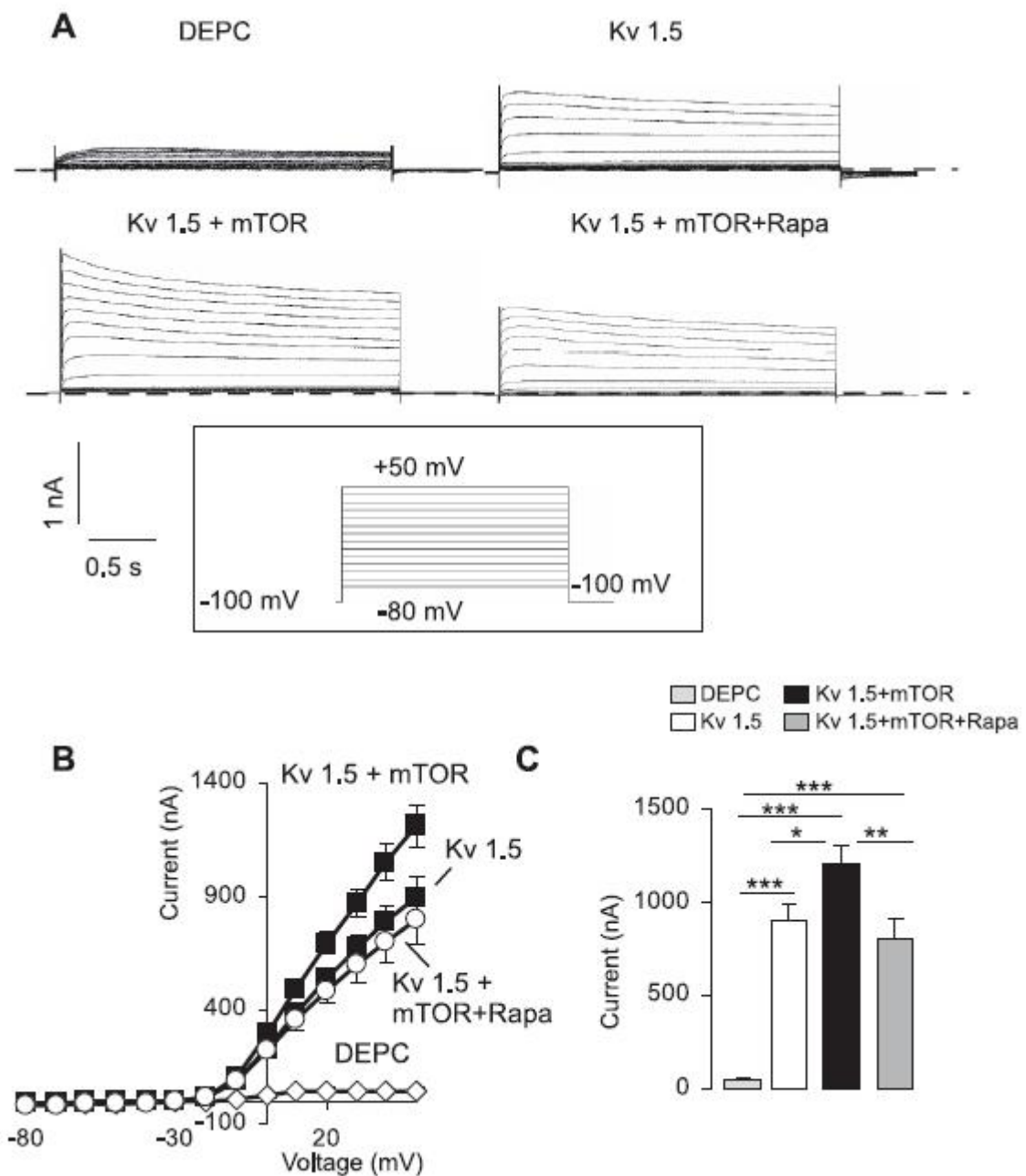
Figure 9. Stimulation of Kv1.5 by mTOR. *A*: representative currents recorded from the oocyte injected with DEPC-H$_2$O (*top left*) or expressing human Kv1.5 (*top right*) or Kv1.5 + mTOR (*bottom left*) or Kv1.5 + mTOR, incubated with rapamycin (75 nM, overnight, *bottom right*). The voltage protocol is shown (not to scale), whereby cells were held at -100 mV and voltage steps were applied in +10-mV increments for 2,000 ms from -80 mV to +50 mV. *B*: mean *I-V* relationships (± SE, *n* = 8–10) of peak Kv1.5 currents in *Xenopus* oocytes injected

64

with water (◊), expressing Kv1.5 alone (■), expressing Kv1.5 + mTOR (■), and expressing Kv1.5 + mTOR, incubated with rapamycin (75 nM, overnight, ○). *C*: mean peak amplitude (± SE, *n* = 8–10) of Kv1.5 currents at +50 mV in *Xenopus* oocytes injected with water (DEPC, light gray bar), expressing Kv1.5 (open bar), expressing Kv1.5 + mTOR (closed bar), and expressing Kv1.5 + mTOR, incubated with rapamycin (75 nM, overnight, dark gray bar). *P < 0.05, **P < 0.01, ***P < 0.001, significant difference between indicated groups (ANOVA).

Analysis of activation and inactivation time constants of Kv1.3 and Kv1.5 (Fig. 10) revealed that mTOR affected τ activation and τ inactivation of Kv1.3, but not of Kv1.5. Coexpression with mTOR resulted in a decreased τ activation and an increased τ inactivation of Kv1.3, suggesting that mTOR causes faster Kv1.3 channel activation and slower Kv1.3 channel inactivation. The stimulating effect of mTOR on Kv1.3 was abrogated by preincubation of the oocytes with rapamycin (Fig. 10).
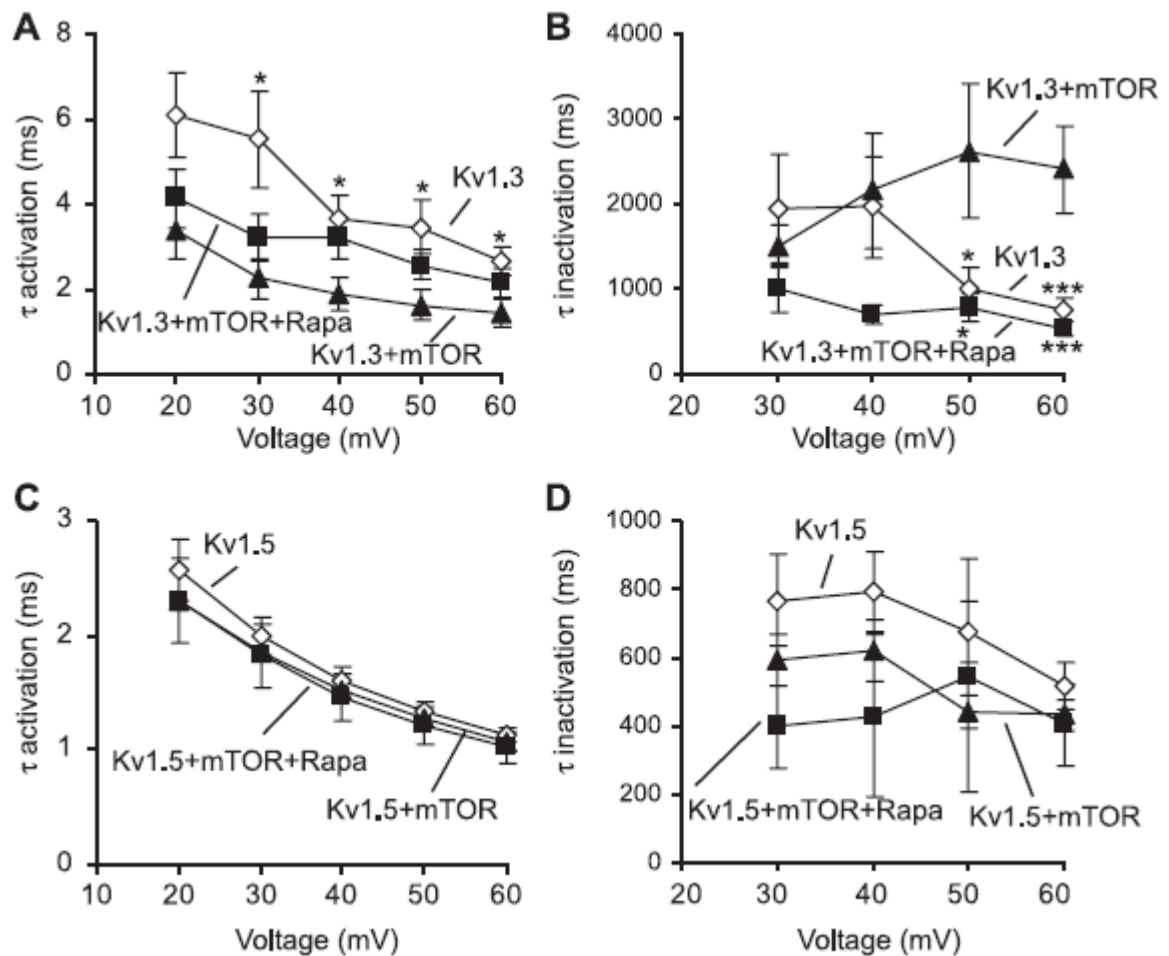
Figure 10. mTOR affects onset of activation and inactivation of Kv1.3 but not Kv1.5. *A* and *C*: activation time constants were determined by fitting single exponential functions to the rising phase of currents at voltages from +20 to +60 mV of Kv1.3, Kv1.3 + mTOR, and Kv1.3 + mTOR + rapamycin (75 nM, overnight, $n = 8$–9) (*A*) or Kv1.5, Kv1.5 + mTOR, and Kv1.5 + mTOR + rapamycin (75 nM, overnight; $n = 8$–10) (*C*). *$P < 0.05$, statistical significance between Kv1.3 and Kv1.3 + mTOR (ANOVA). *B* and *D*: inactivation time constants were determined by fitting single exponential functions to the decaying phase of currents at voltages from +30 to +60 mV of Kv1.3, Kv1.3 + mTOR, and Kv1.3 + mTOR + rapamycin (75 nM, overnight, $n = 14$–19) (*B*) or Kv1.5, Kv1.5 + mTOR, and Kv1.5 + mTOR + rapamycin (75 nM, overnight, $n = 7$–28) (*D*). *$P < 0.05$, ***$P < 0.001$, statistical significance between Kv1.3 and Kv1.3 + mTOR and between Kv1.3 + mTOR and Kv1.3 + mTOR + rapamycin (ANOVA).

3.2. Mast cells.

3.2.1. Effect of rapamycine on Ca^{2+}-activated K^+ channel ($K_{Ca}3.1$) activity in cultured mast cells.

We were interested to analyze whether rapamycin has also effects on non-voltage gated K^+ channels. We performed experiments in mouse bone marrow-derived mast cells (BMMCs), which are known to express Ca^{2+}-activated K^+ channels $K_{Ca}3.1$. Again, ion channel activity in BMMCs was analyzed utilizing whole cell patch-clamp experiments. To stimulate the FcεRI receptor, the BMMCs were incubated with IgE (10 μg/ml, 1h) directed against the hapten dinitrophenyl (DNP), washed and then stimulated with antigen, DNP coupled to the carrier protein human serum albumin (DNP-HSA, 50 ng/ml).

Stimulation of BMMCs through the receptor FcεRI was followed by a rapid increase of the K^+-selective conductance (Fig. 11). The same current could be induced by Ca^{2+} ionophore ionomycin (1 μM). The antigen induced current was significantly smaller in cells treated with rapamycine (100nM, 2 hours, n=8) than in control, nontreated group of BMMCs (n=8) (Fig. 11A). However, when $K_{Ca}3.1$ current was induced by stimulation of the cells with the Ca^{2+} ionophore ionomycin, $K_{Ca}3.1$ current conductance was similar in control group and in cells treated with rapamycine (Fig. 11. B). These observations suggest that rapamycine does not influence $K_{Ca}3.1$ channel activation through increase of cytosolic Ca^{2+} in BMMCs and that the blunted activation of the $K_{Ca}3.1$ channels by antigen in rapamycine-treated BMMCs results rather from rapamycine-induced impaired Ca^{2+} increase upon antigen stimulation.
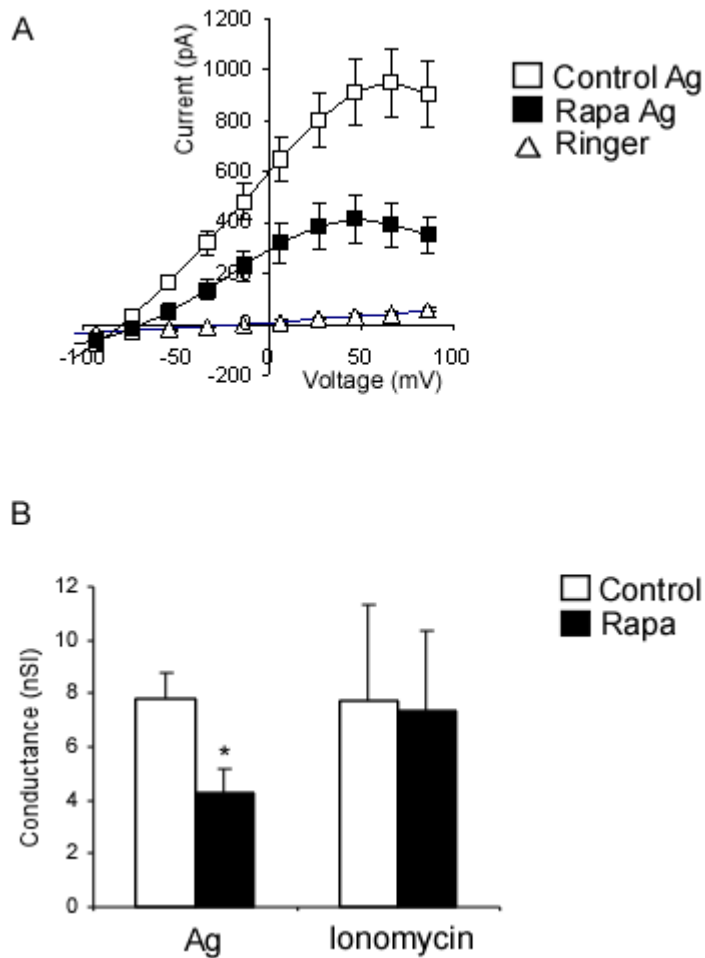
Figure 11. Effect of rapamycine on Ca^{2+}-activated K$^+$ currents in BMMCs. *A*. Mean I-V relationships ($\pm$ SEM, n = 8) prior to (Δ) and 3 min after antigen ($\square$) stimulation of BMMCs untreated (control) and treated with 100nM rapamycine (2h, Rapa Ag, $\blacksquare$). [Here either shown both groups before antigen or none of them] *B*. Mean whole-cell conductance in paired experiments ($\pm$ SEM, n = 8) as recorded in (A) prior to or 3 min after stimulation with antigen ($\square$) or ionomycin (1 μM). Data were calculated by linear regression between -95 and +45 mV. * indicates significant difference between control and Rapa-treated cells ($p<0.05$), ANOVA.

3.2.2. Effects of PDK1 on ion channels in mast cells. Antigen induced Ca^{2+} entry.

In murine mast cells we studied the effect of another kinase of the PI3 kinase pathway, phosphoinositide-dependent kinase 1 (PDK1) , on ion channels and cell functions. The PDK1 knockout mouse is not viable[115]. Thus, mast cells have been isolated from PDK1 hypomorphic mice expressing some 10 to 25% PDK1 (*pdk1^{hm}*) and from age and sex matched wild type mice (*pdk1^{wt}*)[115]

Again before the experiment, BMMCs were incubated with IgE (10 μg/ml, 1h) directed against the hapten dinitrophenyl (DNP), washed and then in course of the experiment stimulated acutely with antigen, DNP coupled to the carrier protein human serum albumin (DNP-HSA, 50 ng/ml).

According to Fura-2 fluorescence, the activation of the FcεRI receptor resulted in a rapid increase of cytosolic Ca^{2+} concentration. The increase was significantly blunted in *pdk1^{hm}* BMMCs (Fig. 12 A, B), i.e. the maximal fluorescence Δratio (peak) and the slope of the ratio (Δratio/ time) upon stimulation with antigen were significantly smaller in *pdk1^{hm}* BMMCs than in *pdk1^{wt}* BMMCs (Fig. 12B). Stimulation of the BMMCs with antigen in Ca^{2+}-free solution allowed an estimate of Ca^{2+} release from intracellular stores (Fig. 12C). This release was not significantly different between the genotypes (Fig. 12D).

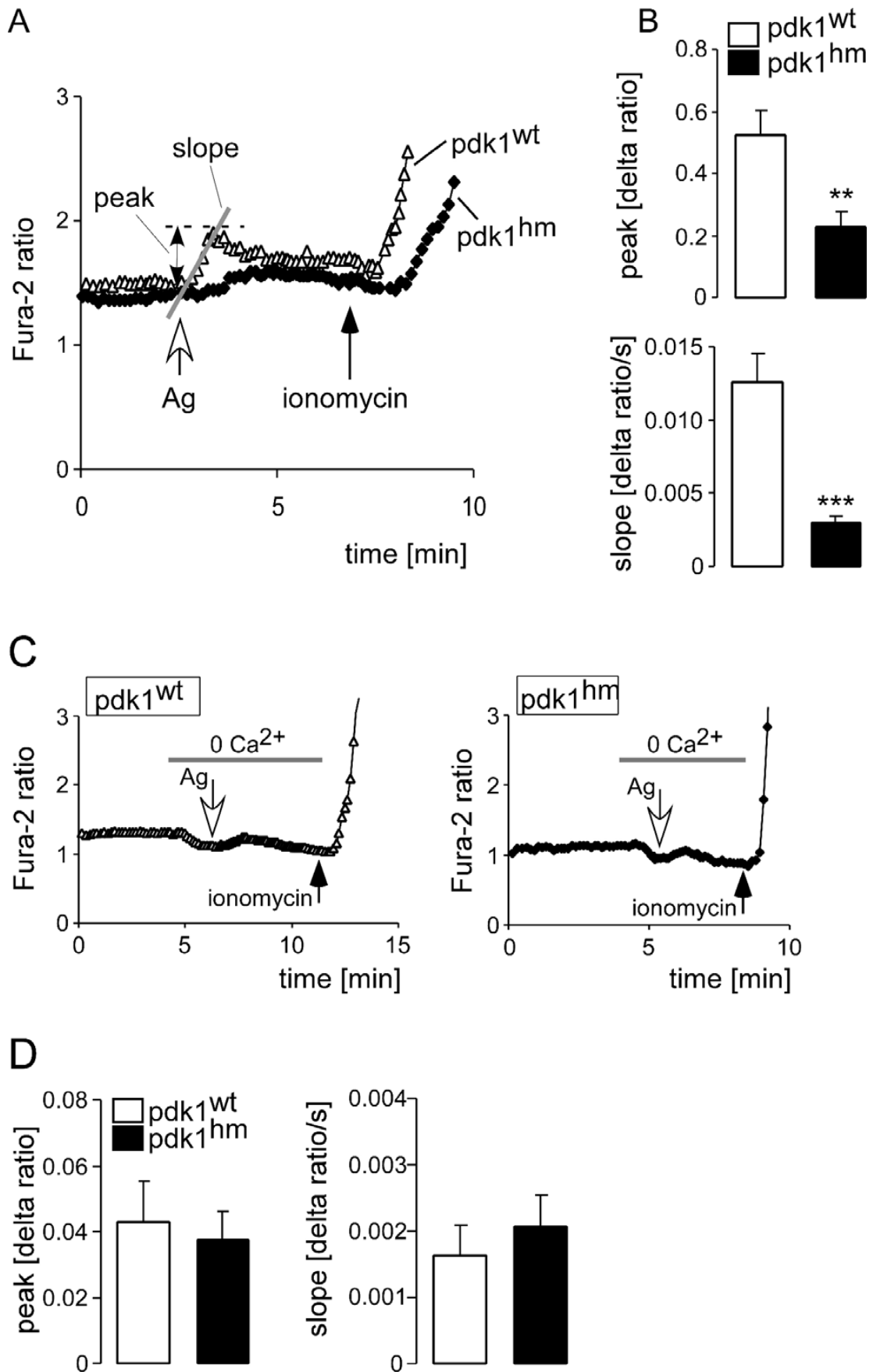**Figure 12. Antigen induced Ca^{2+} entry into BMMCs from *pdk1^{wt}* and *pdk1^{hm}* mice.** *A*.
Representative tracings showing the ratio of 340/380 nm Fura-2 fluorescence in Fura-2/AM

loaded BMMCs prior to and following acute addition of antigen (Ag, 50 ng/ml). At the end of each experiment, ionomycin (10 μM) was added for calibration. For quantification of the Ca^{2+} entry into the BMMCs, the slope (delta ratio/s) and peak (delta ratio) were calculated following addition of Ag. *B*. Mean (± SEM) of the peak (upper panel) and slope (lower panel) of the fluorescence ratio change for *pdk1^{wt}* (n = 25, open bars) and *pdk1^{hm}* (n = 15, closed bars) BMMCs following stimulation with antigen (Ag, 50 ng/ml). ** (p<0.01) and *** (p<0.001) indicate significant difference between both groups (two-tailed unpaired *t*-test). *C*. Representative traces showing the Fura-2 fluorescence ratio before and after addition of Ag (50 ng/ml) in the absence of extracellular Ca^{2+} in Fura-2AM loaded BMMCs. To create a Ca^{2+}-free environment, EGTA (0.5 mM) was added to the Ca^{2+}-free bath solution. Means (± SEM) of the peak value (left side) and slope (right side) of the fluorescence ratio change for *pdk1^{wt}* (n = 4, open bars) and *pdk1^{hm}* (n = 5, closed bars) BMMCs upon stimulation with Ag in Ca^{2+}-free solution.

3.2.3. Effects of PDK1 on ion channels in mast cells. Ca^{2+}-activated K^+ channels.

According to whole cell patch clamp experiments the stimulation of BMMCs with antigen or Ca^{2+} ionophore ionomycin (1 μM). was followed by a rapid increase of $K_{Ca}3.1$ currents (Fig. 13). The antigen induced current was significantly smaller in *pdk1^{hm}* BMMCs than in *pdk1^{wt}* BMMCs (Fig. 13A). Treatment of the cells with ionomycin led to an increase of the K^+ current to similar values in *pdk1^{wt}* and *pdk1^{hm}* BMMCs (Fig. 13B). The observations suggested that the Ca^{2+}-activated K^+ channels were similarly expressed and similarly activated by increase of cytosolic Ca^{2+} in *pdk1^{wt}* and *pdk1^{hm}* BMMCs. The blunted activation of the K^+ channels by antigen in *pdk1^{hm}* BMMCs thus resulted from impaired Ca^{2+} entry.
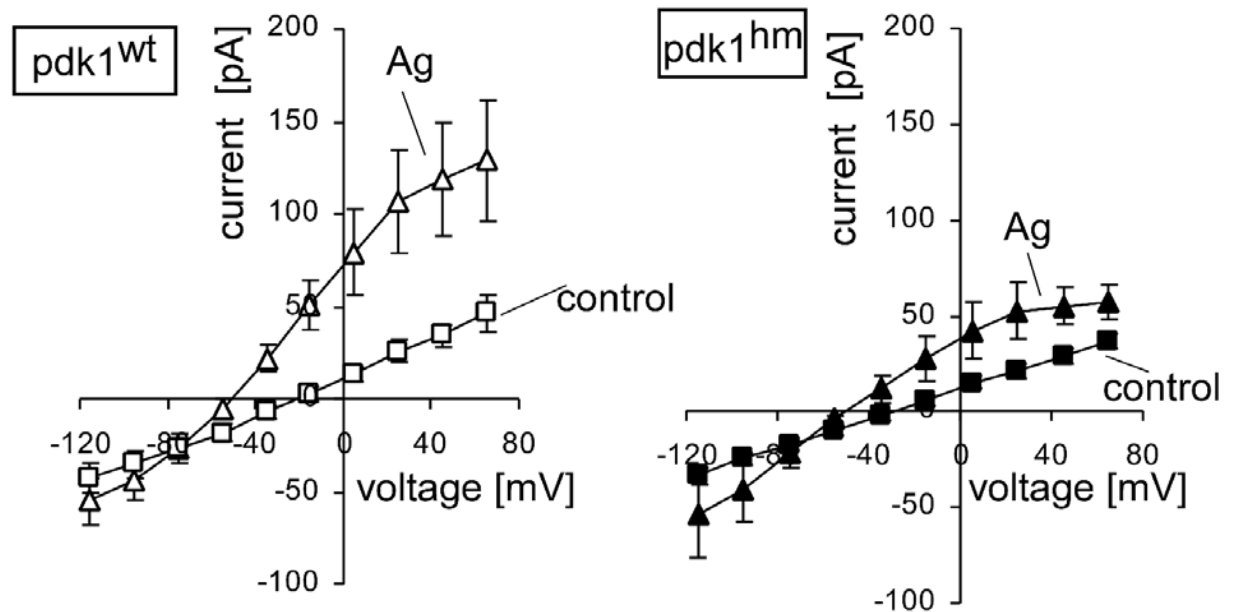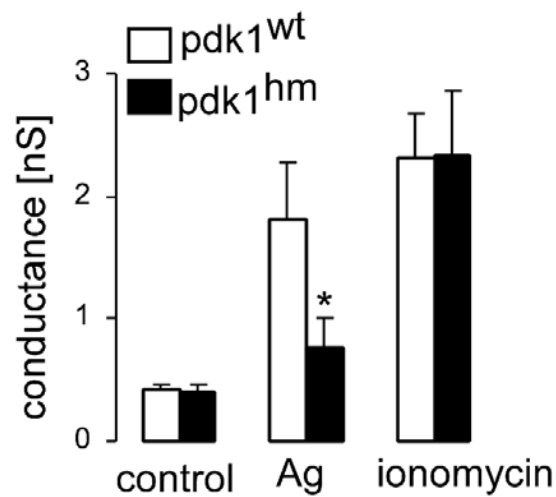
Figure 13. Ca^{2+}-activated K^{+} current K$_{Ca}$3.1 in *pdk1^{wt}* and *pdk1^{hm}* BMMCs upon antigen-IgE-induced or ionomycin-induced stimulation. *A*. Mean I-V relationships ($\pm$ SEM, n = 6) in *pdk1^{wt}* BMMCs (left panel) or *pdk1^{hm}* BMMCs (right panel) prior to (control, squares) or 3 min after stimulation with antigen added to 1 mM Ca^{2+}-containing standard NaCl bath solution (Ag, triangles). *B*. Mean whole-cell conductance in paired experiments ($\pm$ SEM, n = 6-14) as recorded in (*A*) prior to or 3 min after stimulation with antigen or ionomycin (1 μM).

Data were calculated by linear regression between -95 and +45 mV. * indicates significant difference between *pdk1^{wt}* and *pdk1^{hm}* cells ($p < 0.05$; ANOVA).

3.2.4. Histamine and hexosaminidase release from antigen-stimulated pdk^{wt} and pdk^{hm} mast cells.

Additional experiments were performed to explore the effect of antigen exposure on degranulation of *pdk1^{wt}* and *pdk1^{hm}* BMMCs, since mast cell degranulation is known to strongly depend on Ca^{2+} entry[127,128,171,172]. Activation via the FcεRI receptor was followed by release of histamine and of β-hexosaminidase, an enzyme stored in mast cell granules[173]. The release of both histamine (Fig. 14) and β-hexosaminidase (Fig. 15) was similar in *pdk1^{hm}* BMMCs and *pdk1^{wt}* BMMCs.

The lack of difference between histamine and β-hexosaminidase release in *pdk1^{wt}* and *pdk1^{hm}* BMMCs could be due to the opposite effects of PDK1-dependent activation of serum- and glucocorticoid- inducible kinase 1 (SGK1), that is known to positively regulate mast cell degranulation[174] and PDK1 dependent activation of PKCδ, which is a negative regulator of degranulation[175]. Further experiments have been made in the presence of PKCδ-inhibitor rottlerin. As illustrated in Fig. 15, β-hexosaminidase release was significantly enhanced by rottlerin in *pdk1wt* BMMCs but not in *pdk1hm* BMMCs. The observation points to PDK1 sensitive inhibition of mast cell degranulation by PKCδ.
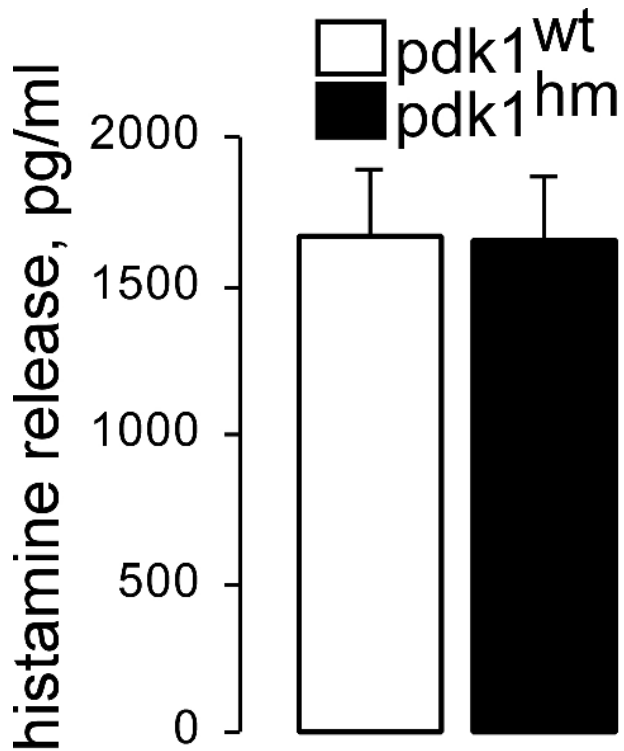
Figure 14. Histamine release from antigen-stimulated *pdk1^wt^* and *pdk1^hm^* BMMCs. Mean histamine release (± SEM, n = 4 individual experiments) from cultured *pdk1^hm^* BMMCs (closed bars*)* and their wild-type littermates *pdk1^wt^* (open bars) stimulated for 15 min with 50 ng/ml antigen. The stimulated histamine release in each experiment was corrected for the spontaneous release.
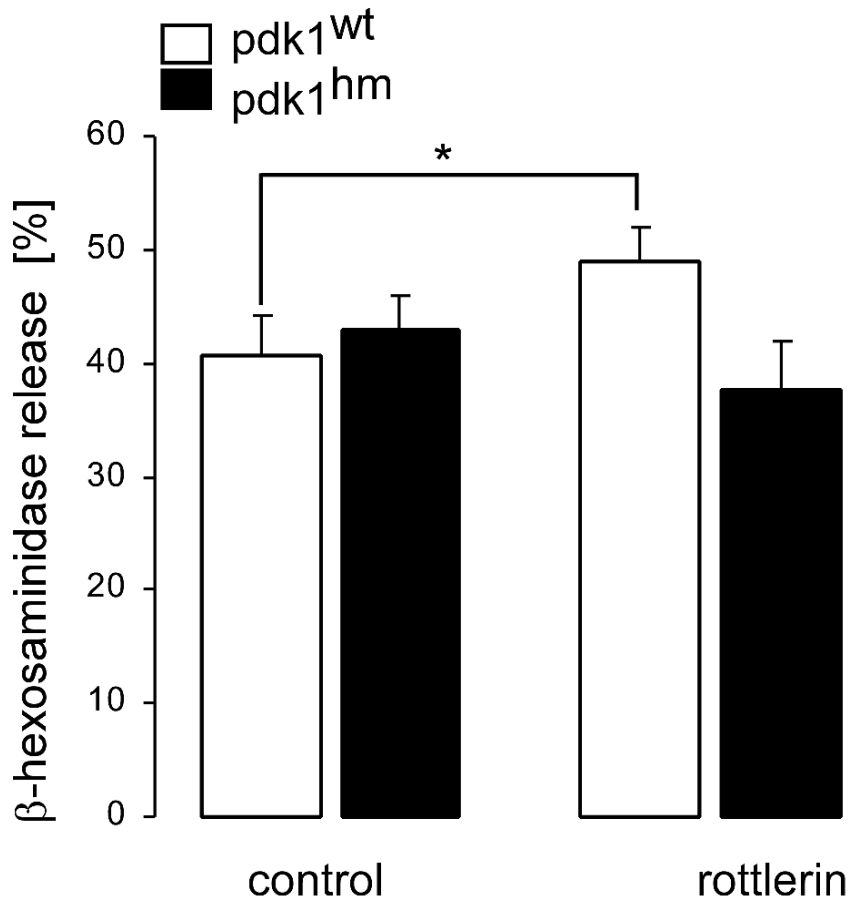
Figure 15. Hexosaminidase release from antigen-stimulated *pdk1^wt* and *pdk1^hm* BMMCs.
Mean β-hexosaminidase release (± SEM, n = 4 individual experiments) from cultured *pdk1^hm*
BMMCs (closed bars*)* and their wild-type littermates *pdk1^wt* (open bars) stimulated for 15 min
with 50 ng/ml antigen. The experiments have been performed in the absence (left bars,
control) and presence (right bars) of PKCδ-inhibitor rottlerin (10 μM). The stimulated β-
hexosaminidase release in each experiment was corrected for the spontaneous release.   *
indicates significant difference (p<0.05; ANOVA).

3.2.5. Phosphorylation status of PKCδ and the SGK1 target NDRG1 in pdk1wt and pdk1hm mast cells.

The activity of the PDK1 sensitive kinases SGK1 and PKCδ was assessed by western blotting of phosphorylated (activated) PKCδ and phosphorylated NDRG1 (N-myc downstream-regulated gene 1), a target of SGK1[176]. Phosphorylation of PKCδ (Thr505) and NDRG (Thr346), a site of SGK1-mediated phosphorylation, was induced by antigen stimulation in *pdk1*^{wt} but not in *pdk1*^{hm} BMMCs (Fig. 16), confirming that both downstream targets of PDK1, SGK1 and PKCδ, are affected upon antigen stimulation in mast cells.
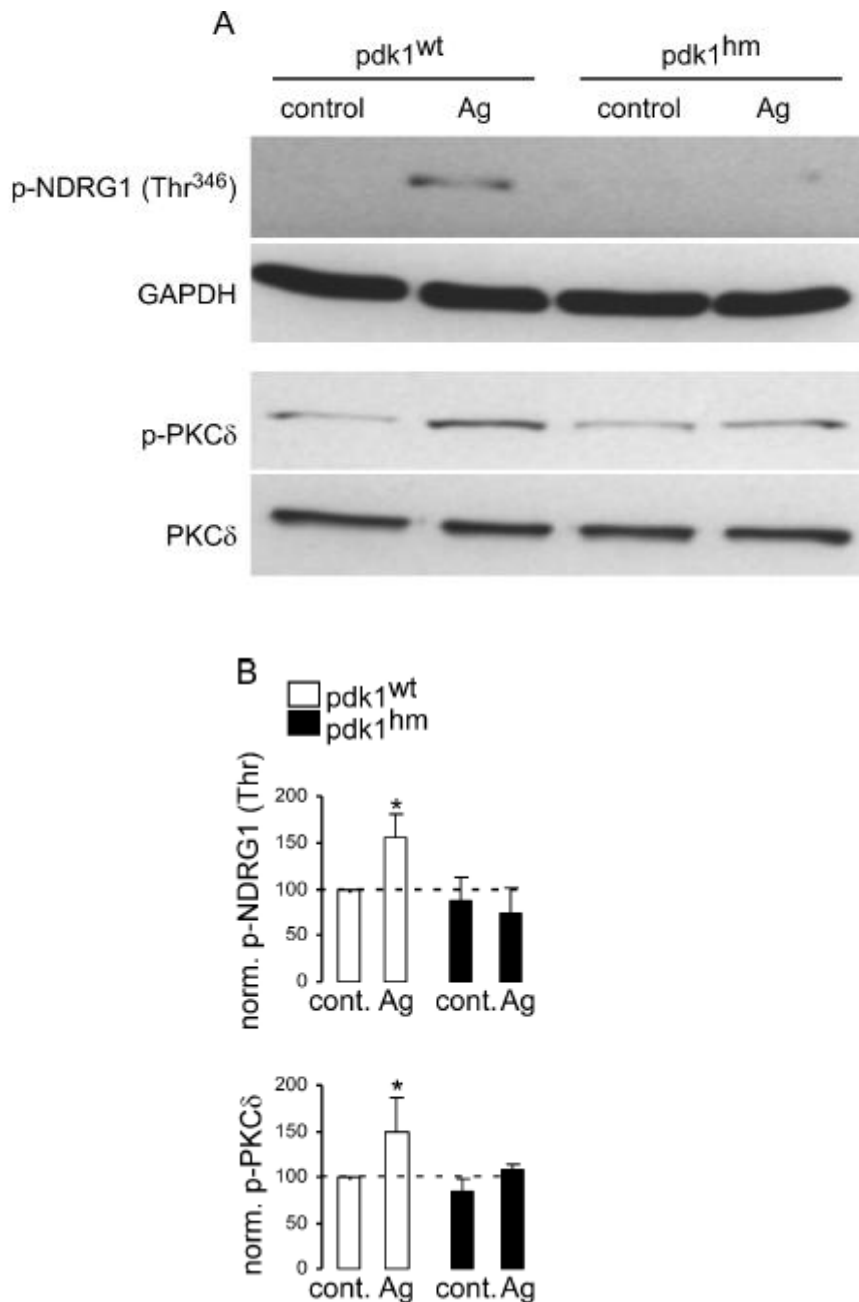
Figure 16. Phosphorylation status of PKCδ and the SGK1 target NDRG1 in *pdk1wt* and *pdk1hm* BMMCs. *A*. Original Western blot of mast cells from *pdk1*^{wt} and *pdk1*^{hm} mice untreated (control) or stimulated for 5 min with 50 ng/ml antigen (Ag). Protein extracts were

analyzed by direct Western blotting using antibodies directed against phospho (p)-NDRG1 (Thr346) and p- PKCδ (Thr505). Equal protein loading was confirmed with GAPDH or PKCδ antibody. *B*. Arithmetic mean ± SEM (n = 4) of the abundance of p-NDRG1 (Thr346) and p-PKCδ (Thr505) as the ratio of p-NDRG1/GAPDH and p-PKCδ/PKCδ normalized to *pdk1wt* (control). * (p<0.05) indicates significant difference from *pdk1wt* (control), ANOVA.

4. Discussion

4.1. Regulation of voltage-gated K$^+$ channels Kv1.3 and Kv1.5 by mTOR in dendritic cells.

The present study confirms previous observations[120,122,124] that bone marrow-derived dendritic cells express voltage-gated K$^+$ (Kv) channels, which are rapidly activated upon cell membrane depolarization. More importantly, the observations disclose a novel regulator of those channels. As apparent from heterologous expression in *Xenopus* oocytes, the Kv1.3 and Kv1.5 channels are upregulated by the mammalian target of rapamycin. Accordingly, Kv channels in DCs are downregulated by rapamycin. Rapamycin concentrations within the human whole blood through therapeutic range are reported as 5–16 nM[177]. Slightly higher concentrations used in the present study (50–100 nM) aimed to fully block mTOR.

In *Xenopus* oocytes, mTOR alters Kv1.3 channel kinetics, accelerating Kv1.3 channel activation and slowing down Kv1.3 channel inactivation, the latter effect abrogated by rapamycin. In DCs the effect of rapamycin required at least 6 h, suggesting that rapamycin may be effective in part by modulating gene expression. However, there was no change in mRNA level of Kv1.3 and Kv1.5 when DCs were incubated with rapamycin (data not shown), pointing to an influence of rapamycin/mTOR on Kv channels in DCs by mechanisms other than regulation of transcription. In Chinese hamster ovary (CHO) cells stably expressing Kv1.3 channels, rapamycin inhibited those channels upon acute drug administration[178]. However, the effect required much higher concentrations (IC$_{50}$ of 6.7 µM) than in our study. In Kv1.3-expressing CHO cells, rapamycin enhanced the rate of current decay, an effect that we also observed at +70 mV in DCs. Another immunosuppressant (and another mTOR inhibitor), FK-506, similarly blocked Kv1.3 and Kv1.5 in stably transfected CHO cells, and FK-506 caused a time-, concentration-, and use-dependent inhibition of Kv1.3 channels[178]. The effect of FK-506 (IC$_{50}$ = 5.6 µM) resulted from a direct interaction with the Kv1.3 channel rather than modifications of the signal transduction pathway, including mTOR, since the effect of FK-506 was observed in excised inside-out patch devoid of diffusible cytosolic molecules required for phosphorylation/dephosphorylation[178].

Earlier dual-electrode voltage-clamp experiments in *Xenopus* oocytes revealed that Kv1.3[179,180] and Kv1.5[181] channels are upregulated by the serum and glucocorticoidinducible kinase (SGK) isoforms SGK1 and SGK3. Similarly, overexpression of SGK1, SGK2, or SGK3 in human embryonic kidney (HEK) cells was shown to upregulate Kv channels[179,182]. The same channels were shown to be activated by treatment of the HEK cells[179] and

fibroblasts[183] with IGF-I. Activation of SGK has previously been shown to involve mTOR[184-186]. Thus, it is tempting to speculate that mTOR is effective through stimulation of the SGK isoforms, which in turn upregulate Kv1.3 and Kv1.5. Inhibition of the PI3K leads, however, to upregulation of Kv channel activity in DCs[122], an effect in seeming contrast to the stimulating effect of SGK isoforms on Kv channels in other cells. Kv channels are further regulated by p38 kinase[187], which is in turn known to upregulate SGK1 expression[159].

Kv1.3 channels are regulated by a variety of further kinases, such as protein kinase A[188,189], protein kinase C[188], Src-kinases[190,191], Lck56[192,193], neurotrophin B receptor kinase[194], and EGF receptor tyrosine kinase[195].

The K^+ channels maintain the cell membrane potential, which in turn provides the electrical driving force for Ca^{2+} entry[196]. Accordingly, Kv channel blockers margatoxin and charybdotoxin decreased capacitative calcium entry in HEK cells[197]. DCs respond to lipopolysaccharide stimulation with a fast increase of intracellular calcium concentration, which is accomplished by both, Ca^{2+} release from intracellular stores and Ca^{2+} influx through Ca^{2+} release-activated channel (CRAC)[124]. The Ca^{2+} influx through CRAC depends on the activity of Kv channels. Inhibition of either CRAC or Kv channels leads to profound changes in DC functions, including changes in maturation, phagocytosis, migration, and cytokine production[124].

4.2. Rapamycin has no direct effect on Ca^{2+}-activated K^+ channels $K_{Ca}3.1$ in mast cells.

Little is known about the signals downstream of PI3K which regulate mast cell homeostasis and function following FcɛRI aggregation.

The present study demonstrates that rapamycin has no direct effect on Ca^{2+}-activated K^+ channels $K_{Ca}3.1$ in mast cells. It is not $K_{Ca}3.1$ that is regulated by rapamycin, but Ca^{2+} entry, due to there is no difference after stimulation with ionomycine, which is an ionophore produced by the bacterium *Streptomyces conglobatus*[198]. It is used in research to raise the intracellular level of Ca^{2+} and as a research tool to understand Ca^{2+} transport across biological membranes.

We explored that rapamycine has direct effect to Kv1.3 and 1.5 in dendritic cells and our next step was to study if other K^+ channels are also influenced by rapamycin. We chose mast cells, due to they express Ca^{2+}-activated K^+ channels[127]. And though we saw an effect on

$K_{Ca}3.1$ upon antigen, but it was not there with ionomycin, meaning that there is no direct effect of Rapa on K+ channel but rather on Ca^{2+} entry.

4.3. Regulation of ion channels by PDK1 in mast cells.

The present study demonstrates that the stimulation of Ca^{2+} entry, but not Ca^{2+} release from intracellular stores, following exposure to antigen is significantly less pronounced in mast cells from PDK1 hypomorphic mice (*pdk1^hm*) than in mast cells from their wild type littermates (*pdk1^wt*). PDK1 deficiency thus blunts Ca^{2+} entry and consequently the currents through Ca^{2+}-activated K^+ channels. The stimulation of the release of inflammatory mediators, as well as the depolymerisation of the cortical F-actin barrier require increase in intracellular Ca^{2+}[127,128,171]. Ca^{2+} further activates Ca^{2+}- sensitive K^+ channels[121,126,171], which maintain the membrane potential and thus the electrical driving force for Ca^{2+} entry[196]

4.4. Regulation of ß-hexosaminidase and histamine-relise in mast cells by PDK1.

The PI3 kinase has previously been shown to regulate mast cell proliferation, adhesion and migration, as well as antigen-IgE-induced degranulation and cytokine release[154]. PDK1 activates the serum- and glucocorticoid- inducible kinase SGK1[157,199,200]. SGK1 is genomically upregulated by glucocorticoids[201], mineralocorticoids[202], 1,25-dihydroxyvitamin D3 (1,25(OH)2D3)[203], cell shrinkage[204], gonadotropins[205], and TGFβ[206].

Surprisingly, partial PDK1 deficiency did not abrogate degranulation despite the reduced Ca^{2+} entry. Accordingly, both β-hexosaminidase release and histamine release were not significantly different between *pdk1^wt* and *pdk1^hm* BMMCs. It should be kept in mind that the *pdk1^hm* still express some 10-25% of regular PDK1. The determination of cytosolic Ca^{2+} concentration and the K^+ channel activity could be more sensitive functions than degranulation. Moreover, degranulation depends on localized increases of cytosolic Ca^{2+} activity, which may not be apparent in Fura2 fluorescence of the whole cell[207]. Alternatively, PDK1 may, in addition to stimulating Ca^{2+} entry, inhibit degranulation by some other mechanism. PDK1 activates protein kinase PKCδ[160] which has in turn been shown to negatively regulate mast cell degranulation[175]. Reduced activity of PDK1 may on the one hand compromise the stimulation of degranulation by decreasing Ca^{2+} entry and on the other

hand disinhibit degranulation by decreasing activation of PKCδ. The net result could be seemingly unchanged degranulation. The observation that the PKCδ-inhibitor rottlerin enhances β-hexosaminidase release in *pdk1^{wt}* BMMCs but not in *pdk1^{hm}* BMMCs is in support of a dual role of PDK1 in the regulation of mast cell degranulation.

4.5. Conclusions

Regarding the initially determined aims of the present work, the regulation of ion channels by mTOR and PDK1 has been characterized in mouse MCs and/or DCs.

The serine/threonine kinase mTOR stimulates the voltage-gated K^+ channels Kv1.3 and Kv1.5, an effect shaping the cell membrane potential and function of bone marrow-derived dendritic cells. mTOR inhibitor rapamycine had no direct effect on Ca^{2+}-activated K^+ channel $K_{Ca}3.1$ in mast cells.

Phosphoinositide-dependent kinase PDK1 upregulates Ca^{2+} entry and consequently also Ca^{2+}- activated K^+ channels in mast cells. At the same time, PDK1 may influence degranulation through activation of SGK1 and PKCδ.

The present observations thus identify further elements of the PI3 kinase signaling pathway in the regulation of ion channels and functions of dendritic and mast cell.

5. Summary

Dendritic cells are antigen-presenting cells, central for the development of optimal T cell immunity, that are able to initiate primary immune responses and to establish immunological memory[5,6]. Mast cells are tissue-based effector cells in allergic diseases, playing a central role in the propagation of IgE-dependent allergic reactions[50], such as allergic rhinitis[51], asthma[52], anaphylaxis and delayed hypersensitivity reactions[52,53]. Upon stimulation of IgE receptors (FcεRI), mast cells release granules containing several mediators including histamine and cytokines, which regulate responses of other inflammatory cells[53]. Dendritic and mast cell functions are regulated by phosphatidylinositol-3 (PI3) kinase signalling pathway[54,122,154,155]. The PI3 kinase is partially effective in dendritic and mast cells through alteration of their ion channel activity [122,156]. Both PI3 kinase on the one hand and ion channels on the other hand are important for the regulation of mast and dendritic cell functions. However, little is known about downstream elements of the PI3 kinase that regulate ion channels in those cells. In the present project the question was addressed whether two PI3 kinase downstream targets, phosphoinositide-dependent kinase 1 (PDK1) and mammalian target of rapamycine (mTOR), regulate ion channels and ion channel-dependent functions in dendritic and mast cell.

We showed that treatment of dendritic cells with rapamycine, the mTOR inhibitor, led to inhibition of the currents through voltage-gated K^+ channels, which in dendritic cells belong to Kv 1.3 and Kv 1.5 families[120]. Analysis of the time constants of activation and inactivation demonstrated that rapamycin caused faster Kv channel inactivation.

To test the hypothesis that Kv1.3 and/or Kv1.5 channels could be regulated by mTOR, cRNA encoding Kv1.3 or Kv1.5 was injected into *Xenopus* oocytes with or without additional injection of cRNA encoding mTOR. The Kv1.3 and Kv1.5 currents were significantly increased by additional coexpression of mTOR, an effect abolished by rapamycin. Analysis of activation and inactivation time constants of Kv1.3 and Kv1.5 revealed that mTOR affected τ activation and τ inactivation of Kv1.3, but not of Kv1.5. Coexpression with mTOR resulted in a decreased τ activation and an increased τ inactivation of Kv1.3, suggesting that mTOR causes faster Kv1.3 channel activation and slower Kv1.3 channel inactivation.

We were interested to analyze whether rapamycin has also effects on non-voltage gated K^+ channels. We performed experiments in mouse bone marrow-derived mast cells (BMMCs), which are known to express Ca^{2+}-activated K^+ channels $K_{Ca}3.1$. Our observations

demonstrated that though rapamycine did not influence $K_{Ca}3.1$ channel activation directly, it impaired antigen-dependent increase of cytosolic Ca^{2+} in BMMCs and that secondary led to the blunted activation of the $K_{Ca}3.1$ channels.

In BMMC we also studied the effect of another kinase of the PI3 kinase pathway, PDK1, on ion channels and cell functions. The present study demonstrated that the stimulation of Ca^{2+} entry, but not Ca^{2+} release from intracellular stores, following exposure to antigen was significantly less pronounced in mast cells from PDK1 hypomorphic mice (*pdk1^{hm}*) than in mast cells from their wild type littermates (*pdk1^{wt}*). PDK1 deficiency thus blunted Ca^{2+} entry and consequently indirectly also the currents through Ca^{2+}-activated K^+ channels $K_{Ca}3.1$. Partial PDK1 deficiency did not abrogate degranulation despite the reduced Ca^{2+} entry in *pdk1^{hm}* BMMCs. Both β-hexosaminidase release and histamine release were not significantly different between *pdk1^{wt}* and *pdk1^{hm}* BMMCs. We provided a possible mechanism explaining unaffected degranulation in *pdk1^{hm}* BMMCs by showing that PDK1 led to the activation of two downstream kinases, SGK1 and PKCδ, positive and negative regulators of mast cell degranulation, respectively.

6. Zusammenfassung

Dendritische Zellen sind Antigen-präsentierende Zellen, die zentral in der Entwicklung einer optimalen T-Zell-Immunität stehen. So können sie primäre Immunantworten einleiten und ein immunologisches Gedächtnis aufbauen[5,6].

Mastzellen sind im Gewebe beheimatete Effektorzellen, die eine zentrale Rolle bei der Ausweitung IgE-abhängiger allergischer Reaktionen einnehmen[50], wie zum Beispiel bei allergischer Rhinitis[51], Asthma[52], Anaphylaxie und verzögerten Hypersensitivitätsreaktionen[52,53]. Nach der Stimulation von IgE-Rezeptoren (Fc$_\varepsilon$RI) setzen Mastzellen Granula mit verschiedenen Mediatoren frei, unter anderem Histamine und Zytokine, welche die Antworten anderer inflammatorischer Zellen regulieren[53]. Die Funktionen von dendritischen und Mastzellen werden über den Phosphatidylinositol-3 (PI3) Kinase Signalweg reguliert[54,122,154,155]. Der PI3 Kinase Signalweg erreicht seine Effektivität in dendritischen und Mastzellen zum Teil durch die Veränderung von Ionenkanal-Aktivitäten [122,156]. Also sind beide, einerseits Pi3K und andererseits Ionenkanäle wichtig für die Regulation von Funktionen dendritischer und Mastzellen. Trotzdem ist wenig bekannt über die Elemente stromabwärts von PI3K, die die Ionenkanäle in diesen Zellen regulieren.

In dem gegenwärtigen Projekt war die Frage, ob zwei der Kinasen die PI3K nachgeschalten sind, phosphoinositid-dependent kinase 1 (PDK1) und mammalian target of rapamycin (mTOR) Ionenkanäle und davon abhängige Funktionen in dendritischen und Mastzellen regulieren.

Wir haben gezeigt, dass die Behandlung dendritischer Zellen mit dem mTOR-Inhibitor Rapamycin zur Inhibierung von Strömen durch spannungsgesteuerte K$^+$ - Kanäle, die in dendritischen Zellen zu den Familien Kv 1.3 und Kv 1.5 gehören, führt[120].

Die Analyse der Zeitkonstanten der Aktivierung und Inaktivierung zeigte, dass Rapamycin eine schnellere Kv-Inaktivierung bewirkt hat.

Um die Hypothese zu testen, dass Kv 1.3 und/oder Kv 1.5 durch mTOR reguliert werden können, wurde cRNA für Kv 1.3 oder Kv 1.5 gleichzeitig mit oder ohne cRNA für mTOR in Xenopus Oocyten injiziert. Die Kv 1.3 – und Kv 1.5 – Ströme wurden signifikant gesteigert durch die zusätzliche Expression von mTOR, ein Effekt, der durch Rapamycin aufgehoben werden konnte. Die Analyse der Aktivierungs- und Inaktivierungszeitkonstanten (τ) von Kv 1.3 und Kv 1.5 ergab, dass mTOR die τ -Aktivierung und –Inaktivierung von Kv 1.3 aber nicht die von Kv 1.5 beeinflusste. Die Koexpression mit mTOR führte zu einer abgeschwächten τ -Aktivierung und einer gesteigerten τ -Inaktivierung, also zu einer schnelleren Aktivierung und langsameren Inaktivierung von Kv 1.3.

Wie waren weiterhin daran interessiert, zu untersuchen, ob Rapamycin auch einen Effekt auf spannungsunabhängige K^+ - Kanäle hat. Die Experimente dazu führten wir in Mastzellen aus dem Knochenmark von Mäusen aus (BMMCs), die bekannter weise die Ca^{2+}- abhängigen K^+ - Kanäle $K_{Ca}3.1$ exprimieren. Unsere Beobachtungen zeigten, dass Rapamycin, obwohl es die $K_{Ca}3.1$ − Kanal − Aktivierung nicht direkt beeinflusste, den Antigen-induzierten Anstieg des cytosolischen Ca^{2+}- Spiegels der BMMCs verminderte, was sekundär zur Dämpfung der $K_{Ca}3.1$ − Kanäle führte. In den BMMCs untersuchten wir außerdem den Effekt einer anderen Kinase im PI3K-Signalweg, PDK1, auf Ionenkanäle und Zellfunktionen. Diese Arbeit bewies, dass die Stimulation des Antigen induzierten Ca^{2+}- Einstroms, aber nicht die Ca^{2+}- Ausschüttung aus intrazellulären Speichern in Mastzellen aus PDK1 hypomorphen Mäusen (*pdk1^{hm}*) weniger stark ausgeprägt war als in Mastzellen aus den Wildtyp-Geschwistertieren (*pdk1^{wt}*). Demnach schwächte der PDK1-Mangel den Ca^{2+}- Einstrom ab und folglich auch indirekt die Ströme durch die Ca^{2+}- aktivierten K^+ - Kanäle $K_{Ca}3.1$. Das partielle PDK1-Defizit verhinderte nicht die Degranulation trotz des geringeren Ca^{2+}- Einstroms in *pdk1^{hm}* BMMCs. Beides, die β-Hexosaminidase- und die Histamin − Ausschüttung waren nicht signifikant unterschiedlich zwischen *pdk1^{wt}* und *pdk1^{hm}* BMMCs. Wir erstellten einen möglichen Mechanismus, der die unbeeinträchtigte Degranulation in *pdk1^{hm}* BMMCs erklärt, indem wir zeigten, dass PDK1 zur Aktivierung zweier nachgeordneter Kinasen, SGK1 und PKCδ führte, wobei erstere die Degranluation in Mastzellen positiv und letztere negativ reguliert.

7. Reference List

1. Hoffmann,J.A., Kafatos,F.C., Janeway,C.A. & Ezekowitz,R.A. Phylogenetic perspectives in innate immunity. *Science* **284**, 1313-1318 (1999).

2. Corthay,A. A three-cell model for activation of naive T helper cells. *Scand. J. Immunol.* **64**, 93-96 (2006).

3. Diebold,S.S. Activation of dendritic cells by toll-like receptors and C-type lectins. *Handb. Exp. Pharmacol.* 3-30 (2009).

4. Takeda,K., Kaisho,T. & Akira,S. Toll-like receptors. *Annu. Rev. Immunol.* **21**, 335-376 (2003).

5. Banchereau,J. & Steinman,R.M. Dendritic cells and the control of immunity. *Nature* **392**, 245-252 (1998).

6. Dubsky,P. *et al.* Human dendritic cell subsets for vaccination. *J. Clin. Immunol.* **25**, 551-572 (2005).

7. Muzio,M., Natoli,G., Saccani,S., Levrero,M. & Mantovani,A. The human Toll signaling pathway: Divergence of NF-kB and JNK/SAPK activation upstream of TRAF6. *European Cytokine Network* **9**, 379 (1998).

8. Brightbill,H.D. *et al.* Host defense mechanisms triggered by microbial lipoproteins through toll-like receptors. *Science* **285**, 732-736 (1999).

9. Espuelas,S., Roth,A., Thumann,C., Frisch,B. & Schuber,F. Effect of synthetic lipopeptides formulated in liposomes on the maturation of human dendritic cells. *Mol. Immunol.* **42**, 721-729 (2005).

10. Hoarau,C., Lagaraine,C., Martin,L., Velge-Roussel,F. & Lebranchu,Y. Supernatant of Bifidobacterium breve induces dendritic cell maturation, activation, and survival through a Toll-like receptor 2 pathway. *J. Allergy Clin. Immunol.* **117**, 696-702 (2006).

11. Katz,J., Zhang,P., Martin,M., Vogel,S.N. & Michalek,S.M. Toll-like receptor 2 is required for inflammatory responses to Francisella tularensis LVS. *Infect. Immun.* **74**, 2809-2816 (2006).

12. Carmona,E.M. *et al.* Pneumocystis cell wall beta-glucans induce dendritic cell costimulatory molecule expression and inflammatory activation through a Fas-Fas ligand mechanism. *J. Immunol.* **177**, 459-467 (2006).

13. Fulcher,J.A. *et al.* Galectin-1-matured human monocyte-derived dendritic cells have enhanced migration through extracellular matrix. *J. Immunol.* **177**, 216-226 (2006).

14. Schakel,K. *et al.* Human 6-sulfo LacNAc-expressing dendritic cells are principal producers of early interleukin-12 and are controlled by erythrocytes. *Immunity.* **24**, 767-777 (2006).

15. Banchereau,J. *et al.* Immunobiology of dendritic cells. *Annu. Rev. Immunol.* **18**, 767-811 (2000).

16. Inaba,K. *et al.* Generation of large numbers of dendritic cells from mouse bone marrow cultures supplemented with granulocyte/macrophage colony-stimulating factor. *J. Exp. Med.* **176**, 1693-1702 (1992).

17. Zanoni,I. & Granucci,F. Regulation of antigen uptake, migration, and lifespan of dendritic cell by Toll-like receptors. *Journal of Molecular Medicine-Jmm* **88**, 873-880 (2010).

18. Ardavin,C., Wu,L., Ferrero,I. & Shortman,K. Mouse Thymic Dendritic Cell Subpopulations. *Immunology Letters* **38**, 19-25 (1993).

19. Shortman,K. & Naik,S.H. Steady-state and inflammatory dendritic-cell development. *Nature Reviews Immunology* **7**, 19-30 (2007).

20. Ardavin,C. *et al.* Origin and differentiation of dendritic cells. *Trends in Immunology* **22**, 691-700 (2001).

21. Ardavin,C. Origin, precursors and differentiation of mouse dendritic cells. *Nature Reviews Immunology* **3**, 582-590 (2003).

22. Wu,L., Ardavin,C., Li,C.L. & Shortman,K. Thymic Dendritic Cells and T-Cells Develop Simultaneously in the Thymus from A Common Precursor Population. *Journal of Leukocyte Biology* 117 (1993).

23. Steinman,R.M., Pack,M. & Inaba,K. Dendritic cells in the T-cell areas of lymphoid organs. *Immunological Reviews* **156**, 25-37 (1997).

24. Leenen,P.J.M. *et al.* Heterogeneity of mouse spleen dendritic cells: In vivo phagocytic activity, expression of macrophage markers, and subpopulation turnover. *Journal of Immunology* **160**, 2166-2173 (1998).

25. Ohteki,T. *et al.* Interleukin 12-dependent interferon gamma production by CD8 alpha(+) lymphoid dendritic cells. *Journal of Experimental Medicine* **189**, 1981-1986 (1999).

26. Kronin,V. *et al.* Subclass of dendritic cells regulates the response of naive CD8 T cells by limiting their IL-2 production. *Journal of Immunology* **157**, 3819-3827 (1996).

27. Maldonado-Lopez,R. *et al.* CD8 alpha(+) and CD8 alpha(-) subclasses of dendritic cells direct the development of distinct T helper cells in vivo. *Journal of Experimental Medicine* **189**, 587-592 (1999).

28. Maraskovsky,E. *et al.* Dramatic increase in the numbers of functionally mature dendritic cells in Flt3 ligand-treated mice: Multiple dendritic cell subpopulations identified. *Journal of Experimental Medicine* **184**, 1953-1962 (1996).

29. Pulendran,B. *et al.* Distinct dendritic cell subsets differentially regulate the class of immune response in vivo. *Proceedings of the National Academy of Sciences of the United States of America* **96**, 1036-1041 (1999).

30. Bell,D. *et al.* In breast carcinoma tissue, immature dendritic cells reside within the tumor, whereas mature dendritic cells are located in peritumoral areas. *Journal of Experimental Medicine* **190**, 1417-1425 (1999).

31. Tang,A.M., Amagai,M., Granger,L.G., Stanley,J.R. & Udey,M.C. Adhesion of Epidermal Langerhans Cells to Keratinocytes Mediated by E-Cadherin. *Nature* **361**, 82-85 (1993).

32. Mommaas,A.M. *et al.* Human epidermal Langerhans cells lack functional mannose receptors and a fully developed endosomal/lysosomal compartment for loading of HLA class II molecules. *European Journal of Immunology* **29**, 571-580 (1999).

33. Fanger,N.A., Wardwell,K., Shen,L.L., Tedder,T.F. & Guyre,P.M. Type I (CD64) and type II (CD32) Fc gamma receptor-mediated phagocytosis by human blood dendritic cells. *Journal of Immunology* **157**, 541-548 (1996).

34. Matsuno,K., Ezaki,T., Kudo,S. & Uehara,Y. A life stage of particle-laden rat dendritic cells in vivo: Their terminal division, active phagocytosis, and translocation from the liver to the draining lymph. *Journal of Experimental Medicine* **183**, 1865-1878 (1996).

35. Albert,M.L. *et al.* Immature dendritic cells phagocytose apoptotic cells via alpha(v)beta(5) and CD36, and cross-present antigens to cytotoxic T lymphocytes. *Journal of Experimental Medicine* **188**, 1359-1368 (1998).

36. Inaba,K., Inaba,M., Naito,M. & Steinman,R.M. Dendritic Cell Progenitors Phagocytose Particulates, Including Bacillus-Calmette-Guerin Organisms, and Sensitize Mice to Mycobacterial Antigens In-Vivo. *Journal of Experimental Medicine* **178**, 479-488 (1993).

37. Moll,H. Epidermal Langerhans Cells Are Critical for Immunoregulation of Cutaneous Leishmaniasis. *Immunology Today* **14**, 383-387 (1993).

38. Rescigno,M., Granucci,F., Citterio,S., Foti,M. & Ricciardi-Castagnoli,P. Coordinated events during bacteria-induced DC maturation. *Immunology Today* **20**, 200-203 (1999).

39. Akbari,O. *et al.* DNA vaccination: Transfection and activation of dendritic cells as key events for immunity. *Journal of Experimental Medicine* **189**, 169-177 (1999).

40. Cella,M. *et al.* Maturation, activation, and protection of dendritic cells induced by double-stranded RNA. *Journal of Experimental Medicine* **189**, 821-829 (1999).

41. Engering,A.J. *et al.* The mannose receptor functions as a high capacity and broad specificity antigen receptor in human dendritic cells. *European Journal of Immunology* **27**, 2417-2425 (1997).

42. Sallusto,F. & Lanzavecchia,A. Efficient Presentation of Soluble-Antigen by Cultured Human Dendritic Cells Is Maintained by Granulocyte-Macrophage Colony-Stimulating Factor Plus Interleukin-4 and Down-Regulated by Tumor-Necrosis-Factor-Alpha. *Journal of Experimental Medicine* **179**, 1109-1118 (1994).

43. Kleijmeer,M.J. *et al.* Mhc Class-Ii Compartments and the Kinetics of Antigen Presentation in Activated Mouse Spleen Dendritic Cells. *Journal of Immunology* **154**, 5715-5724 (1995).

44. Cresswell,P. Invariant chain structure and MHC class II function. *Cell* **84**, 505-507 (1996).

45. Pamer,E. & Cresswell,P. Mechanisms of MHC class I - Restricted antigen processing. *Annual Review of Immunology* **16**, 323-358 (1998).

46. Pfeifer,J.D. *et al.* Phagocytic Processing of Bacterial-Antigens for Class-I Mhc Presentation to T-Cells. *Nature* **361**, 359-362 (1993).

47. Huang,A.Y.C. *et al.* Role of Bone-Marrow-Derived Cells in Presenting Mhc Class I-Restricted Tumor-Antigens. *Science* **264**, 961-965 (1994).

48. Sigal,L.J., Crotty,S., Andino,R. & Rock,K.L. Cytotoxic T-cell immunity to virus-infected non-haematopoietic cells requires presentation of exogenous antigen. *Nature* **398**, 77-80 (1999).

49. Kurts,C. *et al.* CD4(+) T cell help impairs CD8(+) T cell deletion induced by cross-presentation of self-antigens and favors autoimmunity. *Journal of Experimental Medicine* **186**, 2057-2062 (1997).

50. Kawakami,T. & Kitaura,J. Mast cell survival and activation by IgE in the absence of antigen: a consideration of the biologic mechanisms and relevance. *J Immunol.* **175**, 4167-4173 (2005).

51. Pawankar,R. Inflammatory mechanisms in allergic rhinitis. *Current Opinion in Allergy and Clinical Immunology* **7**, 1-4 (2007).

52. Vliagoftis,H. & Befus,A.D. Mast cells at mucosal frontiers. *Current Molecular Medicine* **5**, 573-589 (2005).

53. Galli,S.J., Nakae,S. & Tsai,M. Mast cells in the development of adaptive immune responses. *Nature Immunology* **6**, 135-142 (2005).

54. Gilfillan,A.M. & Tkaczyk,C. Integrated signalling pathways for mast-cell activation. *Nature Reviews Immunology* **6**, 218-230 (2006).

55. Metcalfe,D.D., Baram,D. & Mekori,Y.A. Mast cells. *Physiological Reviews* **77**, 1033-1079 (1997).

56. Aldenborg,F. & Enerback,L. Thymus Dependence of Connective-Tissue Mast-Cells - A Quantitative Cytofluorometric Study of the Growth of Peritoneal Mast-Cells in Normal and Athymic Rats. *International Archives of Allergy and Applied Immunology* **78**, 277-282 (1985).

57. Dvorak,A.M. Human Mast-Cells. *Advances in Anatomy Embryology and Cell Biology* **114**, 1-100 (1989).

58. Dastych,J. & Metcalfe,D.D. Stem-Cell Factor Induces Mast-Cell Adhesion to Fibronectin. *Journal of Immunology* **152**, 213-219 (1994).

59. Fox,C.C., Dvorak,A.M., Peters,S.P., Kageysobotka,A. & Lichtenstein,L.M. Isolation and Characterization of Human Intestinal Mucosal Mast-Cells. *Journal of Immunology* **135**, 483-491 (1985).

60. Serafin,W.E., Dayton,E.T., Gravallese,P.M., Austen,K.R. & Stevens,R.L. Carboxypeptidase-A in Mouse Mast-Cells - Identification, Characterization, and Use As A Differentiation Marker. *Journal of Immunology* **139**, 3771-3776 (1987).

61. Deane,J.A. & Fruman,D.A. Phosphoinositide 3-kinase: Diverse roles in immune cell activation. *Annual Review of Immunology* **22**, 563-598 (2004).

62. Wullschleger,S., Loewith,R. & Hall,M.N. TOR signaling in growth and metabolism. *Cell* **124**, 471-484 (2006).

63. Sekulic,A. *et al.* A direct linkage between the phosphoinositide 3-Kinase-AKT signaling pathway and the mammalian target of rapamycin in mitogen-stimulated and transformed cells. *Cancer Research* **60**, 3504-3513 (2000).

64. Weichhart,T. & Saemann,M.D. The PI3K/Akt/mTOR pathway in innate immune cells: emerging therapeutic applications. *Annals of the Rheumatic Diseases* **67**, 70-74 (2008).

65. Bhattacharyya,S. *et al.* Immunoregulation of dendritic cells by IL-10 is mediated through suppression of the PI3K/Akt pathway and of I kappa B kinase activity. *Blood* **104**, 1100-1109 (2004).

66. Fukao,T. *et al.* PI3K-mediated negative feedback regulation of IL-12 production in DCs. *Nat. Immunol.* **3**, 875-881 (2002).

67. Aksoy,E. *et al.* Inhibition of phosphoinositide 3-kinase enhances TRIF-dependent NF-kappa B activation and IFN-beta synthesis downstream of Toll-like receptor 3 and 4. *European Journal of Immunology* **35**, 2200-2209 (2005).

68. Fukao,T. & Koyasu,S. PI3K and negative regulation of TLR signaling. *Trends Immunol.* **24**, 358-363 (2003).

69. Gangloff,Y.G. *et al.* Disruption of the mouse mTOR gene leads to early postimplantation lethality and prohibits embryonic stem cell development. *Mol. Cell Biol.* **24**, 9508-9516 (2004).

70. Thomson,A.W., Turnquist,H.R. & Raimondi,G. Immunoregulatory functions of mTOR inhibition. *Nature Reviews Immunology* **9**, 324-337 (2009).

71. Potter,C.J., Pedraza,L.G. & Xu,T. Akt regulates growth by directly phosphorylating Tsc2. *Nature Cell Biology* **4**, 658-665 (2002).

72. Yang,Q. & Guan,K.L. Expanding mTOR signaling. *Cell Research* **17**, 666-681 (2007).

73. Staal,F.J.T., Luis,T.C. & Tiemessen,M.M. WNT signalling in the immune system: WNT is spreading its wings. *Nature Reviews Immunology* **8**, 581-593 (2008).

74. Inoki,K. *et al.* TSC2 integrates Wnt and energy signals via a coordinated phosphorylation by AMPK and GSK3 to regulate cell growth. *Cell* **126**, 955-968 (2006).

75. Sarbassov,D.D. *et al.* Rictor, a novel binding partner of mTOR, defines a rapamycin-insensitive and raptor-independent pathway that regulates the cytoskeleton. *Curr. Biol.* **14**, 1296-1302 (2004).

76. Guertin,D.A. *et al.* Ablation in mice of the mTORC components raptor, rictor, or mLST8 reveals that mTORC2 is required for signaling to Akt-FOXO and PKCalpha, but not S6K1. *Dev. Cell* **11**, 859-871 (2006).

77. Hresko,R.C. & Mueckler,M. mTOR center dot RICTOR is the Ser(473) kinase for Akt/protein kinase B in 3T3-L1 adipocytes. *Journal of Biological Chemistry* **280**, 40406-40416 (2005).

78. Jacinto,E. *et al.* Mammalian TOR complex 2 controls the actin cytoskeleton and is rapamycin insensitive. *Nat. Cell Biol.* **6**, 1122-1128 (2004).

79. Astrinidis,A. *et al.* Tuberin, the tuberous sclerosis complex 2 tumor suppressor gene product, regulates Rho activation, cell adhesion and migration. *Oncogene* **21**, 8470-8476 (2002).

80. O'Reilly,K.E. *et al.* mTOR inhibition induces upstream receptor tyrosine kinase signaling and activates Akt. *Cancer Res.* **66**, 1500-1508 (2006).

81. Armstrong,J.L., Bonavaud,S.M., Toole,B.J. & Yeaman,S.J. Regulation of glycogen synthesis by amino acids in cultured human muscle cells. *Journal of Biological Chemistry* **276**, 952-956 (2001).

82. Dames,S.A., Mulet,J.M., Rathgeb-Szabo,K., Hall,M.N. & Grzesiek,S. The solution structure of the FATC domain of the protein kinase target of rapamycin suggests a role for redox-dependent structural and cellular stability. *Journal of Biological Chemistry* **280**, 20558-20564 (2005).

83. Kim,D.H. *et al.* mTOR interacts with raptor to form a nutrient-sensitive complex that signals to the cell growth machinery. *Cell* **110**, 163-175 (2002).

84. Chen,E.J. & Kaiser,C.A. LST8 negatively regulates amino acid biosynthesis as a component of the TOR pathway. *Journal of Cell Biology* **161**, 333-347 (2003).

85. Hackstein,H. *et al.* Rapamycin inhibits IL-4-induced dendritic cell maturation in vitro and dendritic cell mobilization and function in vivo. *Blood* **101**, 4457-4463 (2003).

86. Turnquist,H.R. *et al.* Rapamycin-conditioned dendritic cells are poor stimulators of allogeneic CD4(+) T cells, but enrich for antigen-specific Foxp3(+) T regulatory cells and promote organ transplant tolerance. *Journal of Immunology* **178**, 7018-7031 (2007).

87. Schmitz,F. *et al.* Mammalian target of rapamycin (mTOR) orchestrates the defense program of innate immune cells. *Wiener Klinische Wochenschrift* **120**, 36 (2008).

88. Hackstein,H., Taner,T., Logar,A.J. & Thomson,A.W. Rapamycin inhibits macropinocytosis and mannose receptor-mediated endocytosis by bone marrow-derived dendritic cells. *Blood* **100**, 1084-1087 (2002).

89. Monti,P. *et al.* Rapamycin impairs antigen uptake of human dendritic cells. *Transplantation* **75**, 137-145 (2003).

90. Sordi,V. *et al.* Differential effects of immuno suppressive drugs on chemokine receptor CCR7 in human monocyte-derived dendritic cells: Selective upregulation by rapamycin. *Transplantation* **82**, 826-834 (2006).

91. Reichardt,W. *et al.* Impact of mammalian target of rapamycin inhibition on lymphoid homing and tolerogenic function of nanoparticle-labeled dendritic cells following allogeneic hematopoietic cell transplantation. *Journal of Immunology* **181**, 4770-4779 (2008).

92. Taner,T., Hackstein,H., Wang,Z.L., Morelli,A.E. & Thomson,A.W. Rapamycin-treated, alloantigen-pulsed host dendritic cells induce Ag-specific T cell regulation and prolong graft survival. *American Journal of Transplantation* **5**, 228-236 (2005).

93. Turnquist,H.R. *et al.* IL-I beta-driven ST2L expression promotes maturation resistance in rapamycin-conditioned dendritic cells. *American Journal of Transplantation* **8**, 226 (2008).

94. Schmitz,J. *et al.* IL-33, an interleukin-1-like cytokine that signals via the IL-1 receptor-related protein ST2 and induces T helper type 2-associated cytokines. *Immunity* **23**, 479-490 (2005).

95. Ohtani,M. *et al.* Mammalian target of rapamycin and glycogen synthase kinase 3 differentially regulate lipopolysaccharide-induced interleukin-12 production in dendritic cells. *Blood* **112**, 635-643 (2008).

96. Weichhart,T. *et al.* The TSC-mTOR Signaling Pathway Regulates the Innate Inflammatory Response. *Immunity* **29**, 565-577 (2008).

97. Yang,C.S. *et al.* Intracellular network of phosphatidylinositol 3-kinase, mammalian target of the rapamycin/70 kDa ribosomal S6 kinase 1, and mitogen-activated protein kinases pathways for regulating mycobacteria-induced IL-23 expression in human macrophages. *Cellular Microbiology* **8**, 1158-1171 (2006).

98. Colina,R. *et al.* Translational control of the innate immune response through IRF-7. *Nature* **452**, 323-3U2 (2008).

99. Honda,K. *et al.* IRF-7 is the master regulator of type-I interferon-dependent immune responses. *Nature* **434**, 772-777 (2005).

100. Cao,W.P. *et al.* Toll-like receptor-mediated induction of type I interferon in plasmacytoid dendritic cells requires the rapamycin-sensitive PI(3) K-mTOR-p70S6K pathway. *Nature Immunology* **9**, 1157-1164 (2008).

101. Cao,W.P. *et al.* Toll-like receptor-mediated induction of type I interferon in plasmacytoid dendritic cells requires the rapamycin-sensitive PI(3) K-mTOR-p70S6K pathway. *Nature Immunology* **9**, 1157-1164 (2008).

102. Kim,M.S., Kuehn,H.S., Metcalfe,D.D. & Gilfillan,A.M. Activation and function of the mTORC1 pathway in mast cells. *Journal of Immunology* **180**, 4586-4595 (2008).

103. Andrade,M.V., Hiragun,T. & Beaven,M.A. Dexamethasone suppresses antigen-induced activation of phosphatidylinositol 3-kinase and downstream responses in mast cells. *J Immunol.* **172**, 7254-7262 (2004).

104. Gilfillan,A.M. & Tkaczyk,C. Integrated signalling pathways for mast-cell activation. *Nat Rev Immunol.* **6**, 218-230 (2006).

105. Wymann,M.P. *et al.* Phosphoinositide 3-kinase gamma: a key modulator in inflammation and allergy. *Biochem Soc Trans* **31**, 275-280 (2003).

106. Tkaczyk,C., Beaven,M.A., Brachman,S.M., Metcalfe,D.D. & Gilfillan,A.M. The phospholipase C gamma 1-dependent pathway of Fc epsilon RI-mediated mast cell activation is regulated independently of phosphatidylinositol 3-kinase. *J. Biol. Chem.* **278**, 48474-48484 (2003).

107. Serve,H. *et al.* Differential roles of PI3-kinase and Kit tyrosine 821 in Kit receptor-mediated proliferation, survival and cell adhesion in mast cells. *EMBO J.* **14**, 473-483 (1995).

108. Ali,K. *et al.* Essential role for the p110delta phosphoinositide 3-kinase in the allergic response. *Nature* **431**, 1007-1011 (2004).

109. Ali,K. *et al.* Essential role for the p110delta phosphoinositide 3-kinase in the allergic response. *Nature* **431**, 1007-1011 (2004).

110. Ali,K. *et al.* Essential role for the p110delta phosphoinositide 3-kinase in the allergic response. *Nature* **431**, 1007-1011 (2004).

111. Biondi,R.M. *et al.* High resolution crystal structure of the human PDK1 catalytic domain defines the regulatory phosphopeptide docking site. *Embo Journal* **21**, 4219-4228 (2002).

112. Zaru,R., Mollahan,P. & Watts,C. 3-phosphoinositide-dependent kinase 1 deficiency perturbs toll-like receptor signaling events and actin cytoskeleton dynamics in dendritic cells. *Journal of Biological Chemistry* **283**, 929-939 (2008).

113. Sarbassov,D.D., Guertin,D.A., Ali,S.M. & Sabatini,D.M. Phosphorylation and regulation of Akt/PKB by the rictor-mTOR complex. *Science* **307**, 1098-1101 (2005).

114. Balendran,A. *et al.* A 3-phosphoinositide-dependent protein kinase-1 (PDK1) docking site is required for the phosphorylation of protein kinase C zeta (PKC zeta) and PKC-related kinase 2 by PDK1. *Journal of Biological Chemistry* **275**, 20806-20813 (2000).

115. Lawlor,M.A. *et al.* Essential role of PDK1 in regulating cell size and development in mice. *Embo Journal* **21**, 3728-3738 (2002).

116. Mora,A., Lipina,C., Tronche,F., Sutherland,C. & Alessi,D.R. Deficiency of PDK1 in liver results in glucose intolerance, impairment of insulin-regulated gene expression and liver failure. *Biochemical Journal* **385**, 639-648 (2005).

117. Mora,A., Sakamoto,K., McManus,E.J. & Alessi,D.R. Role of the PDK1-PKB-GSK3 pathway in regulating glycogen synthase and glucose uptake in the heart. *Febs Letters* **579**, 3632-3638 (2005).

118. Nirula,A., Ho,M., Phee,H., Roose,J. & Weiss,A. Phosphoinositide-dependent kinase 1 targets protein kinase A in a pathway that regulates interleukin 4. *Journal of Experimental Medicine* **203**, 1733-1744 (2006).

119. Fischer,H.G. & Eder,C. Voltage-Gated K+ Currents of Mouse Dendritic Cells. *Febs Letters* **373**, 127-130 (1995).

120. Mullen,K.M. *et al.* Potassium channels Kv1.3 and Kv1.5 are expressed on blood-derived dendritic cells in the central nervous system. *Ann. Neurol.* **60**, 118-127 (2006).

121. Shumilina,E. *et al.* Blunted IgE-mediated activation of mast cells in mice lacking the Ca2+-activated K+ channel K(Ca)3.1. *Journal of Immunology* **180**, 8040-8047 (2008).

122. Shumilina,E., Zahir,N., Xuan,N.T. & Lang,F. Phosphoinositide 3-kinase dependent regulation of Kv channels in dendritic cells. *Cell Physiol Biochem.* **20**, 801-808 (2007).

123. Hsu,S.F. *et al.* Fundamental Ca2+ signaling mechanisms in mouse dendritic cells: CRAC is the major Ca2+ entry pathway. *Journal of Immunology* **166**, 6126-6133 (2001).

124. Matzner,N. *et al.* Ion channels modulating mouse dendritic cell functions. *J. Immunol.* **181**, 6803-6809 (2008).

125. Kharrat,R. *et al.* Chemical synthesis and characterization of maurotoxin, a short scorpion toxin with four disulfide bridges that acts on K+ channels. *European Journal of Biochemistry* **242**, 491-498 (1996).

126. Duffy,S.M., Cruse,G., Lawley,W.J. & Bradding,P. beta(2)-Adrenoceptor regulation of the K+ channel iK(Ca)1 in human mast cells. *Faseb Journal* **19**, 1006-+ (2005).

127. Duffy,S.M., Lawley,W.J., Conley,E.C. & Bradding,P. Resting and activation-dependent ion channels in human mast cells. *Journal of Immunology* **167**, 4261-4270 (2001).

128. Duffy,S.M., Leyland,M.L., Conley,E.C. & Bradding,P. Voltage-dependent and calcium-activated ion channels in the human mast cell line HMC-1. *Journal of Leukocyte Biology* **70**, 233-240 (2001).

129. Kahr,H. *et al.* CaT1 knock-down strategies fail to affect CRAC channels in mucosal-type mast cells. *Journal of Physiology-London* **557**, 121-132 (2004).

130. Ching,T.T., Hsu,A.L., Johnson,A.J. & Chen,C.S. Phosphoinositide 3-kinase facilitates antigen-stimulated Ca2+ influx in RBL-2H3 mast cells via a phosphatidylinositol 3,4,5-trisphosphate-sensitive Ca2+ entry mechanism. *Journal of Biological Chemistry* **276**, 14814-14820 (2001).

131. Hoth,M. & Penner,R. Depletion of Intracellular Calcium Stores Activates A Calcium Current in Mast-Cells. *Nature* **355**, 353-356 (1992).

132. Labrecque,G.F., Holowka,D. & Baird,B. Antigen-Triggered Membrane-Potential Changes in Ige-Sensitized Rat Basophilic Leukemia-Cells - Evidence for A

Repolarizing Response That Is Important in the Stimulation of Cellular De-Granulation. *Journal of Immunology* **142**, 236-243 (1989).

133. Narenjkar,J., Marsh,S.J. & Assem,E.S.K. Inhibition of the antigen-induced activation of RBL-2H3 cells by charybdotoxin and cetiedil. *European Journal of Pharmacology* **483**, 95-106 (2004).

134. Coetzee,W.A. *et al.* Molecular diversity of K+ channels. *Ann. N. Y. Acad. Sci.* **868**, 233-285 (1999).

135. Li,M. & Adelman,J.P. ChIPping away at potassium channel regulation. *Nat. Neurosci.* **3**, 202-204 (2000).

136. Xu,J. & Li,M. Auxiliary subunits of Shaker-type potassium channels. *Trends Cardiovasc. Med.* **8**, 229-234 (1998).

137. Cox,R.H. Molecular determinants of voltage-gated potassium currents in vascular smooth muscle. *Cell Biochem. Biophys.* **42**, 167-195 (2005).

138. Yu,W., Xu,J. & Li,M. NAB domain is essential for the subunit assembly of both alpha-alpha and alpha-beta complexes of shaker-like potassium channels. *Neuron* **16**, 441-453 (1996).

139. Cahalan,M.D., Chandy,K.G., Decoursey,T.E. & Gupta,S. A Voltage-Gated Potassium Channel in Human Lymphocytes-T. *Journal of Physiology-London* **358**, 197-237 (1985).

140. Larsson,H.P., Baker,O.S., Dhillon,D.S. & Isacoff,E.Y. Transmembrane movement of the Shaker K+ channel S4. *Neuron* **16**, 387-397 (1996).

141. Chandy,K.G. *et al.* K+ channels as targets for specific immunomodulation. *Trends in Pharmacological Sciences* **25**, 280-289 (2004).

142. Kalman,K. *et al.* ShK-Dap(22), a potent Kv1.3-specific immunosuppressive polypeptide. *Journal of Biological Chemistry* **273**, 32697-32707 (1998).

143. Beeton,C. *et al.* Targeting effector memory T cells with a selective peptide inhibitor of Kv1.3 channels for therapy of autoimmune diseases. *Molecular Pharmacology* **67**, 1369-1381 (2005).

144. Schmitz,A. *et al.* Design of PAP-1, a selective small molecule Kv1.3 blocker, for the suppression of effector memory T cells in autoimmune diseases. *Molecular Pharmacology* **68**, 1254-1270 (2005).

145. Bradding,P. & Wulff,H. The K(+) channels K(Ca)3.1 and K(v)1.3 as novel targets for asthma therapy. *British Journal of Pharmacology* **157**, 1330-1339 (2009).

146. Fanger,C.M. *et al.* Calmodulin mediates calcium-dependent activation of the intermediate conductance K-Ca channel, IKCa1. *Journal of Biological Chemistry* **274**, 5746-5754 (1999).

147. Gerlach,A.C., Gangopadhyay,N.N. & Devor,D.C. Kinase-dependent regulation of the intermediate conductance, calcium-dependent potassium channel, hIK1. *Journal of Biological Chemistry* **275**, 585-598 (2000).

148. Srivastava,S. *et al.* Histidine phosphorylation of the potassium channel KCa3.1 by nucleoside diphosphate kinase B is required for activation of KCa3.1 and CD4 T cells. *Molecular Cell* **24**, 665-675 (2006).

149. Srivastava,S. *et al.* Protein histidine phosphatase 1 negatively regulates CD4 T cells by inhibiting the K(+) channel KCa3.1. *Proceedings of the National Academy of Sciences of the United States of America* **105**, 14442-14446 (2008).

150. Wulff,H. *et al.* Design of a potent and selective inhibitor of the intermediate-conductance Ca2+-activated K+ channel, IKCa1: A potential immunosuppressant. *Proceedings of the National Academy of Sciences of the United States of America* **97**, 8151-8156 (2000).

151. Stocker,J.W. *et al.* ICA-17043, a novel Gardos channel blocker, prevents sickled red blood cell dehydration in vitro and in vivo in SAD mice. *Blood* **101**, 2412-2418 (2003).

152. Pedersen,K.A. *et al.* Activation of the human intermediate-conductance Ca2+-activated K+ channel by 1-ethyl-2-benzimidazolinone is strongly Ca2+-dependent. *Biochimica et Biophysica Acta-Biomembranes* **1420**, 231-240 (1999).

153. Sankaranarayanan,A. *et al.* Naphtho[1,2-d]thiazol-2-ylamine (SKA-31), a New Activator of KCa2 and KCa3.1 Potassium Channels, Potentiates the Endothelium-Derived Hyperpolarizing Factor Response and Lowers Blood Pressure. *Molecular Pharmacology* **75**, 281-295 (2009).

154. Ali,K. *et al.* Essential role for the p110 delta phosphoinositide 3-kinase in the allergic response. *Nature* **431**, 1007-1011 (2004).

155. Andrade,M.V.M., Hiragun,T. & Beaven,M.A. Dexamethasone suppresses antigen-induced activation of phosphatidylinositol 3-kinase and downstream responses in mast cells. *Journal of Immunology* **172**, 7254-7262 (2004).

156. Lam,R.S. *et al.* Phosphatidylinositol-3-kinase regulates mast cell ion channel activity. *Cellular Physiology and Biochemistry* **22**, 169-176 (2008).

157. Alessi,D.R. & Cohen,P. Mechanism of activation and function of protein kinase B. *Current Opinion in Genetics & Development* **8**, 55-62 (1998).

158. Mora,A., Komander,D., van Aalten,D.M.F. & Alessi,D.R. PDK1, the master regulator of AGC kinase signal transduction. *Seminars in Cell & Developmental Biology* **15**, 161-170 (2004).

159. Lang,F. *et al.* (Patho)physiological significance of the serum- and glucocorticoid-inducible kinase isoforms. *Physiological Reviews* **86**, 1151-1178 (2006).

160. Le Good,J.A. *et al.* Protein kinase C isotypes controlled by phosphoinositide 3-kinase through the protein kinase PDK1. *Science* **281**, 2042-2045 (1998).

161. Xia,S.H., Chen,Z.H., Forman,L.W. & Faller,D.V. PKC delta survival signaling in cells containing an activated p21(Ras) protein requires PDK1. *Cellular Signalling* **21**, 502-508 (2009).

162. Hamill,O.P., Marty,A., Neher,E., Sakmann,B. & Sigworth,F.J. Improved patch-clamp techniques for high-resolution current recording from cells and cell-free membrane patches. *Pflugers Arch.* **391**, 85-100 (1981).

163. Barry,P.H. & Lynch,J.W. Liquid Junction Potentials and Small-Cell Effects in Patch-Clamp Analysis. *Journal of Membrane Biology* **121**, 101-117 (1991).

164. Seebohm,G. *et al.* Regulation of KCNQ4 potassium channel prepulse dependence and current amplitude by SGK1 in Xenopus oocytes. *Cell Physiol Biochem.* **16**, 255-262 (2005).

165. Wagner,C.A., Friedrich,B., Setiawan,I., Lang,F. & Broer,S. The use of Xenopus laevis oocytes for the functional characterization of heterologously expressed membrane proteins. *Cell Physiol Biochem.* **10**, 1-12 (2000).

166. Bohmer,C. *et al.* Stimulation of the EAAT4 glutamate transporter by SGK protein kinase isoforms and PKB. *Biochem. Biophys. Res. Commun.* **324**, 1242-1248 (2004).

167. Bohmer,C. *et al.* Stimulation of the EAAT4 glutamate transporter by SGK protein kinase isoforms and PKB. *Biochem Biophys Res. Commun.* **324**, 1242-1248 (2004).

168. Busch,A.E. *et al.* Properties of electrogenic Pi transport by a human renal brush border Na+/Pi transporter. *J. Am. Soc. Nephrol.* **6**, 1547-1551 (1995).

169. Seebohm,G. *et al.* Regulation of KCNQ4 potassium channel prepulse dependence and current amplitude by SGK1 in Xenopus oocytes. *Cell Physiol Biochem.* **16**, 255-262 (2005).

170. Busch,A.E. *et al.* Properties of electrogenic Pi transport by a human renal brush border Na+/Pi transporter. *J. Am. Soc. Nephrol.* **6**, 1547-1551 (1995).

171. Bradding,P., Okayama,Y., Kambe,N. & Saito,H. Ion channel gene expression in human lung, skin, and cord blood-derived mast cells. *Journal of Leukocyte Biology* **73**, 614-620 (2003).

172. Dernick,G., de Toledo,G.A. & Lindau,M. Exocytosis of single chromaffin granules in cell-free inside-out membrane patches. *Nature Cell Biology* **5**, 358-362 (2003).

173. Tkaczyk,C., Beaven,M.A., Brachman,S.M., Metcalfe,D.D. & Gilfillan,A.M. The phospholipase C gamma(1)-dependent pathway of Fc epsilon RI-mediated mast cell activation is regulated independently of phosphatidylinositol 3-kinase. *Journal of Biological Chemistry* **278**, 48474-48484 (2003).

174. Sobiesiak,M. *et al.* Impaired Mast Cell Activation in Gene-Targeted Mice Lacking the Serum- and Glucocorticoid-Inducible Kinase SGK1. *Journal of Immunology* **183**, 4395-4402 (2009).

175. Leitges,M. *et al.* Protein kinase C-delta is a negative regulator of antigen-induced mast cell degranulation. *Molecular and Cellular Biology* **22**, 3970-3980 (2002).

176. Murray,J.T. *et al.* Exploitation of KESTREL to identify NDRG family members as physiological substrates for SGK1 and GSK3. *Biochemical Journal* **384**, 477-488 (2004).

177. MacDonald,A., Scarola,J., Burke,J.T. & Zimmerman,J.J. Clinical pharmacokinetics and therapeutic drug monitoring of sirolimus. *Clinical Therapeutics* **22**, B101-B121 (2000).

178. Ahn,H.S. *et al.* Calcineurin-independent inhibition of KV1.3 by FK-506 (tacrolimus): a novel pharmacological property. *Am. J. Physiol Cell Physiol* **292**, C1714-C1722 (2007).

179. Gamper,N. *et al.* IGF-1 up-regulates K+ channels via PI3-kinase, PDK1 and SGK1. *Pflugers Archiv-European Journal of Physiology* **443**, 625-634 (2002).

180. Henke,G., Maier,G., Wallisch,S., Boehmer,C. & Lang,F. Regulation of the voltage gated K+ channel Kv1.3 by the ubiquitin ligase Nedd4-2 and the serum and glucocorticoid inducible kinase SGK1. *Journal of Cellular Physiology* **199**, 194-199 (2004).

181. Ullrich,S. *et al.* Serum- and glucocorticoid-inducible kinase 1 (SGK1) mediates glucocorticoid-induced inhibition of insulin secretion. *Diabetes* **54**, 1090-1099 (2005).

182. Gamper,N. *et al.* K+ channel activation by all three isoforms of serum- and glucocorticoid-dependent protein kinase SGK. *Pflugers Archiv-European Journal of Physiology* **445**, 60-66 (2002).

183. Shumilina,E. *et al.* Deranged Kv channel regulation in fibroblasts from mice lacking the serum and glucocorticoid inducible kinase SGK1. *Journal of Cellular Physiology* **204**, 87-98 (2005).

184. Dunlop,E.A. & Tee,A.R. Mammalian target of rapamycin complex 1: Signalling inputs, substrates and feedback mechanisms. *Cellular Signalling* **21**, 827-835 (2009).

185. Garcia-Martinez,J.M. & Alessi,D.R. mTOR complex 2 (mTORC2) controls hydrophobic motif phosphorylation and activation of serum- and glucocorticoid-induced protein kinase 1 (SGK1). *Biochemical Journal* **416**, 375-385 (2008).

186. Hong,F. *et al.* mTOR-raptor binds and activates SGK1 to regulate p27 phosphorylation. *Molecular Cell* **30**, 701-711 (2008).

187. Schilling,T. & Eder,C. Effects of kinase inhibitors on TGF-beta induced upregulation of Kv1.3 K+ channels in brain macrophages. *Pflugers Archiv-European Journal of Physiology* **447**, 312-315 (2003).

188. Chung,I. & Schlichter,L.C. Regulation of native Kv1.3 channels by cAMP-dependent protein phosphorylation. *American Journal of Physiology-Cell Physiology* **273**, C622-C633 (1997).

189. Kwak,Y.G. *et al.* Protein kinase A phosphorylation alters Kv beta 1.3 subunit-mediated inactivation of the Kv1.5 potassium channel. *Journal of Biological Chemistry* **274**, 13928-13932 (1999).

190. Cayabyab,F.S., Khanna,R., Jones,O.T. & Schlichter,L.C. Suppression of the rat microglia Kv1.3 current by src-family tyrosine kinases and oxygen/glucose deprivation. *European Journal of Neuroscience* **12**, 1949-1960 (2000).

191. Cook,K.K. & Fadool,D.A. Two adaptor proteins differentially modulate the phosphorylation and biophysics of Kv1.3 ion channel by Src kinase. *Journal of Biological Chemistry* **277**, 13268-13280 (2002).

192. Gulbins,E., Szabo,I., Baltzer,K. & Lang,F. Ceramide-induced inhibition of T lymphocyte voltage-gated potassium channel is mediated by tyrosine kinases. *Proceedings of the National Academy of Sciences of the United States of America* **94**, 7661-7666 (1997).

193. Szabo,I. *et al.* Tyrosine phosphorylation-dependent suppression of a voltage-gated K+ channel in T lymphocytes upon Fas stimulation. *Journal of Biological Chemistry* **271**, 20465-20469 (1996).

194. Colley,B.S., Biju,K.C., Visegrady,A., Campbell,S. & Fadool,D.A. Neurotrophin B receptor kinase increases Kv subfamily member 1.3 (Kv1.3) ion channel half-life and surface expression. *Neuroscience* **144**, 531-546 (2007).

195. Bowlby,M.R., Fadool,D.A., Holmes,T.C. & Levitan,I.B. Modulation of the Kv1.3 potassium channel by receptor tyrosine kinases. *Journal of General Physiology* **110**, 601-610 (1997).

196. Parekh,A.B. & Penner,R. Store depletion and calcium influx. *Physiological Reviews* **77**, 901-930 (1997).

197. Tanneur,V. *et al.* Time-dependent regulation of capacitative Ca2+ entry by IGF-1 in human embryonic kidney cells. *Pflugers Archiv-European Journal of Physiology* **445**, 74-79 (2002).

198. Kumar,D., Hosse,J., von Toerne,C., Noessner,E. & Nelson,P.J. JNK MAPK Pathway Regulates Constitutive Transcription of CCL5 by Human NK Cells through SP1. *Journal of Immunology* **182**, 1011-1020 (2009).

199. Kotani,K. *et al.* Involvement of Phosphoinositide 3-Kinase in Insulin-Induced Or Igf-1-Induced Membrane Ruffling. *Embo Journal* **13**, 2313-2321 (1994).

200. Park,J. *et al.* Serum and glucocorticoid-inducible kinase (SGK) is a target of the PI 3-kinase-stimulated signaling pathway. *Embo Journal* **18**, 3024-3033 (1999).

201. Firestone,G.L., Giampaolo,J.R. & O'Keeffe,B.A. Stimulus-dependent regulation of serum and glucocorticoid inducible protein kinase (SGK) transcription, subcellular localization and enzymatic activity. *Cellular Physiology and Biochemistry* **13**, 1-12 (2003).

202. Chen,S.Y. *et al.* Epithelial sodium channel regulated by aldosterone-induced protein sgk. *Proceedings of the National Academy of Sciences of the United States of America* **96**, 2514-2519 (1999).

203. Akutsu,N. *et al.* Regulation of gene expression by 1 alpha,25-dihydroxyvitamin D-3 and its analog EB1089 under growth-inhibitory conditions in squamous carcinoma cells. *Molecular Endocrinology* **15**, 1127-1139 (2001).

204. Waldegger,S., Barth,P., Raber,G. & Lang,F. Cloning and characterization of a putative human serine/threonine protein kinase transcriptionally modified during anisotonic and isotonic alterations of cell volume. *Proceedings of the National Academy of Sciences of the United States of America* **94**, 4440-4445 (1997).

205. Alliston,T.N., Gonzalez-Robayna,I.J., Buse,P., Firestone,G.L. & Richards,J.S. Expression and localization of serum/glucocorticoid-induced kinase in the rat ovary: Relation to follicular growth and differentiation. *Endocrinology* **141**, 385-395 (2000).

206. Lang,F. *et al.* Deranged transcriptional regulation of cell-volume-sensitive kinase hSGK in diabetic nephropathy. *Proceedings of the National Academy of Sciences of the United States of America* **97**, 8157-8162 (2000).

207. Lang,F. *et al.* Bradykinin-Induced Oscillations of Cell-Membrane Potential in Cells Expressing the Ha-Ras Oncogene. *Journal of Biological Chemistry* **266**, 4938-4942 (1991).

8. Curriculum vitae

Name   Tyan

Name	Tyan
Surname	Leonid
Birth date	21.08.1983
Country	Kyrgyz Republic
Birthplace	Bishkek, Kyrgyz Republic
Languages	Russian (native), English, German (basics)

Education

2008-2012	PhD Studies. Faculty of science, University of Tübingen EBERHARD KARLS. Tübingen, Germany. Dissertation thesis subject: *Regulation of potassium channels through mTOR and PDK1 in dendritic and mast cells.*
2010	Diplomawork at the Institute of Physiology. Faculty of Biology, University of Tübingen, EBERHARD KARLS. Tübingen. Germany. Diploma thesis subject: *Phosphoinositide-dependent kinase PDK1 in the regulation of Ca^{2+} entry into mast cells*
2004-2006	Master degree. Faculty of Biology; Kyrgyz National University named after Jusup Balasagyn, Bishkek, Kyrgyz Republic. Master thesis subject: *Homocysteine. Genes polymorphism of metilenetetrahydrofolate-reductase and atherosclerosis of carotid arteries of patients with hypertonic disease complicated by an insult of a brain.*
2000-2004	Bachelor degree. Faculty of Biology; Kyrgyz National University named after Jusup Balasagyn, Bishkek, Kyrgyz Republic
1990-2000	Elementary school. School #3, Bishkek, Kyrgyz republic.

Specialization.

main field.	Electrophysiology.
other fields.	Immunology, molecular biology.
current research interest.	Role of ion chanells in physiology of dendritic and mast cells.

Laboratory skills and methods	Patch-clamp, Voltage-Clamp, work with culture of cells and immunology methods (migration and adhesion of cells), DNA manipulations (extraction; enzyme restriction; agarose, PAAG gel electrophoresis; PCR, PCR-Flash; biochip analysis), Western Immunobloting, ELISA.

Working experience

2009-2012	Doctoral Researcher, Laboratory of physiology of dendritic and mast cells, Institute of Physiology I, University of Tübingen, Tübingen, Germany
2002-2008	Researcher, Institute of molecular biology and medicine. National Centre of Cardiology and Internal medicine. Bishkek. Kyrgyz Republic.

Supervisory and teaching experience	
2005	Student Teacher. Biochemistry at high school level. Kyrgyz National University named after Jusup Balasagyn, Bishkek, Kyrgyz Republic
Awards	
2011	The best poster presentation. 90th Annual meeting. German Physiological Society. Regensburg University, Regensburg, Germany.
2009	The best poster presentation. 88th Annual meeting. German Physiological Society. Justus Liebich University. Giessen, Germany.
2008-2009	DAAD Fellowship.
2006	The best presentation. Annual meeting of young researchers. Kyrgyz National University named after J.Balasagyn, Bishkek, Kyrgyz Republic.
Scientific congress participation	
2011	90th Annual meeting. German Physiological Society. Regensburg University, Regensburg, Germany (poster presentation). Inhibition of voltage-gated K^+ channels in dendritic cells by rapamycine.
2010	Joint Meeting of the Scandinavian and German Physiological Societies. University of Copenhagen, Copenhagen, Denmark (poster presentation). Amyloid ß-peptide decreases Kv channel activity in dendritic cells via acid sphingomyelinase-dependent formation of ceramide.
2009	88th Annual meeting. German Physiological Society. Justus Liebich University. Giessen, Germany (poster presentation). PIKfive-dependent regulation of the Cl^- channel ClC-2.
2006	Annual meeting of young researchers. Kyrgyz National University named after J.Balasagyn, Bishkek, Kyrgyz Republic. (oral presentation).
2005	Annual meeting of young researchers. Kyrgyz National University named after J.Balasagyn, Bishkek, Kyrgyz Republic. (oral presentation).

9. Publications

Tyan L., Schmid E., Nurbaeva M., Gulbins E., Shumilina E., Lang F. Effect of amyloid peptides on voltage gated K^+ channels in dendritic cells. *[in preparation]*

Schmid E., Bhandaru M., Nurbaeva M., Yang W., Szteyn K., Leibrock C., **Tyan L.**, Pearce D., Shumilina E., Lang F. SGK3 regulates Ca^{2+} entry and migration of dendritic cells *[submitted]*

Bhandaru M, Kempe DS, Rotte A, Capuano P, Pathare G, Sopjani M, Alesutan I, **Tyan L**, Huang DY, Siraskar B, Judenhofer MS, Stange G, Pichler BJ, Biber J, Quintanilla-Martinez L, Wagner CA, Pearce D, Föller M, Lang F. Decreased bone density and increased phosphaturia in gene-targeted mice lacking functional serum- and glucocorticoid-inducible kinase 3. *Kidney Int. 2011 Jul*

Eylenstein A, Gehring EM, Heise N, Shumilina E, Schmidt S, Szteyn K, Münzer P, Nurbaeva MK, Eichenmüller M, **Tyan L**, Regel I, Föller M, Kuhl D, Soboloff J, Penner R, Lang F. Stimulation of Ca^{2+}-channel Orai1/STIM1 by serum- and glucocorticoid-inducible kinase 1 (SGK1). *FASEB J. 2011 Jun*

Shumilina E, Zemtsova IM, Heise N, Schmid E, Eichenmüller M, **Tyan L**, Rexhepaj R, Lang F. Phosphoinositide-dependent kinase PDK1 in the regulation of Ca^{2+} entry into mast cells. *Cell Physiol Biochem. 2010*

Tyan L, Sopjani M, Dërmaku-Sopjani M, Schmid E, Yang W, Xuan NT, Shumilina E, Lang F. Inhibition of voltage-gated K^+ channels in dendritic cells by rapamycin. *Am J Physiol Cell Physiol. 2010 Dec*